

LARRY GARSIDE
NEVADA BUREAU OF MINES
UNIVERSITY OF NEVADA
RENO, NEVADA 89507

University of Nevada

Reno

Time-Variant Hydrogeologic and Geochemical Study
of Selected Thermal Springs in Western Nevada

A thesis submitted in partial fulfillment of the
requirements for the degree of Master of Science
in Hydrology/Hydrogeology

by

Bradley F. Lyles

August 1985

The thesis of Bradley F. Lyles is approved:

Thesis Advisor

Department Chairman

Dean, Graduate School

University of Nevada
Reno

August 1985

Acknowledgements

I gratefully acknowledge the contributions of Dr. Roger Jacobson, Mr. Larry Garside, Dr. Dan Taylor, and Dr. Stephen Wheatcraft, all who served as members of my thesis committee. Special thanks go to my committee chairman Dr. Roger Jacobson whose guidance and critical review were of great help.

I wish to acknowledge Dennis Ghiglieri for his technical assistance with the Desert Research Institute computer facilities, and Jim Heidker at the Desert Research Institute Water Analysis Laboratory. I also thank Bianca Bates of Walley's Hot Spring Resort and Tom Coyle of Washoe County Park and Recreation Department for their cooperation during this study.

Funding for Stable Isotope analysis was supplied by the Desert Research Institute - Water Resources Center.

Special thanks go to my fiancé Leslie for her support, understanding and patience.

Abstract

Infiltrating waters take from 24 weeks to less than two weeks to reach the watertables of individual thermal systems, based on temporal variability of physical and chemical parameters. Steamboat and Walley's hot springs showed nearly instantaneous responses to precipitation events; conversely, Farad and Saratoga hot springs showed lagged responses of six to 24 weeks respectively.

Chemical and isotopic variability suggests that thermal waters have appreciable near-surface mixing, particularly at springs that show rapid responses to precipitation events.

Stable isotopes of oxygen and hydrogen ranged from -16.3 to -11.0 and -132.0 to -102.0 respectively, implying that recharge waters are derived from widely varying elevations. The thermal systems derive most of their recharge from the Sierra Nevada.

Table of Contents

	Page
SIGNATURE PAGE	i
ACKNOWLEDGEMENTS	ii
ABSTRACT	iii
TABLE OF CONTENTS	iv
LIST OF TABLES	1
LIST OF FIGURES	2
INTRODUCTION	3
Purpose	3
Previous Time-series Work	4
METHODS and PROCEDURES	5
Field Methods	5
Analytical Procedures	7
Computational Procedures	8
Statistical Methods	10
Geologic Field Methods	13
REGIONAL ENVIRONMENT	15
Location	15
Geomorphology	15
Geology	17
Climate and Vegetation	18
FARAD HOT SPRING	24
Introduction	24
precise location	24
climate and vegetation	24
previous work	26
Geology	27
lithologic interpretations	27
structure	28
Hydrology	28
Geochemistry	29
major dissolved constituents	30
geothermometry	30
Time-Series Analysis Results	32
Summary	39
STEAMBOAT HOT SPRING	42
Introduction	42
precise location	42
climate	43
previous work	45
Geology	45
lithology	46
structure	48
Hydrology	49
Geochemistry	51
major dissolved constituents	51
geothermometry	53
Time-Series Analysis Results	54
Summary	58
BOWER'S MANSION HOT SPRING	61
Introduction	61
precise location	61

climate and vegetation	63
previous work	64
Geology	64
lithologic interpretations	65
structure	65
Hydrology	66
regional	66
debris flow	69
local	69
Geochemistry	71
major dissolved constituents	71
geothermometry	73
Time-Series Analysis Results	75
Summary	82
STATE PRISON HOT SPRING	85
Introduction	85
precise location	85
climate and vegetation	87
previous work	87
Geology	88
lithologic interpretations	88
structure	89
Hydrology	89
Geochemistry	90
major dissolved constituents	90
geothermometry	91
Time-Series Analysis Results	94
Summary	96
SARATOGA HOT SPRING	98
Introduction	98
precise location	98
climate and vegetation	100
Geology	101
lithologic interpretations	101
mineral deposits	103
structure	103
Hydrology	104
regional	105
local	106
Geochemistry	107
major dissolved constituents	107
mineral precipitants	110
geothermometry	112
Time-Series Analysis Results	112
Summary	119
WALLEY'S RESORT HOT SPRING	121
Introduction	121
precise location	121
climate and vegetation	122
previous work	124
Geology	124
lithologic interpretations	125
structure	126
Hydrology	128
regional	128

local	129
Geochemistry	130
major dissolved constituents	130
geothermometry	130
Time-Series Analysis Results	133
Summary	144
DISCUSSION	146
Similarities	146
Differences	147
CONCLUSIONS	151
FURTHER STUDIES	155
REFERENCES CITED	157
APPENDICES	
A - Descriptive Geology	164
B - Tabulated Data	174
C - Geothermometry Equations	184
D - Program Listings	187
E - Thesis Addendum (Isotope Data)	198

List of Tables

Number		Page
1	Accumulated Precipitation between Sample Dates	21
2	Precipitation Cross-correlation Coefficient Matrix	22
3	Farad Hot Spring WATEQ output	31
4	Farad Hot Spring Chemical Geothermometry Results	33
5	Farad Hot Spring Temporal Data	34
6	Farad Hot Spring Correlation Coefficient Matrix	33
7	Farad Hot Spring Correlation Coefficient Matrix at Six week Lag	33
8	Farad Hot Spring Lead-lag Multiple Regression output	40
9	Steamboat Hot Spring WATEQ output	52
10	Steamboat Hot Spring Chemical Geothermometry Results	55
11	Steamboat Hot Spring Temporal Data	57
12	Steamboat Hot Spring Correlation Coefficient Matrix	55
13	Steamboat Hot Spring Correlation Coefficient Matrix at varying Lag Positions	55
14	Bowers Hot Spring WATEQ output	72
15	Bowers Hot Spring Chemical Geothermometry Results	74
16	Bowers Hot Spring Temporal Data	76
17	Bowers Hot Spring Correlation Coefficient Matrix	74
18	Bowers Hot Spring Correlation Coefficient matrix at Varying Lag Positions	74
19	Bowers Hot Spring Lead-lag Multiple Regression output	77
20	Prison Hot Spring WATEQ output	92
21	Prison Hot Spring Chemical Geothermometry Results	93
22	Prison Hot Spring Temporal Data	95
23	Prison Hot Spring Correlation Coefficient Matrix	93
24	Saratoga Hot Spring WATEQ output	111
25	Saratoga Hot Spring Chemical Geothermometry Results	113
26	Saratoga Hot Spring Temporal Data	114
27	Saratoga Hot Spring Correlation Coefficient Matrix	113
28	Saratoga Hot Spring Correlation Coefficient Matrix at Varying Lag Positions	113
29	Saratoga Hot Spring Lead-lag Multiple Regression output	117
30	Walley's Hot Spring WATEQ output	131
31	Walley's Hot Spring Chemical Geothermometry Results	132
32	Walley's Hot Spring Temporal Data	134
33	Walley's Hot Spring Correlation Coefficient Matrix for 52 weeks of Data	132
34	Walley's Hot Spring Correlation Coefficient Matrix at Varying Lag Positions for 52 weeks of Data	132
35	Walley's Hot Spring Correlation Coefficient Matrix for 38 weeks of Data	139
36	Walley's Hot Spring Correlation Coefficient Matrix at Varying Lag Positions for 38 weeks of Data	139
37	Walley's Hot Spring Lead-lag Multiple Regression output	142
38	FORTTRAN code listing for Program D.1 - Geothermometry	189
39	Example output from Program D.1 - Geothermometry	194
40	FORTTRAN code listing for Program D.3 - pCO ₂	196
41	Stable Isotope Data	199

List of Figures

Number		Page
1	Location Map	16
2	Precipitation Scatter Diagrams	23
3	Farad Hot Spring Geologic Map	25
4	Farad Hot Spring Temperature and Flow vs. Time	36
5	Farad Hot Spring Chloride ion and Flow vs. Time	37
6	Farad Hot Spring Precipitation and Flow vs. Time	38
7	Steamboat Hot Spring area Geologic Map	44
8	Steamboat Hot Spring Geologic Map	47
9	Steamboat Hot Spring Precipitation and Flow vs. Time	59
10	Bowers Hot Spring Geologic Map	62
11	Bowers Hot Spring Hypothetical Geologic Cross-section	67
12	Bowers Hot Spring Flow and Pumping vs. Time	80
13	Bowers Hot Spring Flow and Barometric Press. vs Time	81
14	Flowing Well Discharges West Washoe and Boat Ramp vs. Time	83
15	Prison Hot Spring Geologic Map	86
16	Prison Hot Spring Electrical Conductivity and Temperature vs. Time	97
17	Saratoga Hot Spring Geologic Map	99
18	Carson Valley Area Hypothetical Hydrogeologic Cartoon	108
19	Carson Valley δD vs. $\delta^{18}O$	109
20	Saratoga Hot Spring Precipitation and Flow vs. Time	116
21	Walley's Hot Spring Geologic Map	123
22	Walley's Hot Spring Hypothetical Geologic Cross-section	127
23	Walley's Hot Spring Stage and Flow vs. Time	135
24	Walley's Hot Spring Precipitation and Flow vs. Time	136
25	Walley's Hot Spring Precipitation and Stage vs. Time	138
26	Walley's Hot Spring Temperature and Stage vs. Time	140
27	Durov Diagram of Spring Chemistry	148
28	Stable Isotope Plot δD vs. $\delta^{18}O$	149
29	Conceptual Flowchart of Lead-lag Multiple Step-wise Regression	195
30	Study Area Isotope Plot δD vs. $\delta^{18}O$	201

Introduction

Purpose

Physical and chemical data were collected from September, 1983 to August, 1984, for six hot springs and two flowing wells along the eastern margin of the Sierra Nevada. This study was initiated to further understand the hydrology and geochemistry of thermal reservoirs, utilizing a time-series approach.

To better understand the physical and chemical controls on each reservoir, it was necessary to study the geology at each spring site. Approximately three square miles were studied at each site for major lithologic changes and structural controls. This geologic information was used to justify the individual spring characteristics and to show the physio-chemical similarities and differences of the springs studied.

Temporal isotopic ($\delta^{18}O$ and δD) variabilities were investigated to determine reservoir stability and recharge characteristics. Time-series statistics were used to approximate infiltration rates in the unsaturated zone, to determine interrelationships between measured variables, and to determine which variables are best correlated to spring flow.

Previous Time-series Work

Time-series analysis of hydro-geochemical data have been carried out in several carbonate spring systems; however, little work of this kind has been done on springs in igneous and metamorphic terrains. Many significant relationships have been developed from studies by Bateman (1970), Shuster and White (1971), Jacobson (1974), Babuskin, et al. (1975), and Johnson (1980). General spring discharge characteristics have been modeled and discussed by Mero (1963) and Bear (1979).

Many time-series isotopic studies have been conducted to determine recharge-discharge characteristics and resonance time relationships. Studies of interest have been presented by Fontes (1980), Stewart and Downes (1980), and Gross, et al. (1980).

Studies related to the individual areas are covered in the introductory information of each spring chapter.

Methods and Procedure

Introduction

Spring data were collected from September, 1983 to August, 1984, totaling 312 samples. Field measurements of flow, temperature, and pH were made and water samples were collected on each data collection date (at least biweekly). Laboratory measurements of pH and specific electrical conductivity (EC) were made and analyses for bicarbonate, chloride, and calcium ions were performed on 152 samples (26 samples were also analyzed for sodium ions). Historical chemical analysis results were used in the computer program "WATEQ" and in several chemical geothermometer equations. General statistics were calculated, such as, mean, standard deviation, and coefficients of variation, and time-series analyses (crosscorrelation and lead-lag multiple step-wise regression) were applied to the temporal data. Geologic field mapping was conducted to determine the major lithologic contacts and to determine potential structural controls for the springs.

Field Methods

Flow measurements were made with a 16 liter bucket and a stop watch at Farad and Walley's Hot Springs, and at

two flowing wells in Washoe Valley. Relative stage measurements were made at Steamboat and Prison Hot Springs. V-notch weirs equipped with Stevens Type-F continuous recorders were used at Bowers Mansion and Saratoga Hot Springs (30° V-notch and 90° V-notch respectively). The weirs were constructed of 3/4 inch thick plywood and a stainless steel V-notch was screwed to the wood to insure a sharp crest. Stage at the V-notch center was measured (feet) and converted to flow with the following equation (Daugherty, et al., 1977):

$$\text{FLOW (lps)} = c(\theta) * \tan \theta / 2 * h^{5/2} * \text{conv},$$

$$\begin{aligned} c(\theta) &= 2.5 \text{ if } \theta = 90^\circ \text{ or} \\ c(\theta) &= 0.67 \text{ if } \theta = 30^\circ \\ \theta &= \text{V-notch angle, and} \\ \text{conv} &= 28.32 \text{ lps per cfs.} \end{aligned}$$

Temperatures were measured with a mercury thermometer (0 to 100°C). The measurements were taken in the hottest parts of the springs and the thermometer was allowed to equilibrate before reading

A digital Corning pH meter was used for pH measurements; recalibration was performed at each site with two pH buffers: 6.86 and 9.18. The buffers were placed in the spring water until temperature equilibration was reached. If pH measurements varied substantially from previous measurements, then the meter calibration was checked.

Two water samples were collected for major ion analysis in plastic screw-cap bottles at each site (500 ml each). Neither sample was acidified or filtered. One

sample was sealed with black electrical tape to insure minimal contamination and atmospheric equilibration. The other sample was brought back to the laboratory and analyzed for pH, electrical conductivity, and bicarbonate ion.

An isotope sample was collected at each site in a 10 ml glass vial with a teflon coated cap. These samples were also sealed with black electrical tape.

Analytical Procedures

Laboratory measurements of EC were made on each sample with a YSI Model 33 conductivity meter. A calibration curve was established with known conductivity standards, and all measurements were corrected to 25°C. Readings near 500 $\mu\text{mhos/cm}$ were corrected for a meter scale shift; this was only necessary for samples from Frison Hot Spring.

Laboratory pH measurements were made using the same equipment and technique as the field measurements, but the sample temperatures were uniform (24 to 28°C).

Bicarbonate ion values were measured for each sample. 50 ml of sample was titrated with .02 normal H_2SO_4 and a pH probe was used to monitor the maximum pH shift (HCO_3^- inflection point).

The remaining ions were analyzed in the water analysis laboratory of the Desert Research Institute. Only the byweekly samples were analyzed for chloride,

calcium, and sodium ion concentrations. Analytical error ranged from 3 to 5 percent.

Chloride concentrations were measured for 154 samples, by a colorimetric method. Standards, spikes, and duplicates were used to calibrate curve fitting routines used to calculate the actual sample concentrations (EPA, Method 325.1).

Calcium concentrations were measured for 154 samples and sodium concentrations were measured for 26 samples by Atomic Absorption Spectrometry. Standards, spikes, and duplicates were also used for calibration (EPA, Method 273.1).

Computational Procedures

The computer program "WATEQ" was primarily used to calculate mineral saturations, cation to anion balance, and pCO_2 . This program is basically designed for low TDS water, under 75°C; therefore, the "WATEQ" results are only approximations. One must also keep in mind that just because a mineral is over saturated, it will not precipitate if the sample does not plot within the specific mineral field on the appropriate phase diagram.

The program produces mineral saturation information such as iap/kt (ion activity product / equilibrium constant), $\log iap/kt$, and mineral phase. Values of iap/kt greater than 1.0 and $\log iap/kt$ greater than 0.0, suggest that those minerals are over-saturated;

conversely, values less than 1.0 and 0.0, respectively, are presumably undersaturated.

The cation to anion balance is calculated by dividing the sum EPM cations by the sum EPM anions. If this value is close to one then the analysis is assumed good, or at least no constituents were overlooked.

The partial pressure of CO₂ is computed with the following relationship:

$$pCO_2 = aH_2CO_3 / K_{CO_2},$$

where, aH_2CO_3 is the activity of carbonic acid and K_{CO_2} is the equilibrium constant for CO₂. Samples with calculated values above atmospheric pCO₂ (-3.5) will loose CO₂ (gas) to the atmosphere, increasing the pH; the reverse is also true.

Program D.3 was also used to calculate pCO₂ values for the temporal data. These values were calculated as a function of EC, pH, temperature, and bicarbonate ion concentration from the following equation:

$$pCO_2 = \frac{aH * aHCO_3}{10^{-pK_{CO_2}} * 10^{-pK_1}}.$$

The program is described in detail in Appendix D.

Twelve chemical geothermometers were applied to historical chemical analysis results (see appendix C for equation lists). These equations have been developed through laboratory experimentation, and by thermodynamic and kinetic relationships.

It is sometimes difficult to choose the best chemical geothermometer for a thermal reservoir; the approach used

in this study was to apply all of the geothermometers in program D.1 (appendix D) and then throw out the values that were meaningless. Generally for low-flow springs (less than 200 lpm) certain assumptions should be made (Fournier, et al., OFR):

- 1) use geothermometers that assume conductive cooling, particularly for non-boiling springs,
- 2) consider the possibility of mixed waters of differing temperatures,
- 3) indicate that temperatures calculated by conductive cooling are likely to be a minima, and
- 4) if the Na-K-Ca geothermometer shows a temperature greater than 25°C, assume mixing water conditions.

The stable isotopes of Hydrogen (H^1 Protium and H^2 [or D] Dueterium) and Oxygen (^{18}O and ^{16}O), listed with the temporal data in this study, were analyzed on the mass spectrometer at the Stable Isotope Laboratory, Desert Reserch Institute, Las Vegas, Nevada. All values are reported in del (δ) notation in units of per mill (‰) and were calculated with the following equations:

$$\delta D = \frac{(D/H)_{SAMPLE} - (D/H)_{SMOW}}{(D/H)_{SMOW}} * 1000,$$

$$\delta^{18}O = \frac{(^{18}O/^{16}O)_{SAMPLE} - (^{18}O/^{16}O)_{SMOW}}{(^{18}O/^{16}O)_{SMOW}} * 1000,$$

where SMOW is a standard ("Standard Mean Ocean Water").

Statistical Methods

General statistics such as mean, standard deviation, and coefficient of variation were calculated for each variable. The following equation was used for the coefficient of variation:

$$\text{Coef. Variation} = \frac{\text{Standard Deviation}}{\text{Mean}} * 100 \text{ (units[\%]),}$$

and is expressed - percent variation. This statistic is important for justifying interpretations of temporal data.

A crosscorrelation routine was applied to the data to measure the interrelationships of the variables (Davis, PROG 5.9, 1973). This program calculated the correlation coefficient and t-statistic at each lag position, so a predominant lag between two variables can be determined. This technique loses two degrees of freedom when calculating the t-statistic, or $n-2$; where n equals the number of matches or pairs of observations. The null hypothesis in this case is correlation equals zero:

$$H_0 : \text{correlation} = 0;$$

therefore, the t-statistic is a two-tailed test.

EXAMPLE 1: Farad Hot Spring, Flow vs. Temperature
 zero lag position
 correlation = $-.72$
 computed $t = -5.050$
 H_0 : correlation = 0
 H_a : correlation \neq 0
 $\alpha = .10$ (.05 in each tail)
 $n = 26$ matched positions
 $t(24, .10) = \pm 1.71$

The computed t (-5.050) exceeds the $t(24, .10)$; therefore, reject the null hypothesis and assume that the correlation is not equal to zero, within a

10 percent chance of making a type one error.

The t-statistic allows a measure of correlation validity, but the actual correlation interpretations require some subjective judgements.

Lead-lag multiple step-wise linear regression was applied to the data, in an attempt to produce a meaningful predictive linear equation for each spring. This routine initially uses crosscorrelation techniques to find the best lagged positions between a dependent variable and several independent variables. Data points are then removed from the front of each variable string so that the data is oriented to a maximum correlation position; in other words, the leads and lags are removed from the variable strings. At this point multiple step-wise linear regression is applied, and a linear equation is produced.

The linear equation is produced in a step-wise fashion in that independent variables are considered in the equation one at a time. The variable of highest correlation, at any lagged position, is entered first, the variable of second highest correlation is entered second, and so on. An F-value (analysis of variance) and a t-statistic (analysis of regression coefficient validity) are calculated, so the equation validity can be monitored as each variable is entered.

The analysis of variance (F-test) is calculated with the following equation:

$$F = \frac{MS_R}{MS_D},$$

where MS_R is the mean squares due to regression and MS_D is mean squares due to deviation. This test automatically loses one degree of freedom or $n-1$, where n is the number of observations after points are removed from the data strings. The null hypothesis in this case is lack of fit between the regressed points and the real points.

EXAMPLE 2: Farad Hot Spring

Flow is described by Cl^- , HCO_3^- , and EC

Calculated F-value = 18.335

H_0 = lack of fit

H_a = good fit

α = .01 (one tailed test)

n = 14

	degrees of freedom	
regression	deviation	F-value
1	12	9.33
2	11	7.21
3	10	6.55
4	9	6.42

in this case $df_{REGRESSION} = 3$,

and $df_{DEVIATION} = 10$

F-value critical = 6.55

The computed F-value (18.335) exceeds $F(3,10,.01)$; therefore, reject the null hypothesis and assume that the independent variables adequately describe flow, within a 1 percent chance of making a type one error.

The t-statistic tests for regression coefficient validity. This test is identical to the t-statistic described previously for crosscorrelation coefficient validity (see example 1).

Geologic Field Methods

Geologic mapping was primarily conducted during the spring and summer of 1984. Major lithologic changes and

structures near each hot spring were mapped to further understand the hydrogeologic interrelationships. Aqueous geochemical interpretations were also based on the flowpath mineralogys. Mapping was generally conducted at 1:24,000 scale, and should be considered reconnaissance.

Regional Environment

Location

The study area is located along the eastern flank of the Sierra Nevada Mountains, extending over 80 km from north to south. This geologically complex area contains about 11 geothermal areas (Stewart, 1980); however, only six will be described in this study (figure 1). The springs covered in this study are as follows:

Farad Hot Spring - Sierra County, California
Steamboat Hot Springs - Washoe County, Nevada
Bowers Hot Spring - Washoe County, Nevada
Prison Hot Spring - Carson City, Nevada
Saratoga Hot Spring - Douglas County, Nevada
Walley's Hot Spring - Douglas County, Nevada

All of the springs are accessible year-round, either directly from the highways or via well maintained side roads. Detailed locations and accessibility descriptions are covered in the site-specific introductions.

Geomorphology

The Sierra Nevada crest ranges from 1,219 to 3,962 m and extends for 644 km. The Carson Range parallels the Sierran crest and forms the eastern flank of the Sierra Nevada Mountains within the study area. This crest varies

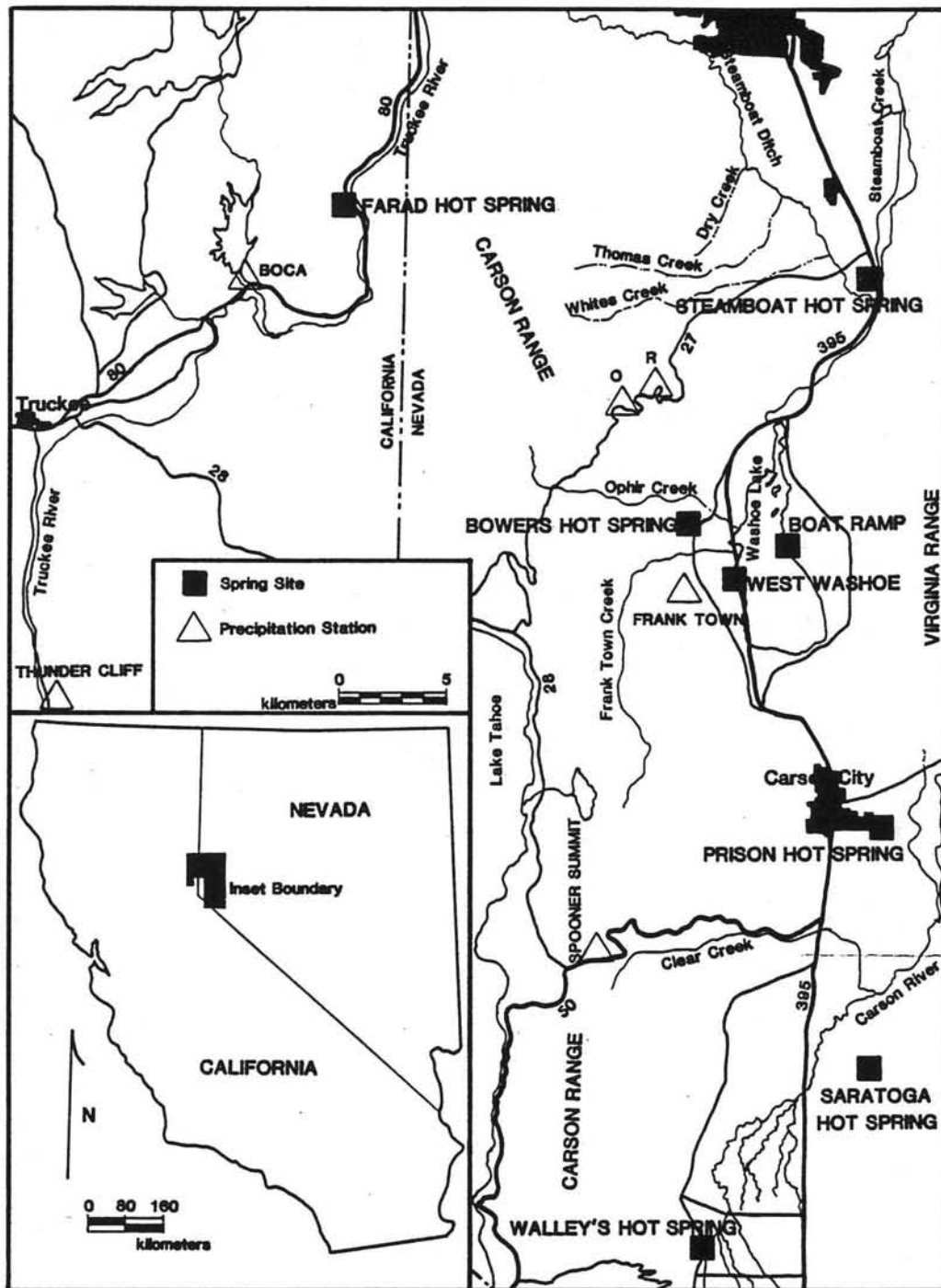


Figure 1. Location Map

from 2,124 to 3,048 m and has a very severe relief, with slopes of 35 degrees. Near the southern portion of the study area the Genoa Fault scarp is quite apparent, suggesting the relative youthfulness of this eastern escarpment.

The Virginia Range and the Pine Nut Mountains make up the mountains on the eastern side of the study area. These mountains vary from 1,828 to 2,743 m high and have a relief similar to the Sierras.

A series of valleys lie between these mountain complexes, paralleling the north-south trending mountains. The valleys are, from north to south, the Truckee Meadows, Washoe Valley, Eagle Valley, and Carson Valley. The valleys are filled with thick terrestrial sedimentary sequences and have elevations from 1,311 to 1,433 m (USGS, map, 1971).

Geology

The study area is located at the boundary between the Basin and Range Province and the Sierra Nevada Province. The Basin and Range Province covers most of Nevada, and is characterized by a series of north-trending mountain ranges separated by alluvial valleys; generally these sub-parallel valleys are accounted for by intense extensional block-faulting (Stewart, 1980). Generally, the lithology in the southern and eastern portion of Nevada is predominantly carbonaceous and sedimentary,

while the northwest portion of Nevada is largely metamorphic and volcanic.

The Sierra Nevada physiographic province extends for approximately 640 km along the California - Nevada border. This province is composed of predominantly igneous and metamorphic rocks; granitic rocks from the Sierra Nevada batholith constitute about 60% of the exposed rocks (Norris, et al., 1976). The Nevadan Orogeny (Mid-Jurassic) produced deformation and uplift of the subjacent rocks (volcanics and metasediments) and formed the Nevadan Mountains - site of the modern Sierra Nevada (Norris, et al., 1976).

Granitic intrusives associated with the Sierran batholith extend into the Basin and Range Province, producing contact and regional metamorphism. Likewise, block-faulting extends into the Sierra Nevada. The study area is entirely within this transition zone and is geologically complex; therefore, local geologic descriptions will be covered in the site-specific sections.

Climate and Vegetation

The temperatures in the study area are similar to those throughout the Northern Basin and Range, with temperatures ranging from -30 to 10°C in the winter and 12 to 38°C in the summer (National Weather Service).

Precipitation predominantly falls in the form of snow

in the Winter and as rain in the Summer. The snow pack in the higher elevations can be up to 4,000 mm, while the valleys may have 0-100 mm. The average precipitation for the area is about 690-760 mm in the Sierra Nevada, 250-300 mm in the Virginia Range and Pine Nut Mountains, and 170-250 mm in the valleys.

The heavier precipitation in the mountains sustains heavy conifer forests, consisting of pines, firs, and cedars. The rain shadow effect caused by the Sierra Nevada produces extreme vegetational changes from the Sierran crest to the valley floors. Many of the valleys have been developed for housing and agriculture, but were previously covered by sage and grasses.

Precipitation data were collected from six monitoring stations in the Sierra Nevada (Klieforth, et al., 1984); table 1 lists the accumulated precipitation over weeks prior to the data listed. The precipitation stations covered the entire study area, from Boca Dam in the North to Spooner Summit in the South (see figure 1).

The temporal uniformity of precipitation events was estimated with crosscorrelation statistics. Correlation coefficients ranged from .91 to .99; the zero lag correlation coefficients are listed in table 2. Based on this analysis, it was assumed that precipitation event frequency was relatively uniform throughout the study area; however, the amount of precipitation that accumulated at each station was highly variable. Mass precipitation variability is caused by several factors: 1)

station elevation, 2) orographic effects, and 3) storm track orientation. Figure 2 shows the mass precipitation between four pairs of precipitation stations, note that the Thunder Cliff station accumulated about twice as much precipitation as any other station.

Table 1 (Accumulated Precipitation
Between Sample Dates (mm))

Station Date	Precipitation Sites					
	Boca	Frank Town	O	R	Spoooner Summit	Thunder Cliff
Elev (m)	1700	1600	1950	1740	2210	1890
8/31/83	-	-	-	-	-	-
9/13/83	3.6	4.8	7.6	1.3	0.0	8.1
9/27/83	45.0	6.4	9.9	5.1	12.7	24.3
10/11/83	31.8	20.6	26.9	12.2	35.1	23.9
10/25/83	10.2	6.6	3.8	1.3	8.6	10.4
11/ 8/83	46.0	21.8	29.0	24.4	30.5	91.2
11/22/84	191.8	210.8	209.3	176.5	232.9	365.8
12/ 6/83	79.5	63.5	109.2	83.8	101.1	125.5
12/20/83	50.3	48.8	60.5	48.8	37.8	101.3
1/ 3/84	79.0	82.8	29.7	35.3	86.9	185.2
1/10/84	0.0	1.8	0.0	0.0	0.0	2.3
1/24/84	8.1	11.7	20.3	18.0	16.0	19.1
2/ 7/83	0.0	0.0	0.3	0.0	0.0	0.0
2/21/84	54.6	63.8	51.6	44.7	82.7	137.7
3/ 6/84	2.5	0.3	14.7	10.9	9.7	6.1
3/20/84	38.6	34.5	34.3	36.1	84.6	73.2
4/ 3/84	0.8	0.0	0.0	0.0	0.0	9.1
4/18/84	26.4	27.7	19.6	25.4	26.9	58.4
5/ 1/84	8.6	3.8	6.4	2.3	3.6	24.4
5/16/84	12.2	9.4	0.0	0.0	1.5	9.1
5/30/84	0.0	0.0	8.4	5.8	0.0	0.0
6/13/84	0.0	7.9	4.1	1.8	16.3	28.4
6/20/84	3.8	12.7	10.4	8.4	0.0	10.7
7/11/84	0.0	0.0	0.0	0.0	1.0	0.0
7/26/84	19.6	4.3	1.8	0.3	6.9	15.2
8/ 9/84	0.0	0.0	11.9	4.8	0.0	1.3
8/23/84	3.8	1.8	0.5	0.0	5.3	0.3
Mean	27.4	24.9	25.7	21.1	30.7	51.3
Stand Dev	41.7	44.5	44.7	37.8	51.6	81.3
Maximum	191.8	210.8	209.3	176.5	232.9	365.8
Total	716.0	645.7	669.8	541.1	799.8	3871.5

* Precipitation amount = total from the previous data to the present date.
O = site on Route 27 at UNR test site.
R = site on Route 27 at Evergreen Hill Road.

Table 2 (Precipitation Crosscorrelation
Coefficient Matrix at Zero Lag)

	Frank Town	Thunder Cliff	Spooner Summit	O	R	Boca
Boca	.97	.97	.96	.93	.95	1
R	.96	.94	.96	.99	1	
O	.94	.91	.94	1		
Spooner Summit	.97	.96	1			
Thunder Cliff	.98	1				
Frank Town	1					

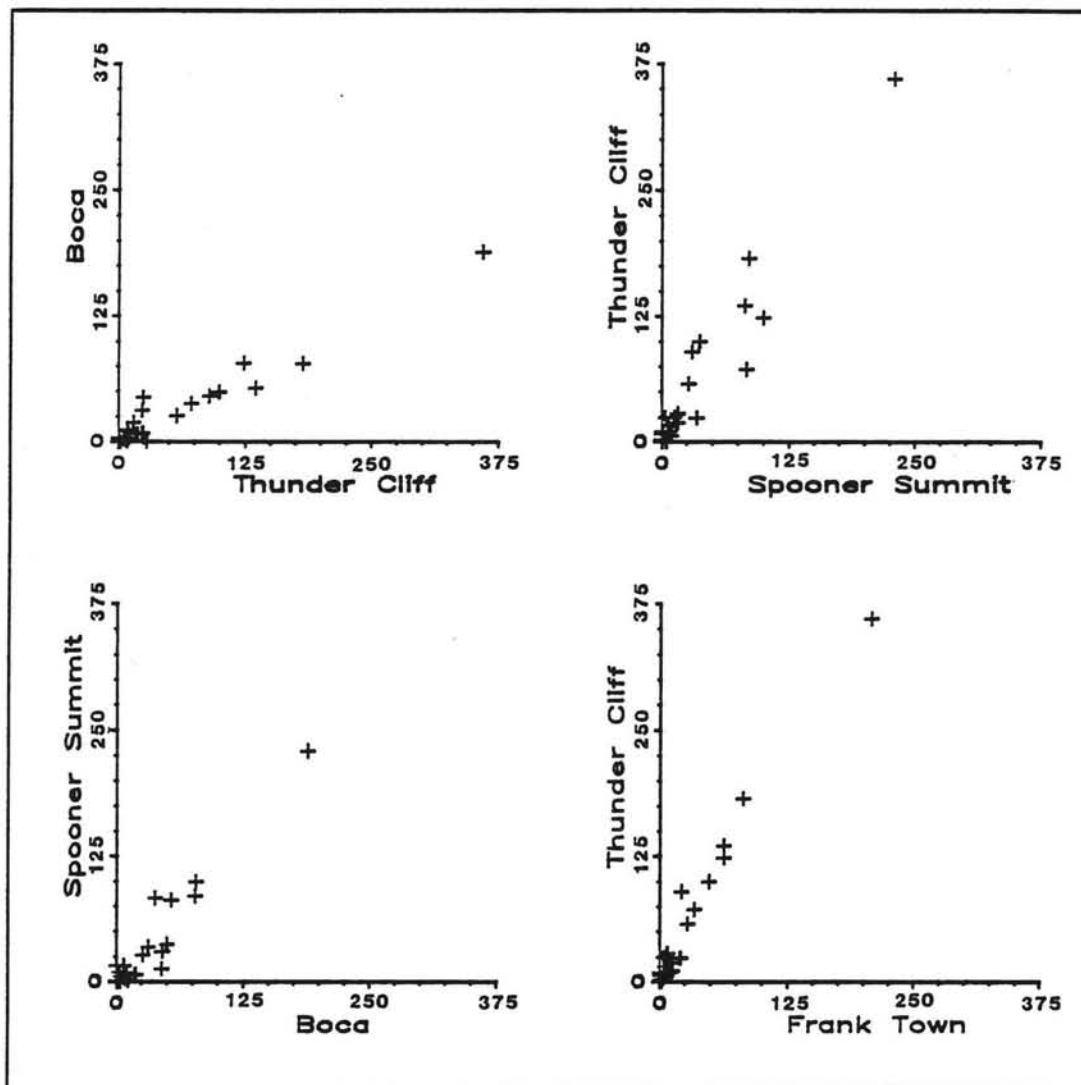


Figure 2. Precipitation Scatter Diagrams
(Accumulated precipitation over 2 weeks (mm))

Farad Hot Spring

Introduction

Precise Location

Farad Hot Spring is in Sierra County, California, about half way between Reno, Nevada and Truckee, California. Approximately ten warm springs issue from the roadcut on the southwest side of Interstate 80, near the Farad Power Plant.

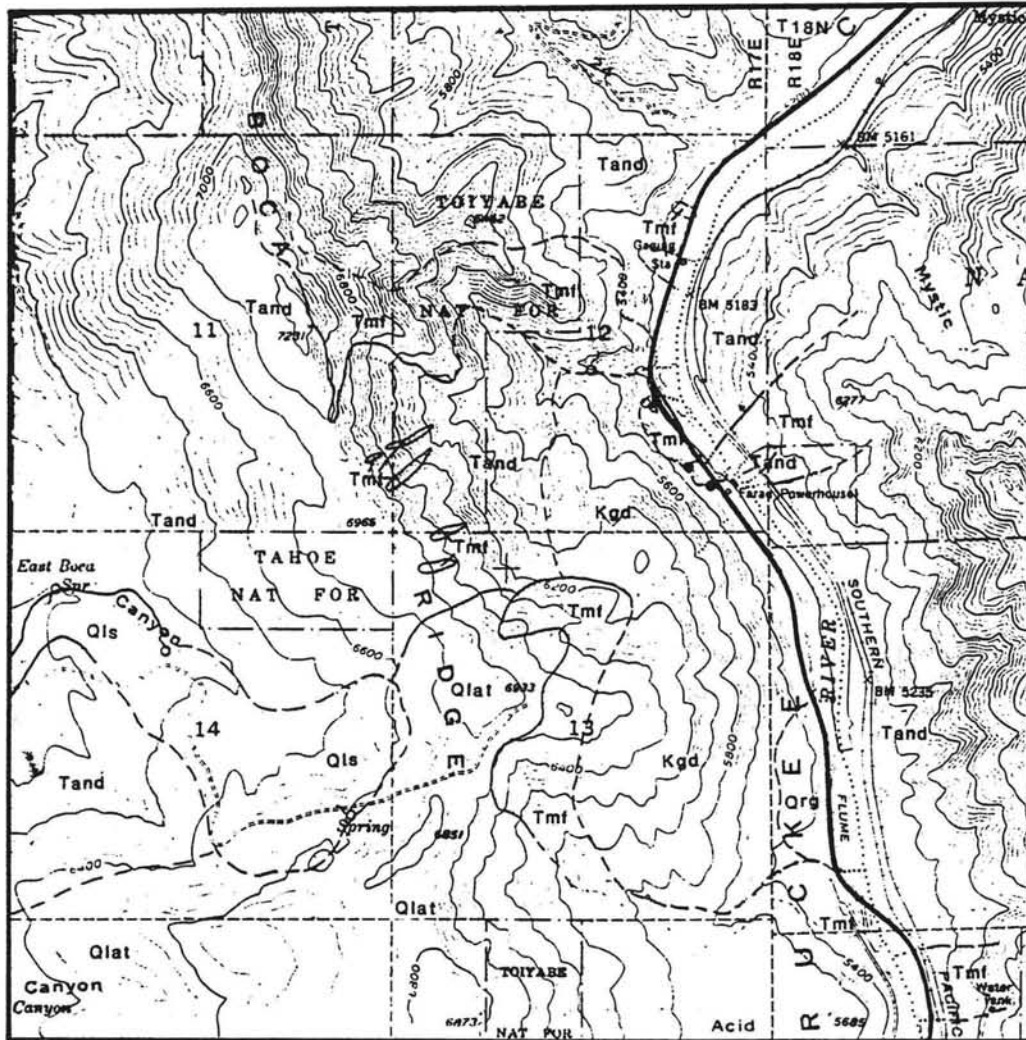
The spring of highest flow was monitored and is located in the SW1/4, SE1/4, SE1/4 of Sec12, T18N, R17E (figure 3). This spring is approximately 0.3 km south of the Farad overpass and can be identified by a 0.3 m section of four inch ABS pipe, cemented in place to collect and divert water.

Climate and Vegetation

Farad Hot Spring is at an elevation of 1,609 m. Temperatures range from a low of -20°C in the winter to a high of $+35^{\circ}\text{C}$ in the summer.

Precipitation in the area generally falls as snow in the winter and as rain in the summer. The winter snow pack varies from a trace to 500 mm at the top of Boca Ridge.

The precipitation station at Boca Reservoir



Geologic Map Farad Hot Spring Area

(geology by B.F. Lyles, 1984)

Qrg - River Gravel

Qls - Landslide

Qlat - Latite

Tmf - Mudflow (Lahar)

Tand - Andesite

Kgd - Hornblende-Biotite Granodiorite

☉ Hot Spring

○ Cold Spring

----- Contact, dashed where approximated,
dotted where concealed

--- Fault, arrow shows dip, dashed where
approximated.

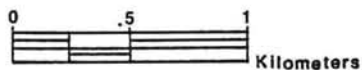


Figure 3. Farad Hot Spring
Geologic Map

(approximately 7 km south of Farad Hot Spring) measured 1,115 mm of precipitation during the study period. Although this precipitation station is at 1,699 m elevation, it is assumed that the precipitation event frequency was relatively uniform from Boca to Farad. Therefore, the Boca precipitation information can be used for time-series relationships at Farad Hot Spring.

Foresteing operations have removed the conifers from the southwest side of Boca Ridge, and Manzanita, Buckbrush, and sage are now predominant in this area. The northeast side of Boca Ridge has many conifers (pines and cedars) as well as the ground cover previously mentioned.

Previous Work

The geology has been described by Birkland (1962,1968) and Lovejoy (1972). Most of this was done on a regional scale; therefore, it was necessary to remap the geology within the study area. Limited data were available on the aqueous geochemistry of the hot spring (DRI, unpublished data).

Geology

Lithologic Interpretation

The Pleistocene geologic history of the area has been covered in detail by Birkland (1962) and Lovejoy (1972). See appendix A for descriptions of geologic units.

The basement rock in the area is hornblende biotite granodiorite (Cretaceous age). The exposures of this unit are restricted to the area near the hot springs (figure 3). These rocks are generally quite competent, forming steep slopes.

The granitic rocks were covered by andesitic rocks during the Miocene. This unit was mapped as a uniform rock type; however, the rocks range from andesite to dacite. Outcrops near the top of Boca Ridge are highly fractured and cooling joints are bent, conforming to the topography of the ridge. The granitic window has been exposed by erosion.

During the Tertiary, mudflows (lahars) covered much of the terrain. This unit is differentially resistant to weathering, producing lahar islands (about 2-3 m thick) resting on the andesitic unit. Breccia fragments are readily obvious from a distance. During the same period a latitic unit was extruded and crops out in the southern portion of the study area.

In more recent time, landslide material and river gravels were deposited. The landslide material is on the

west side of Boca Ridge and was derived primarily from local volcanic and granitic rocks. The river gravels were deposited along the Truckee River during high flow. According to Birkland (1968), flood water velocities of 30 feet per second were probable during the Pleistocene.

Structure

The regional structural geology is very complex; Lake Tahoe Basin, Truckee Basin, and Sierra Valley were once part of a continuous graben structure, which was later separated into basins by andesitic volcanoes (Birkland, 1962). The Truckee River was believed to have originally connected Lake Tahoe to the Feather River, through Sardine Pass; incised streams from Truckee Meadows migrated westward, capturing the northward flow (Lovejoy, 1972).

These eastward flowing streams were undoubtedly partially controlled by fault structures; however, only one small fault was located in the study area. This fault trends N40-50E and dips 60NW, closely paralleling the portion of the Truckee River immediately downstream.

Hydrology

Several cold springs occur on the landslide contact, west of Boca Ridge. The silt-rich material apparently acts as a dam, due to the decreased permeability from the fractured volcanics to the landslide material. These

springs all have approximately the same conductivity (about 100 μ mhos/cm), suggesting similar origins and flow paths.

All of the other springs in the area are located along the granitic - mudflow contacts. Two cold springs occur at the northern portion of the granitic unit. Two hot spring zones also occur in this area, but are separated from the cold springs by a small mudflow outcrop. The cold springs flow approximately 0.05 to 0.5 lps and have a conductivity of about 200 μ mhos/cm, while the hot springs flow approximately 0.05 to 1.8 lps and have a conductivity of about 1,600 to 1,800 μ mhos/cm.

The northern cold springs are apparently controlled by the same mechanisms as the cold springs east of Boca Ridge, but the hot springs issue from joints and fractures in the granitic rocks. It is unclear if there is any significance between the proximity of the hot springs to the mudflow-granitic contact.

Boca Ridge is the most probable recharge area for the hot springs. The canyons above Farad Hot Spring collect several feet of snow each year; however, there is very little surface runoff due to the high permeability of the fractured rocks. It is impossible to tell how deep this water circulates, but it is probable that recharge water may travel as deep as one kilometer before rising to the surface (Ellis and Mahon, 1977).

Geochemistry

Major dissolved Constituents

A water sample was collected at Farad Hot Spring by the Desert Research Institute (DRI) on October 23, 1970, and was analyzed by the Water Analysis Laboratory DRI. The program "WATEQ" was used to calculate cation to anion balance, mineral saturations, $p\text{CO}_2$, etc. (table 3).

The water at Farad Hot Spring is a Na-Cl type water, according to White's classification scheme (1960). All of the sodium minerals calculated are below saturation. Generally, high sodium concentrations can be accounted for two ways; 1) by dissolution of sodium salts, or 2) by dissolution of plagioclase feldspar (Drever, 1982). Likewise, the chloride concentrations can generally be accounted for by dissolution of chloride minerals.

The only minerals near saturation are the silicate minerals chalcedony, cristobalite, quartz, and tremolite. The andesitic and granitic rocks in the area contain more than 50 percent SiO_2 , on an average (Hyndman, 1972); therefore, the observed concentrations of silica can be accounted for primarily by dissolution of silicate minerals (Bricker and Garrels, 1967).

Geothermometry

The results from the water analysis of October 23, 1970 were used in several chemical geothermometers. The

Table 3 (Farad Hot Spring WATEQ output)

*** total concentrations of input species ***				
species	total molality	total mg/liter	epm	epm fraction
-----	-----	-----	----	-----
Ca	0.397058e-03	15.9	0.79	0.060
Mg	0.205842e-04	0.50	0.04	0.003
Na	0.119724e-01	275.0	12.0	0.909
K	0.358355e-03	14.0	0.36	0.027
Cl	0.104456e-01	370.0	10.4	0.798
SO4	0.502206e-03	48.2	1.00	0.077
HCO3	0.163705e-02	99.8	1.64	0.125
SiO2 tot	0.101613e-02	61.0		

tds = 884.40				
***description of solution ***				
	analytical	ph		
epmcat	13.166	7.99	pco2 = 0.102495e-02	
epman	13.087		log pco2 = -2.9893	
cation/anion	1.01	temperature	EC = 1518.0	
		31.00 deg c	ionic strength	
			0.138384e-01	
mineral saturations				
	iap/kt	log iap/kt	phase	
	0.3389e-02	-2.46991	ANHYDRITE	
	0.4232e+00	-0.37350	ARAGONITE	
	0.6916e-08	-8.16012	ARTINITE	
	0.4549e-05	-5.34208	BRUCITE	
	0.5568e+00	-0.25426	CALCITE	
	0.2867e+01	0.45747	CHALCEDONY	
		-40.50313	CHRYSOTILE	
	0.3226e+01	0.50867	CRISTOBALITE	
		-1.98576	DIOPSIDE	
	0.2110e-01	-1.67576	DOLOMITE	
	0.3611e-08	-8.44240	FORSTERITE	
	0.2805e-02	-2.55212	GYPSUM	
	0.2451e-05	-5.61059	HALITE	
	0.1172e-01	-1.93123	MAGNESIITE	
	0.9451e-08	-8.02450	NATRON	
	0.8265e+01	0.91726	QUARTZ	
	0.9971e-01	-1.00126	SEPIOLITE(C)	
	0.9016e+00	-0.04500	SiO2(A,L)	
		-1.31478	TALC	
	0.4912e-07	-7.30874	THENARDITE	
		0.95204	TREMOLITE	
	0.1301e-12	-12.88577	TRONA	
		-4.85227	SEPIOLITE(A)	

temperatures calculated ranged from 60.8°C to 165.8°C (table 4). These temperatures are in question due to the possibility of significant dilution or mixing of hot and cold waters near the ground surface (within 20 meters).

The SiO₂ geothermometers are less susceptible to reactions or reequilibrations due to dilution than the Na-K and Na-K-Ca geothermometers (Fournier, et al., OFR; Benjamin, 1983); therefore, the reservoir temperature is probably about 110 ± 25°C.

Time Series Analysis Results

Data were collected for approximately one year at Farad Hot Spring, from September 13, 1983 to August 23, 1984. During the later portion of the study, data were collected weekly; however, during this period every other data point was ignored and the mean sample interval was 13.52 days (Standard Deviation = 2.00 days) (table 5).

Crosscorrelation coefficient results, at zero lag, are presented in table 6. Only four of the values are greater than 50 percent, of which only two are greater than 70 percent. There also exist several significant correlations at varying lag positions; however, only the lagged correlation coefficients of precipitation exceed 60 percent.

There is an inverse relationship between flow and temperature, and flow and chloride ion at the zero lag position (figure 4 and 5 respectively). This suggests

Table 4 (Farad Hot Spring Chemical
Geothermoter Results)

Thermometer	SiO ₂	SiO ₂	SiO ₂	Na-K	Na-K-Ca	Na-K-Ca
Equation	1	2	4	6	8	10
Calculated Temperature (C)	60.78	82.73	111.32	165.22	156.02	165.78

Table 6 (Farad Hot Spring Correlation
Coefficient Matrix)

	Ca	Cl	EC	HCO ₃	pH	pCO ₂	FLOW	TEMP
TEMP	.40	.40	0	.38	.33	-.56	-.72	1
FLOW	-.49	-.78	0	-.50	-.36	.56	1	
pCO ₂	0	0	0	-.37	-1.0	1		
pH	0	0	0	.44	1			
HCO ₃	0	0	0	1				
EC	.37	.37	1					
Cl	.61	1						
Ca	1							

Table 7 (Farad Hot Spring Correlation
Coefficient Matrix at Six Week Lag)

	Ca	Cl	EC	HCO ₃	pH	FLOW	TEMP	Precip
Precip	-.40	-.63	0	-.38	0	.79	-.59	1

Table 5 (Farad Hot Spring temporal data)

Date	Time	T(C)	Flow l/s	EC µmhos	pH field	pH lab	HCO ₃ mg/l	Cl mg/l	Ca mg/l	log pCO ₂	σ ¹⁰⁰ %	σD %
9/13/83	8:10	36.0	-	1560	-	7.61	97.6	356.	28.98	-2.56	-	-108
9/27/83	8:32	36.0	1.62	1645	-	7.58	97.6	367.	30.88	-2.53	-	-
10/11/83	8:05	35.5	1.59	1800	-	7.62	104.9	371.	30.88	-2.54	-	-
10/25/83	8:05	36.0	1.58	1642	7.65	7.67	100.0	366.	31.35	-2.61	-	-
11/ 8/83	7:42	35.5	1.59	1771	7.69	7.74	98.9	377.	31.59	-2.69	-	-115
11/22/83	8:02	35.0	1.57	1712	7.30	7.67	101.3	378.	31.12	-2.61	-	-
12/ 6/83	7:47	35.0	1.67	1676	7.65	7.67	98.8	371.	30.40	-2.62	-	-
12/20/83	8:50	35.0	1.80	1873	-	7.70	100.0	362.	29.46	-2.65	-	-
1/ 3/84	8:05	34.5	1.99	1672	-	7.62	100.0	337.	27.56	-2.57	-13.8	-106
1/10/84	7:32	34.5	1.90	1599	7.31	7.36	98.8	349.	28.27	-2.31	-	-
1/24/84	7:12	35.0	1.67	1727	(7.80)	7.35	100.0	362.	28.98	-2.30	-	-
2/ 7/84	7:18	35.0	1.60	1608	7.70	7.63	101.3	373.	29.22	-2.57	-	-
2/21/84	6:74	35.0	1.64	1673	7.51	7.51	101.3	365.	29.46	-2.45	-	-
‡ 2/28/84	6:36	35.0	1.62	1673	7.73	7.47	102.5	-	-	-	-	-
3/ 6/84	6:39	35.0	1.62	1684	7.60	7.49	100.0	363.	29.22	-2.43	-	-107
‡ 3/13/84	6:40	35.0	1.61	1675	7.71	7.69	100.0	-	-	-	-	-
3/20/84	6:37	-	1.66	1668	7.82	7.62	100.0	358.	29.22	-2.56	-	-
‡ 3/27/84	6:35	35.0	1.76	1583	7.56	7.66	100.0	-	-	-	-	-
4/ 3/84	6:45	35.0	1.69	1638	7.65	7.63	100.0	362.	28.98	-2.57	-	-
‡ 4/10/84	6:38	35.0	1.64	1644	7.66	7.66	98.8	-	-	-	-	-
4/18/84	7:47	-	1.62	1608	-	7.56	101.3	362.	28.74	-2.50	-	-
‡ 4/24/84	6:30	36.0	1.63	1644	7.60	7.59	101.3	-	-	-	-	-
5/ 1/84	6:45	36.0	1.61	1617	-	7.65	103.7	360.	28.51	-2.57	-	-
‡ 5/ 8/84	6:25	35.5	1.61	1673	7.66	7.50	100.0	-	-	-	-	-
5/16/84	7:40	36.0	1.55	1617	7.59	7.86	106.1	362.	28.74	-2.77	-	-102
‡ 5/23/84	9:24	36.0	1.56	1617	7.48	7.80	108.6	-	-	-	-	-
5/30/84	7:34	36.0	1.54	1673	7.58	7.64	101.3	362.	29.22	-2.57	-	-
‡ 6/ 6/84	7:59	35.5	1.53	1673	7.64	7.77	97.6	-	-	-	-	-
6/13/84	8:00	35.5	1.52	1693	7.65	8.01	104.9	365.	29.46	-2.93	-	-
6/20/84	7:52	35.5	1.52	1653	7.60	7.73	102.5	365.	29.46	-2.66	-	-
‡ 7/ 5/84	9:45	36.0	1.52	1653	7.66	7.54	102.5	-	-	-	-	-
7/11/84	8:08	36.0	1.51	1727	7.71	7.61	102.5	373.	37.98	-2.54	-13.7	-106
‡ 7/17/84	6:54	36.0	1.50	1680	7.64	7.69	104.9	-	-	-	-	-
7/26/84	8:03	36.0	1.50	1680	7.57	7.61	103.7	376.	30.88	-2.53	-	-
‡ 8/ 2/84	7:47	36.0	1.51	1754	7.71	7.64	102.5	-	-	-	-	-
8/ 9/84	7:56	36.0	1.52	1705	7.70	7.58	104.9	378.	30.88	-2.50	-	-
‡ 8/16/84	7:16	35.5	1.49	1747	7.50	7.62	102.5	-	-	-	-	-
8/23/84	8:00	35.5	1.47	1747	7.76	7.62	102.5	380.	31.59	-2.55	-	-
Mean		35.4	1.62	1679		7.63	102.4	365.	30.04	-2.57		
Stand Dev		0.5	0.12	67.5		0.13	2.0	9.6	1.96	0.13		
Coef Variance		1.42	7.34	4.0		1.72	2.0	2.6	6.54	5.06		

that increases in flow are primarily caused by local mixing of recharge waters. The recharge water is presumably cooler and fresher (lower in chloride concentration) than the thermal reservoir water. The coefficients of variation for flow and temperature (7.34 % and 1.42 % respectively) suggest that the correlation between them is real and not caused by analytical or sampling errors. However, the coefficient of variation for the chloride ions (2.61 %) suggests that chloride variation can be caused by analytical and sampling errors.

There is a weak direct relationship between calcium and chloride ions and there is a weak inverse relationship between flow and bicarbonate ions. Although the coefficient of variation for calcium ion (6.54 %) suggests a significant real variation, the variation in the chloride ions is not significant; therefore, the crosscorrelation is not valid. The coefficient of variation of the bicarbonate ions (1.95 %) shows that the variation may be due to errors; the correlation is not valid.

There is a good direct relationship between precipitation and flow at a six week lag (table 7). About six weeks after a precipitation event an increase in flow is noted (figure 6). Several other correlations exist between precipitation and the independent variables at a four to six week lag, ranging from -0.38 to $+0.79$.

Lead-lag multiple step-wise regression was applied to the temporal data to get a predictive linear equation.

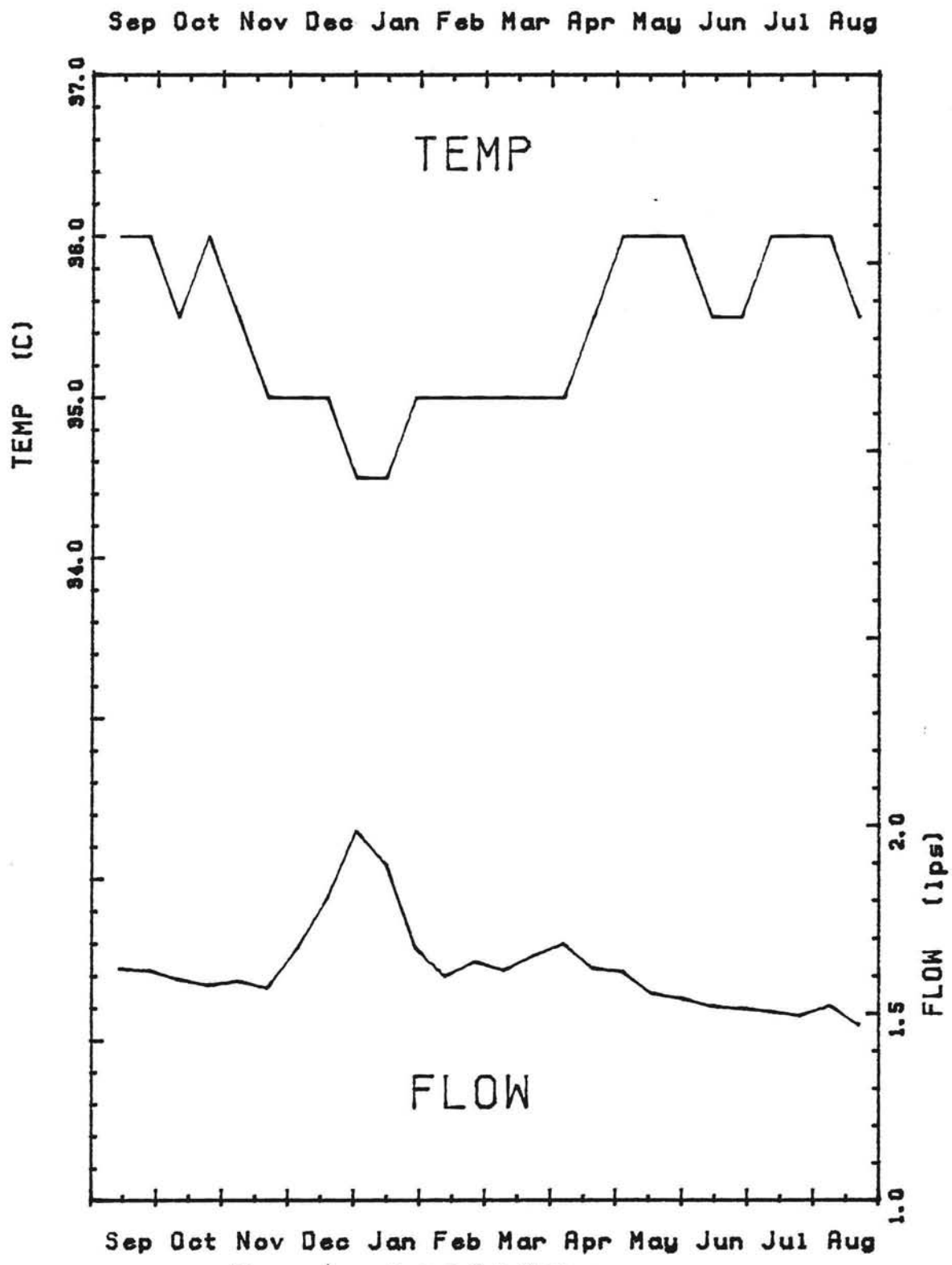


Figure 4. Farad Hot Spring
Temperature and Flow vs. Time

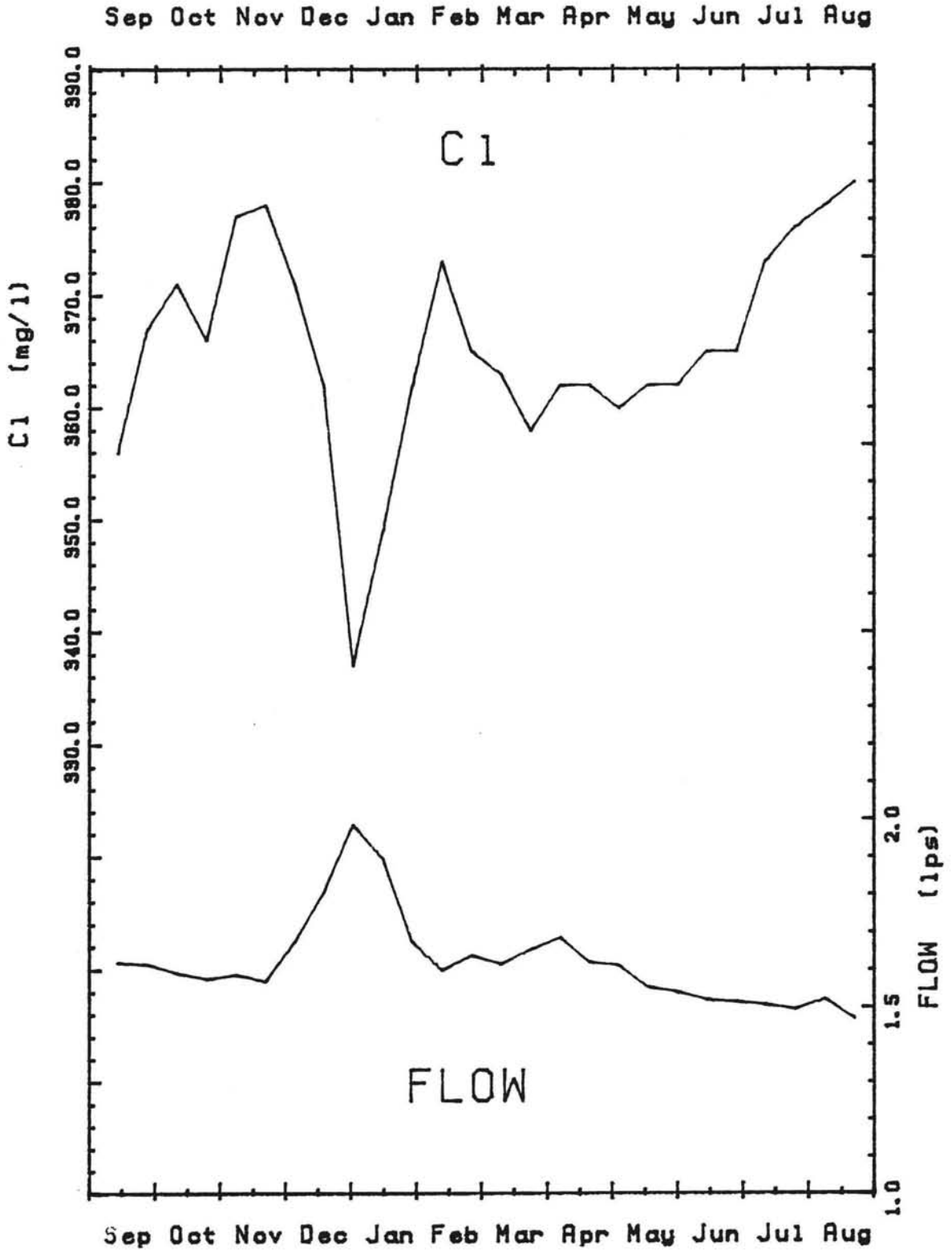


Figure 5. Farad Hot Spring
 . Chloride ion and Flow vs. Time

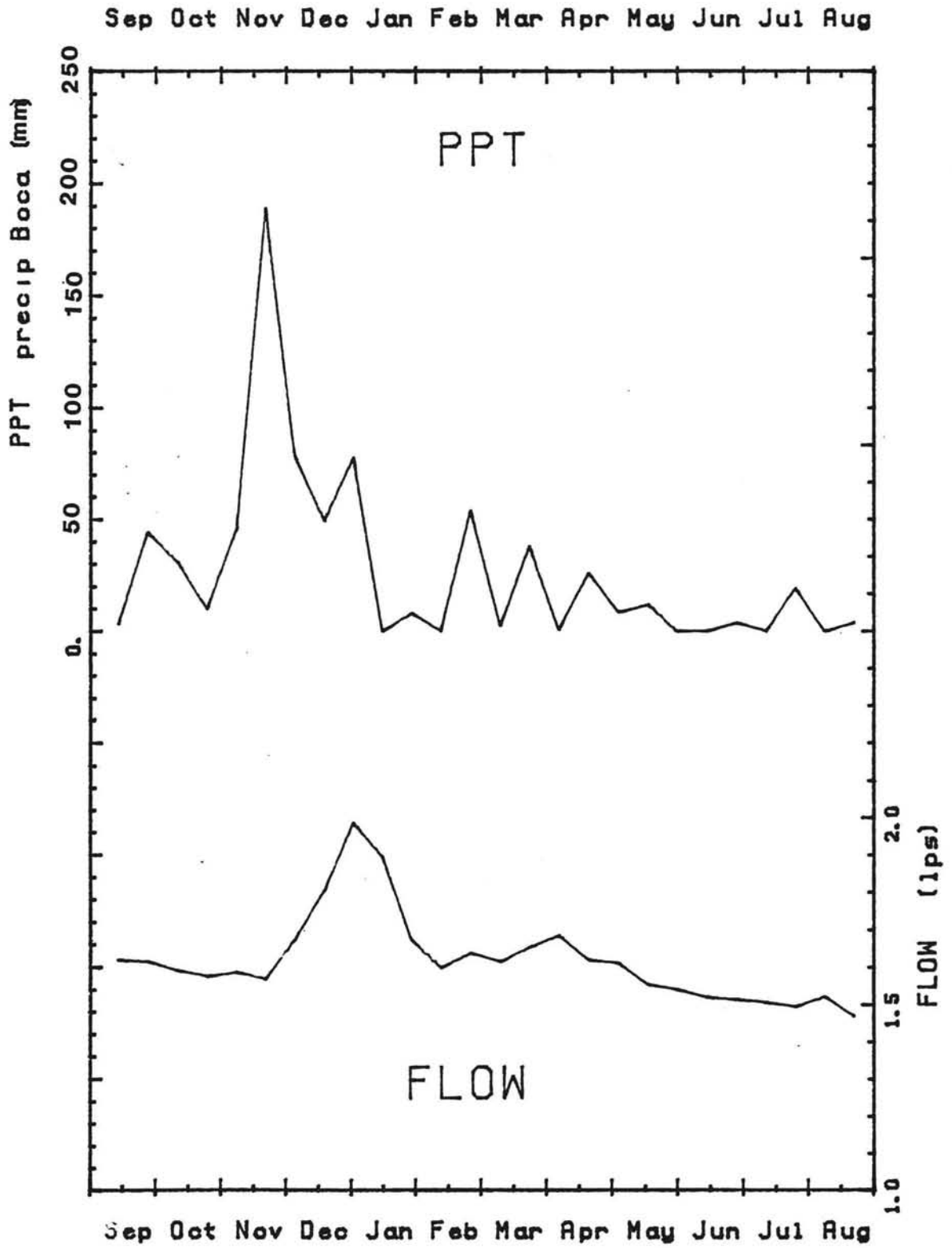


Figure 6. Farad Hot Spring
Precipitation and Flow vs. Time

When solving for flow, the best fit was found with three variables entered (table 8) (refer to page 10 for statistical technique).

The analysis of variance produced an F-value of 35.90, which surpassed the critical $F(3,10,.01)$ equal to 6.55. Therefore reject the null hypothesis of "lack of fit" and conclude that there is a good fit between the regressed points and the real points.

The analysis of regression coefficient validity produced t-values less than -3.14 and greater than 2.53, which surpassed the critical $t(13,.025)$ equal to ± 2.16 ; therefore, reject the null hypothesis that β is equal to 0 (regression coefficient = 0) and assume each coefficient is valid.

The predictive equation is as follows:

$$\text{FLOW} = 6.79 - 5.90 \times 10^{-3} * \text{Cl} - 8.61 \times 10^{-2} * \text{TEMP} + 2.34 \times 10^{-2} * \text{PPT}. \quad (1)$$

Summary

Several cold springs occur in the area along with two hot spring zones. The two hot spring zones issue from fractured granitic rocks, while the cold springs occur at contacts between high- and low-permeability geologic formations. Recharge to the thermal reservoir is primarily from rainfall along Boca Ridge and generally takes about six weeks to infiltrate to the reservoir.

The water at Farad Hot Spring is a Na-Cl type water,

Table 8 (Farad Hot Spring Lead-lag
Multiple Regression output)

Dependent Variable = Flow			
Number of Points = 23			
Step 1			
Variable Entered = C1			
Sum of Squares Reduced in this Step ..			.227
Proportion Reduced in this Step640
Multiple Corr. Coef. Adj. for D.F.800
F-value for Analysis of Variance			37.303
Variable	Regression Coefficient	Std. Error of Reg. Coef.	Computed t-value
C1	-.01024	.00168	-6.108
Intercept	5.36540		
Step 2			
Variable Entered = Temp			
Sum of Squares Reduced in this Step ..			.057
Proportion Reduced in this Step160
Multiple Corr. Coef. Adj. for D.F.894
F-value for Analysis of Variance			39.875
Variable	Regression Coefficient	Std. Error of Reg. Coef.	Computed t-value
C1	-.00791	.00141	-5.612
Temp	-.11347	.02843	-3.991
Intercept	8.52101		
Step 3			
Variable Entered = Precip			
Sum of Squares Reduced in this Step ..			.018
Proportion Reduced in this Step051
Multiple Corr. Coef. Adj. for D.F.922
F-value for Analysis of Variance			35.900
Variable	Regression Coefficient	Std. Error of Reg. Coef.	Computed t-value
C1	-.00590	.00148	-3.983
Temp	-.08613	.02744	-3.138
precip	.02341	.00925	2.531
Intercept	6.79315		

has an average temperature of 35.4°C, and has an average conductivity of 1,679 μ mhos/cm. This water is near saturation with the silicate minerals chalcedony, cristobalite, quartz, and tremolite. Chalcedony and quartz chemical geothermometers yield a reservoir temperature of $110 \pm 25^\circ\text{C}$.

Temporal variations show that infiltration of surface water (cold, low chloride) causes increased spring discharge. A linear equation was developed from the temporal data, solving for flow from measured independent variables.

Steamboat Hot Springs

Introduction

Early settlers and miners in the area named the hot springs 'Steamboat', because the fumarole sounds reminded them of a puffing steamboat (Garside and Schilling, 1979). Several spas were located here about the time of the Comstock Lode mining.

Many attempts have been made to utilize the resources at Steamboat since these early times. Some of the spas have used names like Reno Hot Springs, Mount Rose Hot Springs, and Radium Hot Spring (Garside and Schilling, 1979). The only spa currently operating is the Steamboat Mineral Spa. Phillips Petroleum Company drilled a 930 m deep well and is in the process of putting in a geothermally powered electric test-plant.

Precise Location

The Steamboat thermal area is in Washoe County, Nevada, about 20 km south of Reno on Highway 395. Most of the presently discharging springs, fumarols, and gysers are on the Main Terrace, on the west side of Highway 395 (south of State Route 27).

The spring monitored for this study is on the Main Terrace (number 24 of White, 1968) and is located in the

SW1/4, SW1/4, SE1/4 of Section 28, T18N, R20E (figure 7). The spring issues from a northerly trending fracture (approximately 10 m long and 0.1 m wide). This spring can be most easily found by hiking about 0.3 km at N80W from the Steamboat Post office.

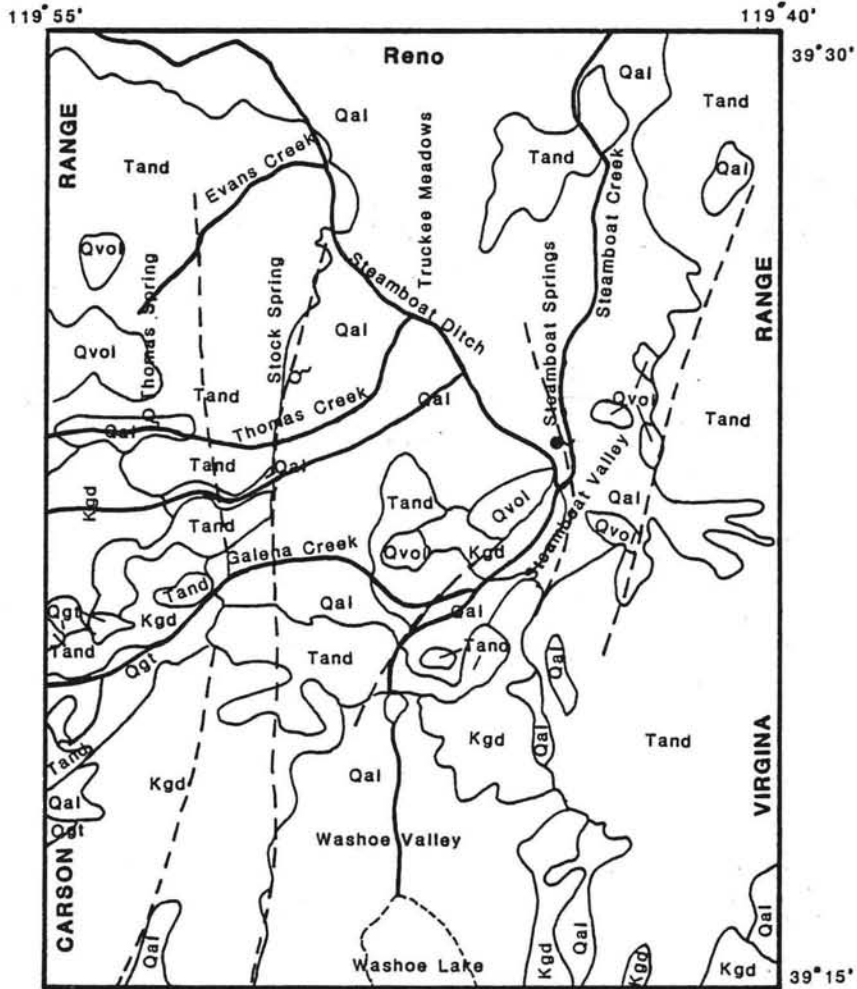
Many interesting fumaroles and gysers occur along the eastern edge of the Main Terrace. Several flowing and gysering wells also occur in the area, such as Nevada Thermal Power No. 1 on the east side of Highway 395 near the main terrace.

Climate

Steamboat is at an average elevation of about 1,448 m. Temperatures in nearby Reno range from -10 to 5°C in the winter and from 21 to 38°C in the summer.

Precipitation in the area generally falls as rain; minor accumulations of snow (about 30 mm) were observed during this study. Precipitation in the recharge area generally falls as snow in the winter and as rain in the summer, and was estimated by precipitation information collected near the maintenance station on the Mount Rose Highway (State Route 27). This station is at 1,737 m elevation and collected 547.12 mm of precipitation during the study period (Kleiforth, et al., 1984).





Although discharge data is no longer collected for Whites and Thomas Creeks, in 1982 the discharge hydrographs showed peaks during June; this suggests that



Geologic Map Steamboat Area

(Nehring, 1980)

- Qal - Lake Deposits and Stream Gravels
- Qgt - Glacial Till
- Qvol - Volcanic Rocks
- Tand - Andesite
- Kgd - Granodiorite and
Meta-Volcanic Rocks

-  Hot Spring
-  Cold Spring
-  Contact
-  Fault

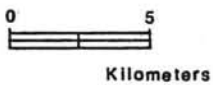


Figure 7. Steamboat Springs Area
Geologic Map

June was the period of highest snow melt and therefore is also the period of highest potential recharge to the Steamboat Thermal System. This June peak was also noticed at Galena Creek in 1982 and 1983 (Water Resources Data Nevada, 1982 and 1983).

Previous Work

Steamboat Hot Springs is one of the best known and most highly studied thermal springs in the world. References to the mineralization in the area were made as long ago as the 1870's, primarily due to Steamboats close proximity to Virginia City and the Comstock Lode. A listing of these early works has been compiled by Garside and Schilling (1979).

An extensive geologic and time-series evaluation was initiated by Thomas, White, and Sandberg in the 1940's. This work is encompassed in three papers by the U.S. Geological Survey: Thompson and White, (1964), White, et al. (1964), and White, (1968).

Several preliminary isotopic studies were conducted in the 1950's and 1960's by White (1968). A recent study of environmental isotopes was conducted by Nehring (1980).

Geothermal resource evaluations have been conducted by Bateman and Scheibach (1975), Yeamans (1983), and Flynn and Ghushn (1984).

Geology

In about 1945 the U.S. Geological Survey started a detailed study of the Steamboat Springs area. The reports by Thompson and White, (1964), and White, et al. (1964) give very detailed geologic descriptions and should be reviewed by the reader, as the geologic map and lithologic descriptions are primarily from these sources.

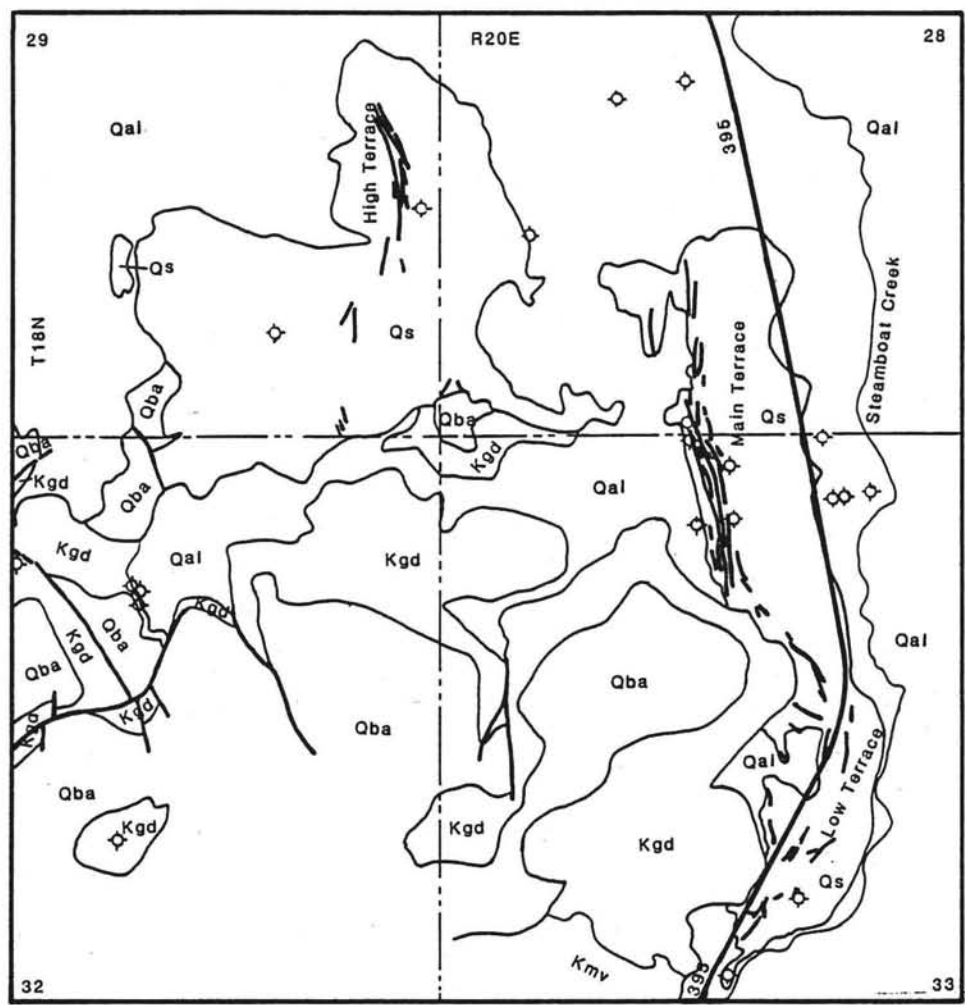
Lithology

There are five major lithologic units in the area: 1) meta-sedimentary rocks, 2) hornblende-biotite granodiorite, 3) basaltic andesite, 4) alluvium, and 5) sinter (figure 8).

The meta-sedimentary rocks cropout in the southern portion of the study area. According to Thompson and White, (1964), these rocks are Triassic hornfels with local schist and tectite; the most intense metamorphism is near the granitic contact.

The regional granitic composition ranges from granodiorite to quartz monzonite, but granitics in the study area are predominantly Cretaceous hornblende-biotite granodiorite (Thompson and White, 1964). Granitic outcrops cover much of the study area; outcrops are moderately to highly fractured, and are in varying stages of decomposition due to intense hydrothermal alteration.

The basaltic andesite is Pliocene to Pleistocene according to Thompson and White, (1964), and White, et



Geologic Map Steamboat Hot Springs Area (White, et al., 1964)

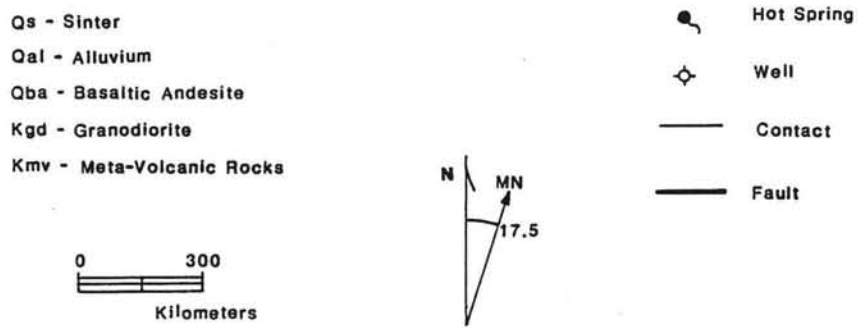


Figure 8. Steamboat Hot Springs. Geologic Map

al., (1964). Flows in the western portion of the study area are vitric basalts, with small hornblende and olivine crystals noticeable on fresh surfaces. These flows cover most of the granitic rocks in the southern 1/4 of the study area (figure 8). Hydrothermal alteration is not as noticeable in these rocks as in the granitics.

The alluvium is composed of coarse sand and gravel at the bottom of the unit and boulder gravel near the surface (White, et al., 1964). No distinction was made between pre-Lake Lahontan sediments and post-Lake Lahontan sediments on the geologic map (figure 8); however, White, et al., (1964) break the Quaternary rocks into 14 different units.

Sinter has been deposited in two distinct areas at Steamboat: 1) High Terrace, and 2) Main Terrace and Low Terrace. According to White (1968), sinter deposition in the High Terrace started at least 3 million years ago (dated by a basaltic flow covering the sinter). The High Terrace is predominantly composed of opal, while the younger (main and lower) terraces are composed of chalcedonic deposits. The younger sinter has been deposited somewhat uniformly for the past 0.1 million years (White, 1983).

Structure

The meta-sedimentary rocks in the area were folded by pre-Cenozoic tectonism; presently the rocks trend N30-50E

and dip 45° to 90° (Thompson and White, 1964). Cenozoic block faulting caused doming in the northern Carson Range, raising the range as a normal fault block (Thompson and White, 1964).

Three major sets of faults have been identified in the Steamboat Hills area: 1) a set trending northeast, paralleling the axis of the hills, 2) a set trending northwest, at nearly right angles to the first, and 3) a set trending north, predominantly in the hot springs area (Thompson and White, 1964). Thermal studies by Phillips Petroleum show a distinct thermal boundary south of Steamboat Hill, trending approximately northeast and dipping steeply southeasterly (Yeaman, 1983). This boundary coincides with a northeast trending fault; this fault apparently does not allow warm water to migrate southeast toward Steamboat Valley.

The north-trending faults dip to the east and act as a conduit for the ascending hot water. Siesmic activity in the area has been relatively moderate for approximately the past 100 years (White, 1983), but minor earthquakes in the area have a direct effect on the discharge characteristics of the springs (White, 1968).

Hydrology

Steamboat Creek is the most prominent stream in the area; this stream flows northerly from Washoe Lake to the Truckee River, east of Sparks (figure 7). Average annual

flow in Steamboat Creek near the hot springs is about 10,408 hm³/year (for 22 years of record) (Water Resources Data Nevada, 1983). Galena, Whites, and Thomas Creeks are west of Steamboat in the Carson Range and flow easterly, with flows of 0.25 m³/sec, 0.33 m³/sec, and 0.24 m³/sec respectively (Water Resources Data Nevada, 1982). Flow from Galena Creek is diverted for irrigation or flows into Steamboat Creek, while the other two creeks (Thomas and Whites) recharge the alluvial aquifer west of Steamboat and eventually flow into Steamboat Ditch.

A hypothesis was posed by White (1950) that most of the thermal system recharge was from Steamboat Creek, based on local hydrologic parameters and hydrothermal conduction theories; however, recent work by Nehring (1980) showed isotopic evidence disproving this and suggesting a bulk of the recharge is derived from collection basins to the west. Nehring (1980) also showed the recharge waters are primarily derived from the watersheds between Galena Creek and Evans Creek (about 15 km²) (figure 7).

Recharge waters near the Carson Range frontal fault would have about 400 m of head above the water table at the Steamboat Main Terrace, equaling about 4.1×10^6 N/m² (600 psi) (White, 1983). White (1968) hypothesized a deep convective magma body (100 km³) as the heat source at Steamboat; this magma conducts heat through relatively silicified rock, heating meteoric water, producing a convective cell as water becomes less dense. This type of

system has been termed a mixed convection system (combination of free and forced convection) by Combarrous and Bories (1975).

Discharge at Steamboat is accounted for three ways: 1) from spring discharge, 2) from well discharge, and 3) from subsurface flow to Steamboat Creek, all totaling $3.7 \times 10^{-2} \text{ m}^3/\text{s}$ (590 GPM) (White, 1968). Temporal observations of spring and well discharge characteristics were highly variable; discharge varied from predominantly flowing, to gysering, to fumarolic activity. Fortunately, the spring monitored in this study remained flowing for the entire study period.

Geochemistry

Major Dissolved Constituents

A water sample was collected by Nehring on June 11, 1977 at spring number 23; spring 23 is 20 m due north, along the same fracture as the spring in this study (White's spring 24, 1968). The analysis results (Nehring, 1980) were entered into the computer program "WATEQ" to calculate mineral saturations, cation to anion balance, pCO_2 , etc. (table 9).

The water at Steamboat is a Na-Cl type water. The sodium is primarily derived from dissolution of plagioclase feldspar and dissolution of sodium salts; likewise, chloride is thought to come from dissolution of

Table 9 (Steamboat Hot Spring WATEQ output)

*** total concentrations of input species ***				
species	total molality	total mg/liter	epm	epm fraction
Ca	0.105053e-03	4.2	0.21	0.007
Mg	0.700999e-06	0.017	0.00	0.000
Na	0.294346e-01	675.0	29.4	0.927
K	0.210234e-02	82.0	2.10	0.066
Cl	0.253646e-01	897.0	25.3	0.740
SO4	0.147149e-02	141.0	2.93	0.086
HCO3	0.596407e-02	363.0	5.95	0.174
SiO2 tot	0.478857e-02	287.0		
F	0.116090e-03	2.2		
B tot	0.417326e-02	45.0		
Li	0.112690e-02	7.8		

tds = 2504.22				
*** description of solution ***				
epmcat	analytical 32.875	ph 7.30	pco2 = .0561221	
epman	34.388		log pco2 = -1.25	
cation/anion	0.956	temperature 95.50 deg c	ec = 3600.0	
			ionic strength 0.345559e-01	
*** mineral saturation ***				
	iap/kt	log iap/kt	phase	
	0.3100e-02	-2.50865	ANHYDRITE	
	0.1191e+00	-0.92421	ARAGONITE	
	0.7645e-05	-5.11665	BRUCITE	
	0.5334e+00	-0.27292	CALCITE	
	0.3527e+01	0.54739	CHALCEDONY	
		-35.40408	CHRYSOTILE	
	0.1558e-02	-2.80732	CLINOENSTITE	
	0.3071e+01	0.48733	CRISTOBALITE	
	0.1515e-01	-1.81949	DIOPSIDE	
	0.9614e-02	-2.01711	DOLOMITE	
		-56.60659	FLUORITE	
	0.2921e-02	-2.53445	GYPSUM	
	0.9545e-05	-5.02021	HALITE	
	0.3345e+03	2.52445	MAGADIITE	
	0.1417e-02	-2.84852	MAGNESITE	
	0.6389e+01	0.80541	QUARTZ	
	0.1532e-01	-1.81463	SEPIOLITE (C)	
	0.1167e+01	0.06692	SiO2 (A,L)	
		-3.30212	TALC	
		-1.07360	TREMOLITE	
		-2.17800	SEPIOLITE (A)	

minerals (Drever, 1983) and evaporative concentration.

The only minerals found in the water near saturation were the silicate minerals chalcedony, cristobalite, magadiite, and quartz. Silica is primarily derived from dissolution of silicate minerals along the flow path (Bricker and Garrels, 1967).

As previously mentioned, sinter, composed of opal and chalcedony, make up the major terraces at Steamboat. Gold and silver have been detected in the sinter, and dark grey silicious spring precipitates contain as much as 15 ppm Au, 150 ppm Ag, 0.01 percent Hg, and 3.9 percent Sb (Silberman, et al., 1979, and White, 1983). The dark precipitate generally forms during high flow (White, 1983) and was first observed during this study on May 16, 1984.

in wells cause problems in producing geothermal wells. Precipitates are deposited in the well bore and discharge pipes as the fluids ascend, due to CO₂ gas enrichment and decreases in pressure (White, 1968). As CO₂ gas is evolved in vapor phase, equilibria shifts, HCO₃⁻ ion decreases, and CO₃²⁻ increases ($2\text{HCO}_3^- \leftrightarrow \text{CO}_2(\text{g}) + \text{H}_2\text{O}(\text{g}) + \text{CO}_3^{2-}$). This phenomena causes the pH to increase dramatically (from 8.5 to 8.9 in wells, compared to 6.0 to 8.2 in springs) and allows suitable conditions for abundant mineral growth (White, 1968).

Geothermometry

The water analysis from Nehring (1980) was used in several chemical geothermometers, for results see table 10. Calculated reservoir temperatures ranged from 157.5 to 283.3°C. The SiO₂ geothermometers gave the lowest readings, undoubtedly due to precipitation of silicate minerals. The reservoir temperature is probably about 230±20°C, which is in agreement with Nehring's (1980) results and is very close to the highest observed temperature of 227°C (Yeaman, 1983).

Time Series Analysis Results

A time-series study was conducted by White from 1945 to 1952 (White, 1968); White found that four major factors influenced discharge characteristics at springs, vents, and wells: 1) barometric pressure, 2) precipitation events, 3) earth tides, and 4) seismic activity. An inverse relationship was noticed between barometric pressure and water level (or flow); a direct relationship was observed between precipitation and discharge, with precipitation leading discharge by one to three days (depending on soil saturation and precipitation volume) (White, 1968). Earth tides and seismic activity appeared to be less responsible for discharge variations, but did in some cases have an observed effect.

For this study, data were collected for approximately one year at Steamboat Hot Springs from September 29, 1983 to August 23, 1984. The mean sample interval was 13.60

Table 10 (Steamboat Hot Spring Chemical Geothermometer Results)

Thermometer	SiO ₂	SiO ₂	SiO ₂	SiO ₂	SiO ₂
Equation	1	2	3	4	5
Calculated Temperature (C)	157.49	180.34	170.03	205.97	189.17
Thermometer	Na-K	Na-K	Na-K-Ca	Na-K-Ca	Na-Li
Equation	6	7	8	10	11
Calculated Temperature (C)	234.25	215.72	236.19	230.60	283.30

Table 12 (Steamboat Hot Spring Correlation Coefficient Matrix)

	Ca	Cl	EC	HCO ₃	pCO ₂	pH	TEMP	FLOW	PRCIP
PRECIP	0	0	0	-.50	-.42	.36	0	.52	1
FLOW	0	-.57	-.61	-.70	-.62	.60	0	1	
TEMP	0	-.59	0	0	0	0	1		
pH	0	0	-.46	-.39	-1.0	1			
pCO ₂	0	0	.47	.45	1				
HCO ₃	.46	.50	.36	1					
EC	0	.37	1						
Cl	0	1							
Ca	1								

Table 13 (Steamboat Hot Spring Correlation Coefficient Matrix at Varying Lag Positions)

Var 1	Var 2	Lag	Corr. Coef.
PRECIP	leads Cl	by 16 weeks	.61
pH	leads HCO ₃	by 8 weeks	-.61
EC	leads HCO ₃	by 8 weeks	.58

days (standard deviation = 2.20 days) (table 11). A concrete weir was cemented to the sinter for flow measurements, unfortunately the weir was stolen by vandals sometime between February 21 and 28; therefore, only six months of flow data was recorded.

Crosscorrelation coefficient results at zero lag are presented in table 12. Eight of the values are 50 percent or greater, but one is 70 percent or greater. There are also several significant lagged correlations (table 13).

There is an inverse relationship between flow and bicarbonate ion, which suggests that during the first six months of the study when flow increased a decrease in bicarbonate ion was observed; however, the coefficient of variation for bicarbonate ion shows that all of the variation can be accounted for by analytical and sampling errors.

An inverse relationship exists between flow and electrical conductivity, suggesting that increased flow is caused by fresher water; a direct relationship also exists between flow and pH, which may be a similar phenomena to the EC relationship. These relationships are also questionable due to the low coefficients of variation.

There is a fair direct correlation between flow and precipitation, which suggests that infiltration to the water table occurs in less than two weeks (figure 9). White, (1968) noticed flow changes one to three days after precipitation events.

Due to the extremely complex nature of this

Table 11 (Steamboat Hot Spring temporal data)

Date	Time	T(C)	FLOW (lps)	EC µmhos	pH field	pH lab	HCO ₃ ⁻ mg/l	Cl mg/l	Ca mg/l	log pCO ₂	σ ¹⁸ O ‰	σD ‰
9/29/83	11:45	87.0	0.86	3570	-	7.20	307.	917.	5.24	-1.51	-	-
10/11/83	8:58	86.0	0.73	3660	-	7.18	312.	897.	5.16	-1.49	-	-
10/25/83	9:09	84.5	0.76	3587	7.23	7.34	317.	904.	5.18	-1.65	-11.8	-112
11/ 8/83	9:02	87.0	0.86	3718	7.42	7.32	323.	904.	5.24	-1.61	-	-
11/22/83	9:44	91.0	1.12	3541	7.35	7.34	285.	876.	5.31	-1.68	-	-
12/ 6/83	9:02	88.0	1.04	3541	7.85	7.51	305.	873.	5.91	-1.82	-	-
12/20/83	9:44	92.5	1.04	3645	-	7.25	306.	876.	5.80	-1.56	-	-109
1/ 3/84	9:22	93.0	0.77	3812	-	7.06	307.	883.	5.54	-1.36	-	-
1/10/84	8:32	90.5	0.77	3581	7.18	6.89	305.	876.	5.80	-1.20	-	-
1/24/84	8:11	91.0	0.75	3773	-	6.69	311.	890.	5.52	-0.99	-	-
2/ 7/84	8:19	89.5	0.67	3654	7.68	7.05	314.	904.	5.52	-1.35	-	-
2/21/84	7:47	88.5	0.49	3791	7.12	7.02	321.	904.	5.57	-1.31	-	-106
‡ 2/28/84	7:36	90.5	-	3770	6.88	6.90	327.	-	-	-	-	-
‡ 3/ 6/84	7:44	89.0	-	3716	6.86	6.82	320.	938.	5.44	-1.11	-	-
‡ 3/13/84	7:33	89.0	-	3806	7.47	7.22	333.	-	-	-	-	-
3/20/84	7:36	-	-	3694	6.71	6.85	320.	897.	5.65	-1.14	-	-
‡ 3/27/84	7:36	90.0	-	3631	6.80	6.89	322.	-	-	-	-	-
‡ 4/ 3/84	7:46	90.0	-	3658	6.76	6.77	321.	879.	5.86	-1.06	-	-
‡ 4/10/84	7:43	88.0	-	3715	7.20	7.00	322.	-	-	-	-	-
‡ 4/18/84	9:08	88.0	-	3776	-	6.97	332.	938.	5.88	-1.25	-10.8	-105
‡ 4/24/84	7:36	92.0	-	3837	6.90	6.81	329.	-	-	-	-	-
‡ 5/ 1/84	7:36	89.0	-	3624	-	7.04	328.	917.	5.86	-1.32	-	-
‡ 5/ 8/84	7:22	91.0	-	3680	6.55	7.06	327.	-	-	-	-	-
‡ 5/16/84	8:48	92.0	-	3625	6.54	6.94	331.	897.	5.57	-1.21	-	-
‡ 5/23/84	10:17	91.0	-	3596	7.18	7.02	333.	-	-	-	-	-
5/30/84	8:33	92.0	-	3625	6.92	7.04	333.	873.	5.96	-1.31	-	-
‡ 6/ 6/84	9:06	90.0	-	3568	6.96	7.21	328.	-	-	-	-	-
‡ 6/13/84	8:59	91.0	-	3658	6.74	7.13	318.	873.	6.25	-1.42	-	-
‡ 6/20/84	8:42	91.5	-	3576	7.03	7.15	314.	866.	5.62	-1.44	-	-109
‡ 7/ 5/84	10:37	94.0	-	3576	6.83	7.05	312.	-	-	-	-	-
7/11/84	9:00	92.0	-	3622	6.85	6.88	309.	890.	5.49	-1.18	-	-
‡ 7/17/84	8:01	92.5	-	3675	6.88	7.15	310.	-	-	-	-	-
‡ 7/26/84	8:56	91.0	-	3649	6.80	7.04	305.	879.	4.88	-1.35	-	-
‡ 8/ 2/84	8:53	91.0	-	3610	6.84	7.10	303.	-	-	-	-	-
‡ 8/ 9/84	8:57	92.0	-	3635	6.89	7.16	304.	866.	4.73	-1.47	-	-
‡ 8/16/84	8:16	86.0	-	3667	7.19	7.36	300.	-	-	-	-	-
‡ 8/23/84	9:20	93.0	-	3667	6.75	7.36	300.	866.	4.85	-1.67	-	-120
Mean		89.8	.82	3656		7.07	314.	892.	5.54	-1.38		
Stand Dev		4.8	.18	76.6		.20	11.2	20.6	0.35	0.21		
Coef Variation		2.5	21.2	2.1		2.84	3.6	2.3	6.41	15.5		

hydrothermal system, it is impossible to decipher the lagged correlation results; therefore, no attempt will be made to analyze these relationships.

Lead-lag multiple step-wise regression was not applied to this data, due to the limited amount of flow data collected.

Summary

The Steamboat thermal system has been studied extensively over the past 30 years by research institutions and by geothermal development companies. Several geothermal wells have been drilled in the area; monitoring of these wells and several hot and cold springs have yielded significant results.

Isotopic studies show that most of the recharge comes from the Carson Range to the west; however, time-series analysis show a quick discharge response after precipitation events (less than two weeks) and is primarily caused by near-spring infiltration. Mountain-front infiltrating water migrates downward along fractures and faults, and is heated by rocks in contact with a convecting magma body. After heating, fluids ascend along fractures due to convection and a hydraulic gradient (mixed convection).

Approximately 3.7×10^{-2} cubic meters of moderately saline water are discharged from Steamboat thermal system each second, via three paths: 1) from spring discharge, 2)

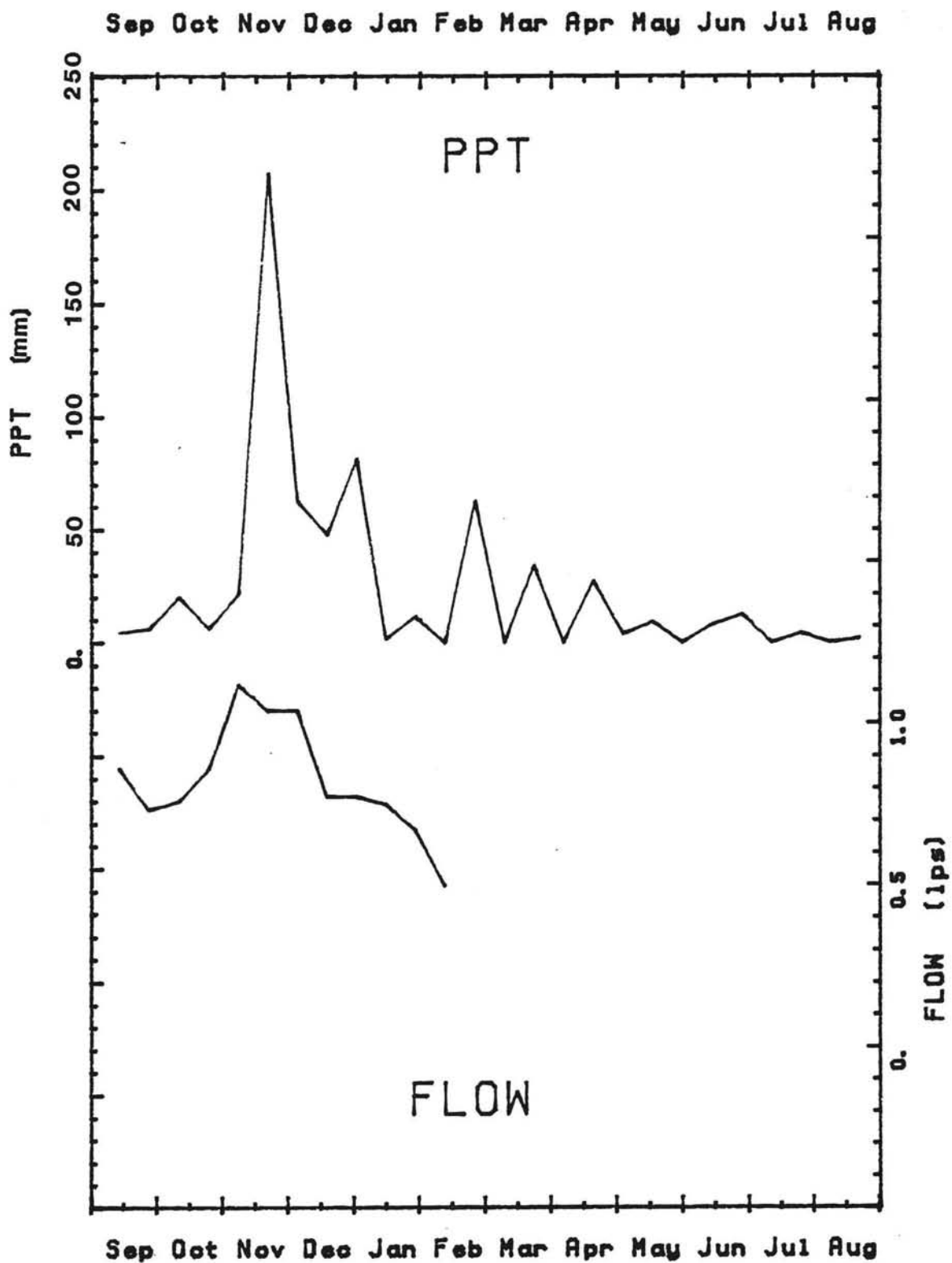


Figure 9. Steamboat Hot Spring
Precipitation and Flow vs. Time

from well discharge, and 3) from subsurface flow to Steamboat Creek.

The water at Steamboat Hot Spring is a Na-Cl type water, has an average temperature of 89.8°C, and has an average electrical conductivity of 3,656 $\mu\text{mhos/cm}$. Thick sinter deposits in the area were composed of opal and chalcedony, and spring water was near saturation in the silicate minerals chalcedony, cristobalite, magadiite, and quartz. Dark grey spring precipitates contained measurable concentrations of gold and silver, and precipitation was observed during high discharge. Carbonate mineral precipitation has been observed in wells and is formed due to rapid changes in pressure and temperature.

Most of the hot springs in the area are near boiling (about 90°C). Na-K and Na-K-Ca chemical geothermometers yielded a reservoir temperature of $230 \pm 20^\circ\text{C}$, which is close to the highest observed down-hole temperature of 227°C.

The highest variations were observed on the parameters of flow, pCO_2 , and calcium ion. Significant correlations were observed between flow versus bicarbonate ion, flow versus EC, and flow versus precipitation.

Bowers Mansion Hot Spring

Introduction

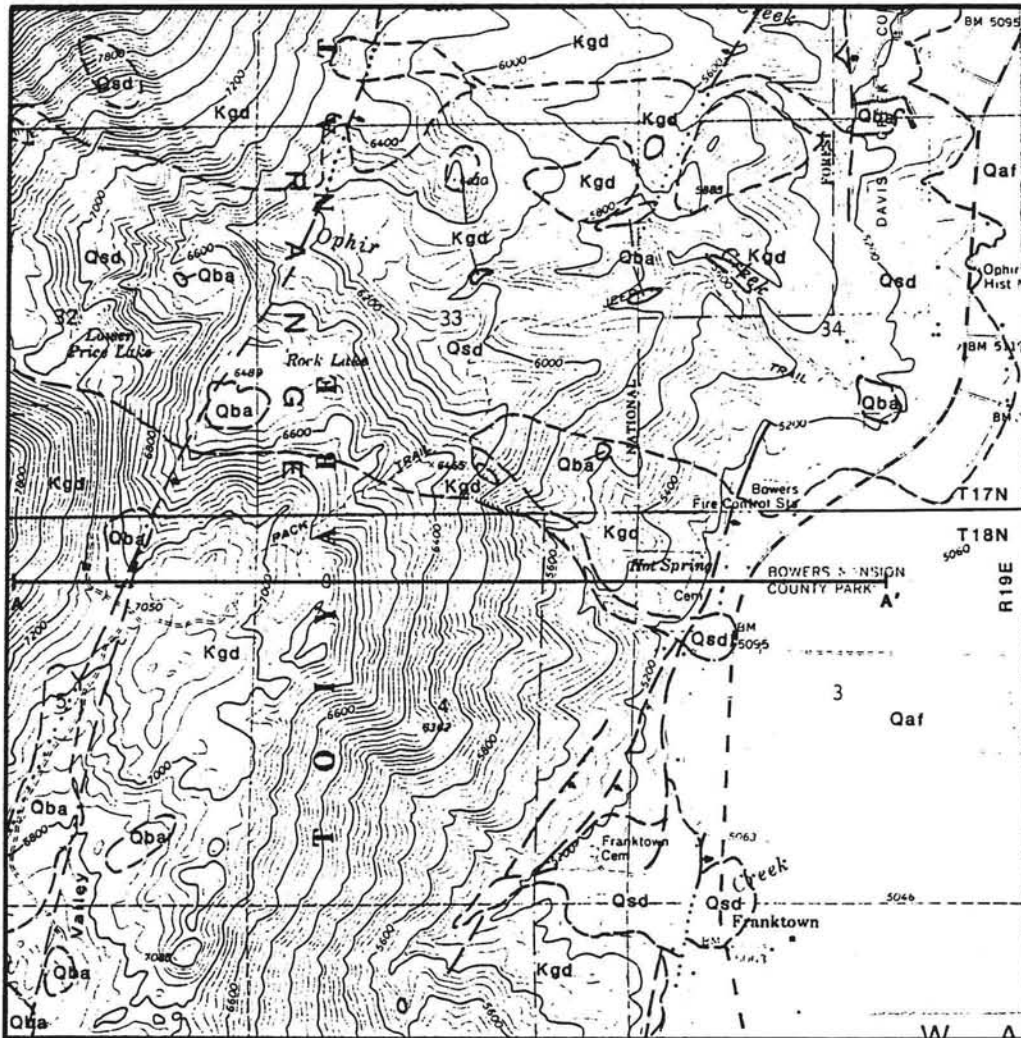
Bowers Mansion was built by the Bowers family, who were involved with banking in Virginia City during mining of the Comstock Lode. The mansion was donated to Washoe County and is now a county park. The hot spring was previously used to heat a swimming pool, but the spring is no longer used.

Precise Location

Bowers Mansion Hot Spring is in Washoe County, Nevada, about halfway between Reno, Nevada and Carson City, Nevada. Bowers Mansion is a State historical Landmark and is run by the Washoe County Parks and Recreation Department.

The county park is on Old Highway 395, about 1.5 km south of the north junction of Old and New Highway 395. The hot spring issues from a fault immediately behind the ranger's house, and is located in the SE1/4, NW1/4, NW1/4 of Section 3, T16N, R19E (figure 10). The hot spring flows into a concrete collection box (2 m long, 1 m wide, and 1 m deep) and is diverted via a steel culvert for approximately 10 m to an old swimming pool; this old pool now acts as an irrigation water supply for the park.

Two flowing wells were also monitored in Washoe



Geologic Map Bowers Mansion Hot Spring Area

(Modified from Tabor, et al., 1975)

Qaf - Alluvial Fan
 Qba - Basin Alluvium
 Qsd - Slide Mountain Debris Flows
 Kgd - Hornblende-Biotite Granodiorite

— ····· Contact, dashed where approximated,
 dotted where concealed
 — — — — — Fault, dashed where inferred or
 approximated, arrow shows dip.

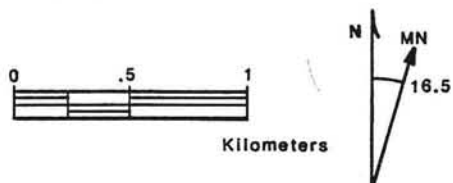


Figure 10. Bowers Hot Spring
 Geologic Map

Valley, one on the east side and one on the west side of Washoe Lake. West Washoe flowing well is approximately 10 meters west of new Highway 395 South and is about 3 km north of the Belview Exit (NW1/4, NW1/4, SE1/4 Sec 11, T16N, R19E). The well discharges into a small ditch which flows to a pond near the center of section 11. Boat Ramp flowing well is at the Washoe County boat ramp, west of Lakeside Drive in New Washoe City (NE1/4, SE1/4, SE1/4, Section 1, T16N, R19E). This well discharges into a ditch connected to Washoe Lake.

Climate and Vegetation

Bowers Mansion Hot Spring is at an elevation of about 1,561 m. Temperatures range from -10 to 5°C in the winter and from 21 to 38°C in the summer.

Precipitation generally falls as rain, but approximately 200 mm of snow accumulated during the study period. A precipitation monitoring station at Franktown (about 1 km south, elevation = 1,600 m) recorded 645.7 mm of precipitation during this study (Kleiforth, et al., 1984). Although data were not available from the Little Valley monitoring station, Little Valley has historically accumulated about 18 percent more precipitation than the Franktown site.

Vegetation in the Sierra Nevada consists of thick coniferous forests, primarily pines and cedars. Young deciduous trees occur along streams and at springs.

Manzonita and buckbrush are generally thicker on south-facing slopes than on north-facing slopes, and meadows are covered with grasses, tobacco weed, bitter brush, and holly. The alluvial basin is covered with grasses and sages.

Previous Work

Geologic studies have been conducted in the area by Thompson and White (1964) and by Tabor and Ellen (1975). geotechnical studies have been conducted in the Slide Mountain area by Tabor and others (1983) and by Watters (1983).

The hydrogeology of Washoe Valley has been extensively described by Rush (1967) and by Arteaga and Nichols (1983), while the hydrogeochemistry has been described by White and others (1964) and by Armstrong and Fordham (1977). Selected Sierran cold springs were sampled for major ions and stable isotopes by Nehring (1980).

Geology

The Geology near Bowers Mansion has been described by Thompson and White (1964), and has been mapped by Tabor and Ellen (1975). In conjunction with the Ophir Creek Debris flow (May, 1983), more recent geologic / geotechnical studies have been conducted by Tabor and

others (1983), and by Watters (1983). The geologic map by Tabor and Ellen (1975) was used in this study, with only slight modification (figure 10). Refer to appendix A for descriptive geology.

Lithologic Interpretations

The oldest rocks in the study area are Cretaceous granitic rocks (Tabor, et al., 1975), and have been mapped as hornblende-biotite granodiorite. Outcrops are moderately to highly fractured, and jointing is abundant near Slide Mountain. Most of the granitic outcrops in Little Valley are in varying stages of decomposition and most of the sediments in Little Valley are derived from weathered granitic rocks.

Three Quaternary units were mapped in the study area; however, about 20 units were distinguished by Tabor and Ellen (1975). The mapped units are as follows: 1) basin alluvium composed predominantly of granitic sands, gravels, and boulders, 2) Slide Mountain debris flows are composed of granitic silt to boulder sized material, derived from Slide Mountain and are generally located along the Ophir Creek flood-path, and 3) alluvial fan material is composed of granitic sand and gravels located east of the mountain front.

Structure

A distinct, high angle, normal fault controls the hot spring at Bowers Mansion. This range front fault trends about N10E and is mappable for several kilometers north and south of the hot spring (figure 10).

A second major N10-20E trending fault occurs about 2 km west of Bowers Mansion. This fault is located at the base of Slide Mountain and controls Little Valley; it is mappable for more than 20 km. Field approximations of fault dip were used to generate a hypothetical geologic cross-section (figure 11).

Geotechnical studies by Watters (1983) concluded that joint failure planes within the granitic rock of Slide Mountain caused a May 1983 rock avalanche, and produced a debris flow as slide material displaced the water in Upper and Lower Price Lakes.

Hydrology

The regional hydrology of Washoe Valley has been studied by Rush (1967) and by Arteaga (1984). Water quality investigations have been conducted by Rush (1967) and by Armstrong and Fordham (1977).

Regional

The predominant aquifer in Washoe Valley is formed by alluvium; the aquifer covers approximately 7,285 hm² and is about 152 m thick (Rush, 1967). Rush (1967) estimated

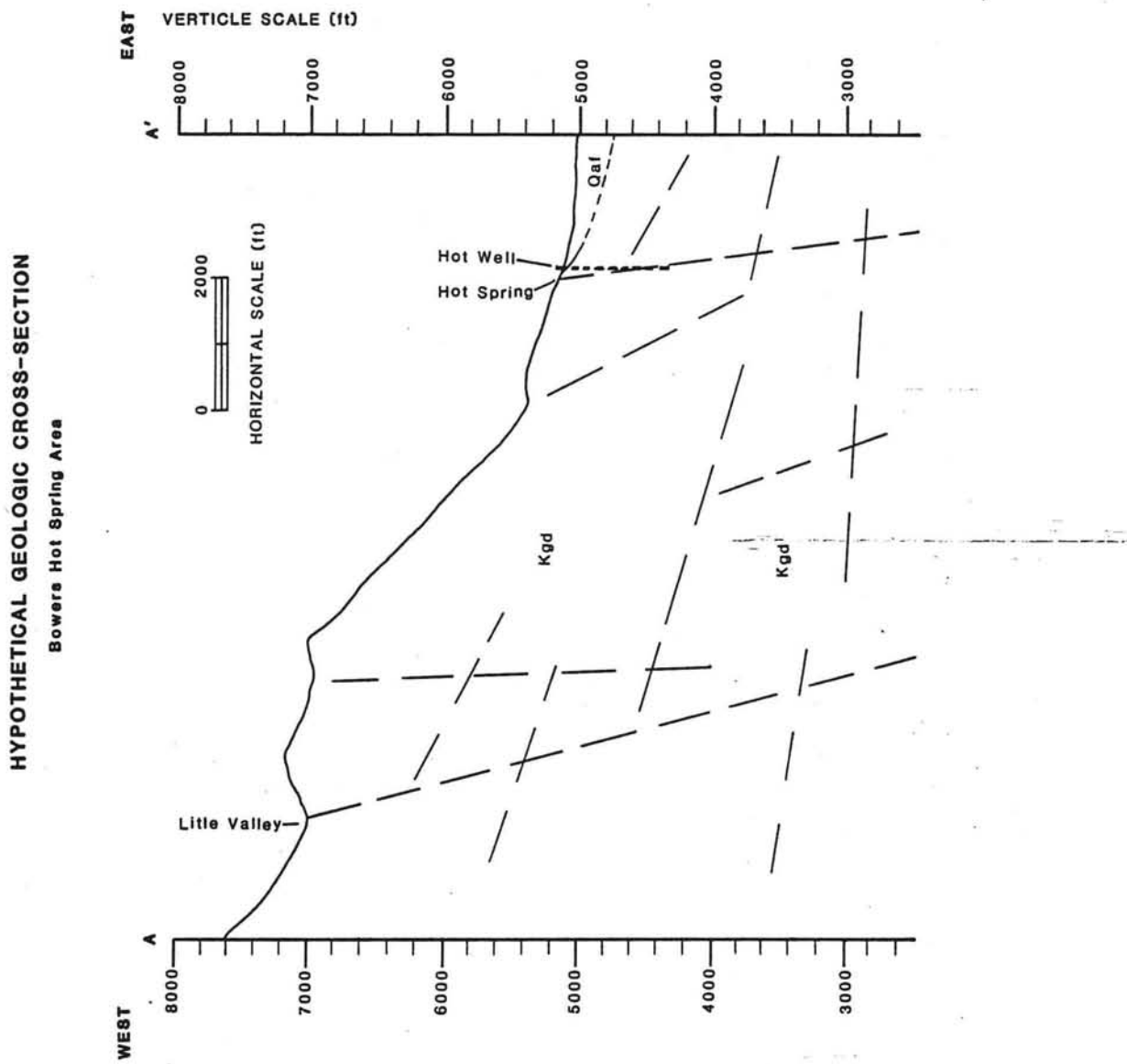


Figure 11. Bowers Hot Spring
Hypothetical Geologic Cross-section

the transmissability to be $0.0072 \text{ m}^2/\text{sec}$ to $0.0216 \text{ m}^2/\text{sec}$ and the storage coefficient was approximately equal to the specific yield - 15 percent.

Recharge to the valley aquifer is accounted for several ways: 1) by precipitation infiltration, 2) by seepage loss from streams on the valley floor, and 3) by underflow from consolidated rocks (Rush, 1967). A groundwater level contour map was developed by Rush (1967) and by Arteaga, et al. (1983); groundwater flows toward Washoe Lake, which discharges at the north end of the valley into Steamboat Creek (figure 7).

A water budget was proposed by Rush (1967) for 1965 conditions and is summarized as follows:

inflow = $40.69 \text{ hm}^3/\text{yr}$,

outflow = $38.22 \text{ hm}^3/\text{yr}$, and

difference = $+2.47 \text{ hm}^3/\text{yr}$;

therefore, 2.47 hm^3 of water per year are in excess.

Arteaga and Nichols (1983) proposed a new water budget using refined techniques, and suggested inflow equaled outflow ($65,455 \text{ hm}^3/\text{year}$, each); therefore, it was suggested that no further development of Washoe Valley be allowed.

Water quality varied markedly from one side of Washoe Valley to the other, and differing hardness and conductivity zones have been delineated by Rush (1967). A detailed water quality study in New Washoe City was conducted by Armstrong and Fordham (1977) and showed zones of high fluoride, nitrate, and iron; these ions are not

derived from surface waters and are presumably from the geologic formations.

Debris Flow

On May 30, 1983, an avalanche on Slide Mountain displaced the water in Upper and Lower Price Lakes; this caused a water-flood debris flow in Ophir Creek. Because the area has been historically prone to debris flows, an extensive study was carried out in 1977 and the 100 year peak flow was estimated to be $55 \text{ m}^3/\text{sec}$ (Glancey, et al., 1977). According to Glancey (personal communication, 1983), the previous peak flow estimate was off by one to two orders of magnitude due to the unexpected lake water displacements.

The 1983 debris flow covered about 2 km of Old Highway 395 and deposited approximately 100,000 to 150,000 m^3 of material over about 200,000 m^2 of valley floor (Watters, 1983). The flood stage was from six to seven meters above the stream-bed at the canyon mouth (Watters, 1983).

Local

Bowers Mansion Hot Spring issues from fractures, near ground level, along the range front fault previously mentioned. The hot spring discharges into the old Bowers Mansion swimming pool, via a steel culvert. A 30° V-notch

weir was installed between the culvert and the pool, and a Stevens type-F continuous recorder was installed so that flow measurements could be made. A four inch (10 cm) steel pipe also runs from the concrete collection box to the old pool; no measurements could be made from this pipe, because the discharge was below water level. The average flow at the spring was 2.59 liters per second, varying markedly due to local pumping. The hot spring was used in the past to heat the old swimming pool (now used for an irrigation water source), and may be used in the future for space heating.

An olympic size swimming pool exists approximately 100 m north of the hot spring and about 60 m from the range front fault. During excavation for this pool, another hot spring was found; this spring flows unregulated through a grate in the pool floor and, along with a hot well, is used as the heat source for the pool (Tom Coyle, personal communication, 1984).

A hot well was drilled on January 24, 1963, about 100 meters north of the original hot spring; it is about halfway between the new pool and the range front fault. The well log submitted by the driller indicated the total depth as 304 m; the upper 232 m were sealed with concrete to decrease the cooling effect of surface water. This well intersected the range front-fault at a depth of about 230 m (figure 11). The well pumping volume was monitored during the study at an in-line flow meter between the pump and the pressure tank; the well pumped 14,114 m³ during

the 2.5 month summer swim season and approximately 26,206 m³ during the off season.

Stable isotopes ($\delta D = -102.3$, $\delta^{18}O = -14.79$, Garside and Schilling, 1979) suggest that the recharge is primarily derived from about the same elevation as the recharge to Slide Mountain Spring ($\delta D = -105.5$, $\delta^{18}O = -14.94$; Nehring, 1980). Although this relationship does not pin-down the exact recharge area, it does suggest some kind of slight anomalous isotopic enrichment is occurring in this recharge area. Topographic and geologic controls show Tahoe Meadows and Little Valley as the most suitable locations for recharge to Bowers Mansion Hot Spring.

Geochemistry

Major Dissolved Constituents

A water sample analysis result was obtained from Washoe County Park data files. This data was entered into the program "WATEQ" to calculate mineral saturations, cation to anion balance, pCO₂, etc. (table 14).

The water at Bowers Mansion Hot Spring is a Na-HCO₃ type water. Sodium is generally accounted for two ways: 1) by dissolution of plagioclase feldspar, and 2) by dissolution of sodium salt minerals (Drever, 1982). Bicarbonate ion is a secondary product of carbonic acid, which in granitic terrains is derived several ways: 1) through weathering and dissolution of granitic minerals

Table 14 (Bowers Hot Spring WATEQ output)

*** total concentrations of input species ***					
species	total molality	total mg/liter	epm	epm fraction	
Ca	0.499151e-04	2.0	0.10	0.044	
Mg	0.	0.	0.00	0.000	
Na	0.217553e-02	50.0	2.17	0.953	
K	0.665126e-05	0.26	0.01	0.003	
Cl	0.110038e-03	3.9	0.11	0.049	
SO4	0.322806e-03	31.0	0.65	0.290	
HCO3	0.146789e-02	89.54	1.47	0.660	
SiO2 tot	0.187291e-02	112.5			
PO4	0.263316e-05	0.25			
Fe	0.100304e-05	0.056			
Li	0.158572e-04	0.11			
Sr	0.605065e-04	5.3			
Be	0.203935e-05	0.28			

tds = 298.596					
*** description of solution ***					
epmcat	analytical 2.803	ph 9.40	pco2 = 0.939750e-05		
epman	2.231		log pco2 = -5.0270		
cation/anion	1.256	temperature 43.00 deg c	EC = 250.0		
			ionic strength 0.280656e-02		
*** mineral saturations ***					
iap/kt	log iap/kt	phase	iap/kt	log iap/kt	phase
0.5386e-03	-3.26876	ANHYDRITE	0.5998e+01	0.77803	QUARTZ
0.4352e-00	-0.36132	ARAGONITE	0.2000e+01	0.30109	SIDERITE
0.2080e+01	0.31808	BARITE	0.7317e+00	-0.13568	SiO2(A,L)
0.6215e+00	-0.20657	CALCITE	0.3871e+01	0.58778	STRONTIANITE
0.3639e-01	-1.43900	CELESTITE	0.1632e-08	-8.78719	THENARDITE
0.2302e+01	0.36201	CHALCEDONY	0.1716e-09	-9.76557	THERMONATR
0.2450e+01	0.38908	CRISTOBALITE	0.3383e-14	-14.47064	TRONA
0.3817e-03	-3.41831	GYPHUM	0.2551e-01	-1.59328	WITHERITE
0.5015e-08	-8.29970	HALITE	0.5905e-01	-1.22879	MHCALC
0.8331e+03	2.92067	HYDROXYAPATI			
0.8810e+08	7.94495	MACKINAWIITE			
0.5207e-02	-2.28338	MAGADIITE			
0.2144e-08	-8.66879	MIRABILITE			
0.1360e-05	-5.86650	NAHCOLITE			
0.7872e-09	-9.10390	NATRON			

such as plagioclase feldspar, potassium feldspar, and biotite, which causes subsequent buffering of pH (Bohm, 1984), 2) by hydrolyzation of soil CO₂ gas (Feth, et al., 1964; Drever, 1982), and 3) from possible CO₂ sources at depth such as dissolution of Limestone at low pH, metamorphic reactions and/or magmatic emanations (Bohm, 1984).

The computer program "WATEQ" showed several minerals above saturation, including silicates, sulfates, carbonates, and hydrolysates. Although most of the minerals are near saturation limits, some of the silicates are highly saturated. The only observed precipitant was a light blue mineral precipitating on a copper pipe that discharged into a chlorine tank; this mineral was presumably chalcantite.

Geothermometry

The water analysis results from the Bowers Mansion files were entered into several chemical geothermometers; for results see table 15. The calculated temperatures ranged from 11.6 to 143.9°C. The calculated temperatures are in question due to the possibility of near-surface mixing. The SiO₂ geothermometers are generally less susceptible to reactions and reequilibrations than the Na-K and Na-K-Ca thermometers (Fournier, et al., OFR; Benjamin, 1983). Therefore, reservoir temperature is estimated at about 100±20°C.

Table 15 (Bowers Hot Spring Chemical Geothermometer Results)

Thermometer	SiO ₂	SiO ₂	SiO ₂	Na-K	Na-K	Na-K-Ca	Na-K-Ca	Na-Li
Equation	1	2	4	6	7	8	8	11
Calculated Temperature (C)	93.31	115.82	143.88	49.92	11.56	29.79	68.87	127.08

Table 17 (Bowers Hot Spring Correlation Coefficient Matrix)

	Ca	Cl	EC	HCO ₃	pCO ₂	pH	FLOW	TEMP	PRECIP
PRECIP	0	0	0	0	.42	-.42	0	0	1
TEMP	0	0	0	0	0	0	0	1	
FLOW	.57	0	0	0	0	0	1		
pH	0	0	.48	0	-1.0	1			
pCO ₂	0	0	-.48	0	1				
HCO ₃	0	0	0	1					
EC	0	.72	1						
Cl	0	1							
Ca	1								

Table 18 (Bowers Hot Spring Correlation Coefficient Matrix at Varying Lag Positions)

Var 1		Var 2		Lag	Corr. Coef.
HCO ₃	leads	Ca	by	2 weeks	-.58
EC	leads	Ca	by	12 weeks	.64
Cl	leads	Ca	by	12 weeks	.73
Cl	leads	HCO ₃	by	8 weeks	-.63
EC	leads	HCO ₃	by	4 weeks	-.56
PPT	leads	EC	by	16 weeks	.67
PPT	leads	TEMP	by	4 weeks	.48

Time Series Analysis Results

Data were collected at Bowers Mansion Hot Spring for approximately one year, from September 13, 1983 to August 31, 1984. The average sample interval was 13.5 days (standard deviation = 2.00 days) (table 16).

Crosscorrelation coefficient results are presented in table 17. Only two coefficients were greater than 50 percent, with one greater than 70 percent. A good direct correlation exists between EC and chloride ion, suggesting that most of the variation in EC can be accounted for by variation in chloride ion concentration; however, the coefficient of variation suggests that all of the chloride variability may be due to analytical and sampling errors. Therefore, this relationship has limited validity.

The only other correlation of significance is between flow and calcium ion. This phenomena is presumably caused by increased dissolution of calcium salts from fractures that are normally dry during low flow. Several statistically significant lagged correlations are listed in table 18.

Lead-lag multiple step-wise linear regression was applied to the data in an attempt to produce a predictive equation for the spring (table 19). This statistical approach cannot be used in this case because the variability in flow cannot be suitably accounted for by the independent variables; this is analogous to a poor cation to anion balance that suggests that one of the

Table 16 (Bowers Hot Spring temporal data)

Date	Time	T(C)	Flow l/s	EC µmhos	pH field	pH lab	HCO ₃ ⁻ mg/l	Cl mg/l	Ca mg/l	log pCO ₂	σ ¹⁸ O ‰	σD ‰
9/15/83	11:41	46.0	1.23	230	-	8.90	83.	4.2	2.93	-3.85	-	-109
9/27/83	12:03	45.0	0.55	230	-	9.13	84.	3.8	2.93	-4.07	-	-
10/11/83	9:44	45.0	2.17	240	-	9.23	87.	3.8	3.07	-4.16	-	-105
10/25/83	10:07	46.0	(2.2)	243	-	9.07	84.	3.9	3.22	-4.01	-	-
11/ 8/83	9:56	46.0	(2.4)	239	8.49	8.83	85.	4.0	3.27	-3.77	-14.8	-104
11/22/83	10:52	45.5	(2.4)	239	8.72	8.79	83.	4.2	3.27	-3.74	-	-
12/ 6/83	10:06	45.0	(2.4)	239	-	8.80	83.	4.2	3.22	-3.75	-	-105
12/20/83	11:09	44.5	(2.2)	247	-	(9.31)	85.	4.2	3.12	-4.25	-	-
1/ 3/84	10:19	45.0	(2.2)	262	-	(9.29)	85.	4.1	3.20	-4.23	-	-
1/10/84	9:36	44.5	(2.2)	250	8.78	8.91	84.	4.2	3.20	-3.86	-	-108
1/24/84	9:05	45.0	(2.4)	250	-	8.98	87.	4.1	3.14	-3.91	-	-
2/ 7/84	9:22	45.5	(2.4)	232	8.76	9.27	85.	4.2	3.12	-4.21	-14.9	-106
2/21/84	8:49	45.0	(2.6)	256	8.75	9.11	84.	4.2	3.12	-4.06	-	-
* 2/28/84	8:26	45.0	(2.6)	249	8.72	9.47	85.	-	-	-	-	-
* 3/ 3/84	13:41	45.0	2.58	No Sample.	-	-	-	-	-	-	-	-
3/ 6/84	8:42	45.0	2.44	307	8.70	9.39	87.	4.2	3.12	-4.33	-	-103
* 3/13/84	8:40	45.0	2.58	251	8.75	9.32	88.	-	-	-	-	-
3/20/84	8:47	-	2.58	245	8.75	9.22	87.	4.2	3.10	-4.15	-	-
* 3/27/84	8:36	45.0	2.23	248	8.68	9.36	84.	-	-	-	-	-
4/ 3/84	8:46	45.0	2.23	248	8.64	9.35	83.	4.3	3.07	-4.30	-	-
* 4/10/84	8:41	45.0	2.58	252	8.74	8.89	83.	-	-	-	-	-
4/18/84	9:55	45.5	3.35	252	-	8.90	83.	4.3	3.25	-3.85	-	-102
* 4/24/84	8:20	45.0	2.95	259	8.84	8.92	84.	-	-	-	-	-
5/ 1/84	8:09	45.5	3.35	253	-	9.10	78.	4.2	3.15	-4.08	-	-
* 5/ 8/84	8:24	45.0	3.35	259	8.91	9.21	83.	-	-	-	-	-
5/16/84	9:34	45.5	3.35	259	9.26	9.18	81.	4.4	3.79	-4.14	-14.5	-105
* 5/23/84	11:13	46.0	2.72	265	8.95	9.23	83.	-	-	-	-	-
5/30/84	9:31	46.0	3.03	253	9.04	9.32	85.	4.2	3.93	-4.26	-	-
* 6/ 6/84	10:13	45.0	3.03	259	8.84	9.42	84.	-	-	-	-	-
6/13/84	9:53	45.0	2.44	254	9.11	9.39	83.	4.6	3.05	-4.34	-	-101
6/20/84	9:39	45.0	1.28	251	9.12	9.14	82.	4.3	3.02	-4.10	-	-
* 6/28/84	12:47	-	1.92	No sample.	-	-	-	-	-	-	-	-
* 7/ 5/84	11:30	46.0	2.95	271	9.11	9.40	83.	-	-	-	-	-
7/11/84	9:52	46.0	1.92	281	9.20	9.25	84.	4.2	3.05	-4.19	-	-104
* 7/17/84	9:04	46.0	3.35	261	9.07	9.27	83.	-	-	-	-	-
7/26/84	9:51	46.0	2.58	261	9.01	9.34	83.	4.2	3.05	-4.29	-	-
* 8/ 2/84	9:44	45.5	2.04	260	8.95	9.33	85.	-	-	-	-	-
8/ 9/84	9:46	46.0	2.95	254	9.04	9.33	84.	4.0	3.12	-4.27	-	-
* 8/16/84	9:15	45.0	2.95	260	8.95	9.27	84.	-	-	-	-	-
8/23/84	10:34	45.0	2.58	260	9.07	9.27	84.	4.4	3.07	-4.22	-14.7	-105
* 8/31/84	14:54	45.5	2.58	-	9.05	-	-	-	-	-	-	-
Mean		45.2	2.59	250		9.14	83.9	4.3	3.20	-4.09		
Stand Dev		0.48	0.55	16.9		0.21	2.4	0.1	0.27	0.19		
Coef Variation		1.1	21.1	6.7		2.29	2.8	3.3	8.3	4.67		

Table 19 (Bowers Hot Spring Lead-lag
Multiple Regression Output)

Dependent Variable = Flow			
Number of Points = 16			
Step 1			
Variable Entered HCO ₃			
Sum of Squares Reduced in this Step ..		2.149	
Proportion Reduced in this Step481	
Multiple Corr. Coef. Adj. for D.F.693	
F-value for Analysis of Variance		12.971	
Variable	Regression Coefficient	Std. Error of Reg. Coef.	Computed t-value
HCO ₃	.16018	.04448	3.602
Intercept	-10.84252		
Step 2			
Variable Entered pH			
Sum of Squares Reduced in this Step ..		.848	
Proportion Reduced in this Step190	
Multiple Corr. Coef. Adj. for D.F.819	
F-value for Analysis of Variance		13.239	
Variable	Regression Coefficient	Std. Error of Reg. Coef.	Computed t-value
HCO ₃	.15160	.03689	4.109
pH	1.14264	.41745	2.737
Intercept	-20.57172		
Step 3			
Variable Entered Ca			
Sum of Squares Reduced in this Step ..		.354	
Proportion Reduced in this Step079	
Multiple Corr. Coef. Adj. for D.F.844	
F-value for Analysis of Variance		12.000	
Variable	Regression Coefficient	Std. Error of Reg. Coef.	Computed t-value
HCO ₃	.13676	.03431	3.985
pH	.92409	.39481	2.341
Ca	.62084	.31822	1.951
Intercept	-19.31296		

Table 19 continued

Step 4			
Variable Entered Temp			
Sum of Squares Reduced in this Step ..	.129		
Proportion Reduced in this Step029		
Multiple Corr. Coef. Adj. for D.F.883		
F-value for Analysis of Variance	9.690		
Variable	Regression Coefficient	Std. Error of Reg. Coef.	Computed t-value
HCO ₃	.13817	.03372	4.097
pH	.73415	.41881	1.753
Ca	.50657	.32672	1.550
Temp	-.22661	.18881	-1.200
Intercept	-7.08953		
Step 5			
Variable Entered Cl			
Sum of Squares Reduced in this Step ..	.057		
Proportion Reduced in this Step013		
Multiple Corr. Coef. Adj. for D.F.846		
F-value for Analysis of Variance	7.606		
Variable	Regression Coefficient	Std. Error of Reg. Coef.	Computed t-value
HCO ₃	.11375	.04630	2.457
pH	.62821	.44709	1.405
Ca	.52852	.33372	1.584
Temp	-.21917	.19242	-1.139
Cl	-.00879	.01119	-.786
Intercept	-4.42068		
Step 6			
Variable Entered = EC			
Sum of Squares Reduced in this Step ..	.256		
Proportion Reduced in this Step057		
Multiple Corr. Coef. Adj. for D.F.880		
F-value for Analysis of Variance	8.446		
Variable	Regression Coefficient	Std. Error of Reg. Coef.	Computed t-value
HCO ₃	.10501	.04180	2.512
pH	.28814	.44120	.653
Ca	.84840	.34571	2.454
Temp	-.11346	.18183	-.624
Cl	-.04497	.02198	-2.046
EC	.02197	.01187	1.851
Intercept	-11.63359		

constituents was omitted. In this case, the pumping rate from the fracture was not monitored adequately (appendix B.1).

During the summer, volumetric flow measurements were made approximately twice daily - when the pool inlet water was turned on and when it was turned off. These measurements gave a general idea of how much water was pumped during a given time, but the pumping rate was not constant because the pump was on a pressure system (figure 12). Crosscorrelation was not attempted to show the relationship between spring flow and pumping rate, due to the ambiguity of the pumping rate at any given time.

A continuous recording barometer was located at Bowers Mansion from August 31, 1984 to September 2, 1984 (figure 13 and appendix B.3). Time series studies by White (1968) at Steamboat Hot Springs showed a significant inverse correlation between barometric pressure and stage; the stage would rise to a new equilibrium when the atmospheric pressure decreased, and vice versa. This phenomena was also observed in Carson Valley flowing wells (Maurer, 1984). Crosscorrelation was not a powerful enough technique to measure a correlation between these two parameters, and no further analysis will be made on this data.

Temporal data was also collected on two flowing wells in Washoe Valley, one on the east and one on the west side of Washoe Lake (see appendix B.4 and B.5, respectively). A direct correlation of .96 was calculated between the

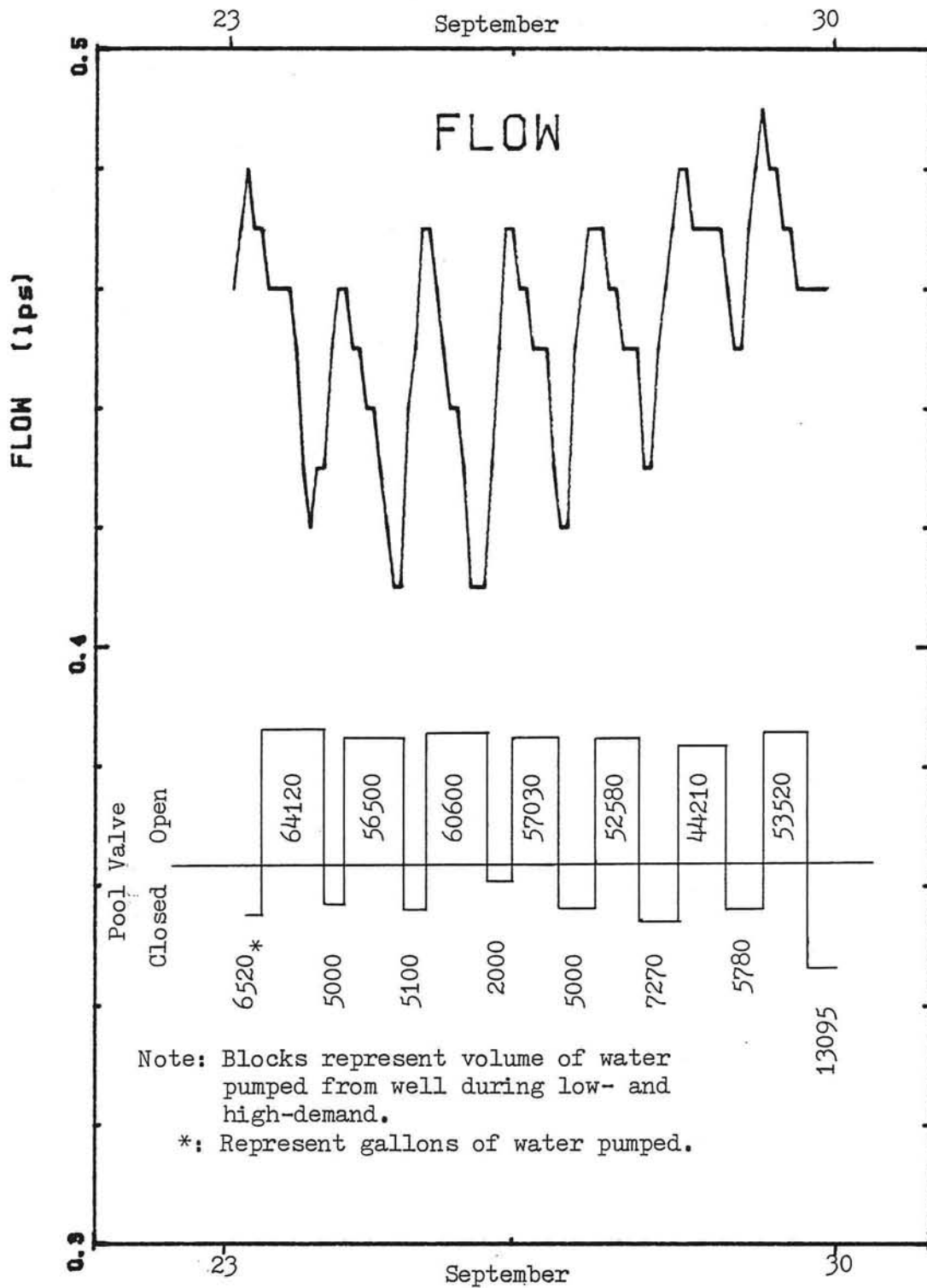


Figure 12. Bowers Hot Spring
 Flow and Pumping vs. Time

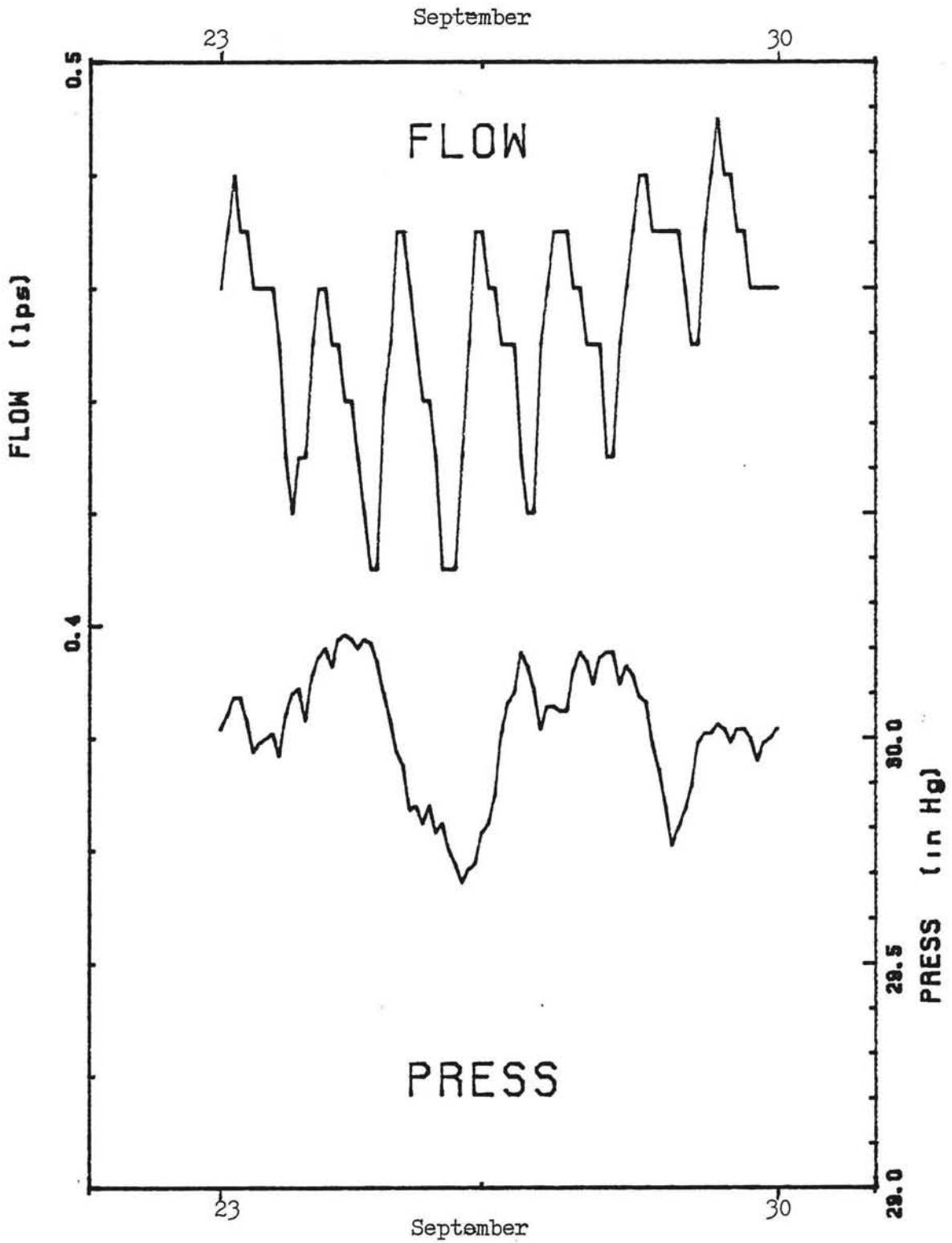


Figure 13. Bowers Hot Spring
Flow and Barometric Pressure vs. Time

flow measurements of the two flowing wells (figure 14). The fluctuations in well discharge were caused by precipitation events and variations in lake level. No significant correlations were observed between the flowing well discharges and Bowers Mansion Hot Spring discharge.

Summary

Bowers Hot Spring is apparently controlled by a high-angle normal fault, at a contact between granitic basement rocks and valley-fill alluvium. A well intersects this fault at about 230 m; pumping directly affects the spring discharge. The hot spring discharge was measured with a 30° V-notch weir equipped with a continuous recorder; average flow equaled 2.59 lps.

The water at Bowers Hot Spring is a Na-HCO₃ type water and had an average EC of 250 μmhos/cm. The dissolved ions are presumably derived from the dissolution of minerals such as plagioclase feldspar and potassium feldspar, from hydrolyzation of soil CO₂, and from possible CO₂ sources at depth. Silica chemical geothermometry suggested a reservoir temperature of 100 ±20°C.

Temporal analysis showed that increased calcium ion may be caused by dissolution of calcium salts from fractures during high flow. Lead-lag multiple step-wise linear regression showed that the independent variables measured cannot account for the high variability in flow;

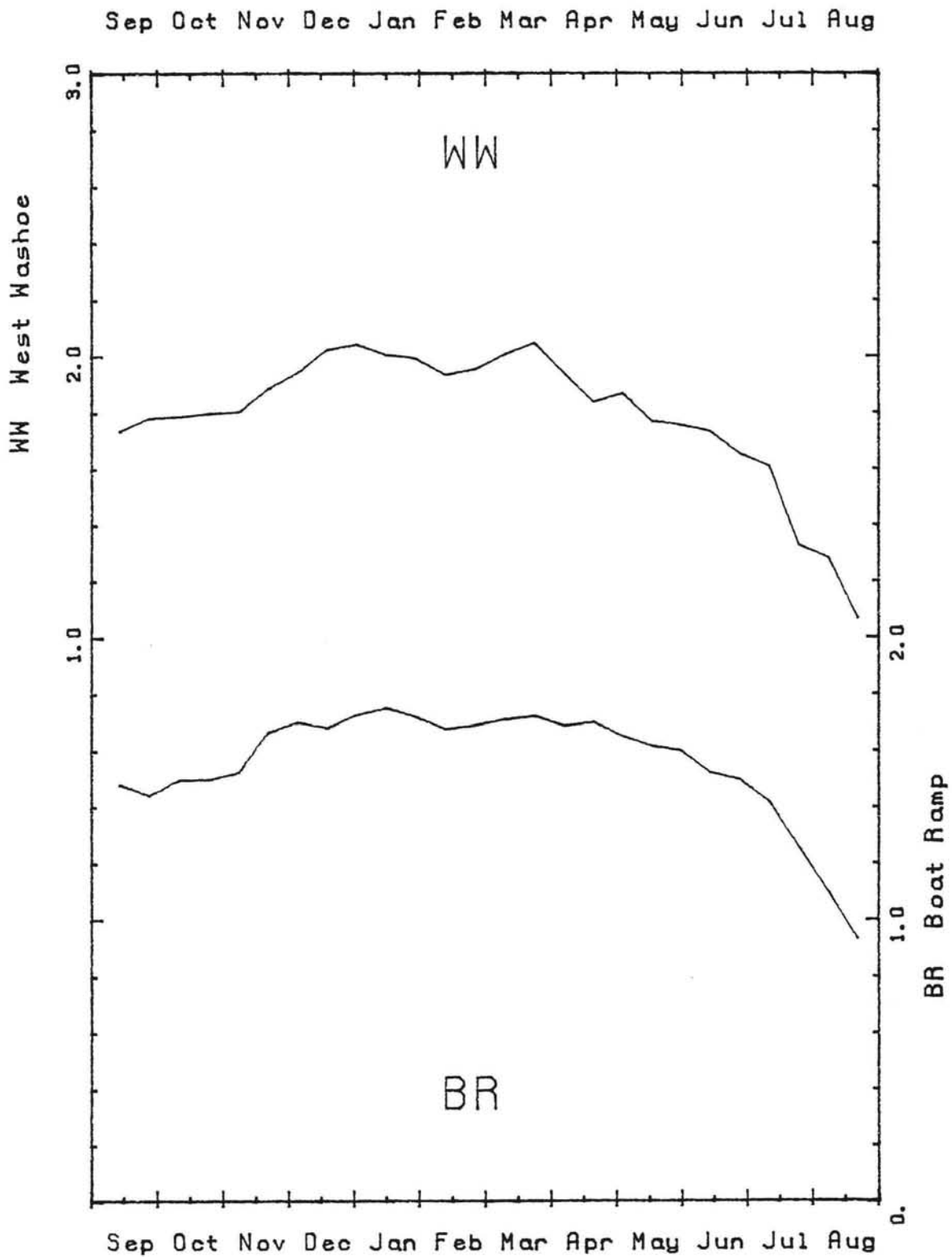


Figure 14. Flowing Well Discharge West West Washoe and Boat Ramp vs. Time (gps)

this is presumably due to the erratic pumping from the hot well.

Time-series comparisons of flow from the two wells in Washoe Valley show that flow is predominantly controlled by stage fluctuations in Washoe Lake. The flow variability at Bowers Hot Well was independent of the flowing well fluctuations. Chemical variations in the flowing wells appeared to be very stable; therefore, correlations between these variables were considered insignificant.

Prison Hot Spring

Introduction

The Maximum Security Prison was originally the Governor's Mansion, and the hot spring was used to supply spas for the Mansion guests. When the Mansion was converted into a prison, the hot spring was used to heat a greenhouse which supplied flowers to the state offices in downtown Carson City. Prisoner riots caused a prison lock-down in the 1970's; at that time the greenhouse was abandoned and the hot spring was no longer utilized.

Precise Location

Prison Hot Spring is at the Maximum Security Prison, Carson City, Nevada. The spring discharge is inside a greenhouse about 30 meters southwest of the main prison gate.

The spring is located in the SE1/4, NW1/4, SE1/4 of Section 16, T15N, R20E (figure 15). The spring issues from fractured rock in the bottom of a concrete walled channel (20 m long, .75 m wide, and .90 m deep). The channel discharges into a duck pond below water level; therefore, the duck pond water level directly influences the channel stage, making the stage measurements relative at best.

Climate and Vegetation

Prison Hot Spring is at an elevation of 1,411 m. Most of the precipitation at this elevation falls as rain, with up to 60 mm accumulating as snow in the Winter. Annually, approximately 250 mm of precipitation fall in Eagle Valley, about 760 mm in the Sierra Nevada, and about 500 mm in the Pine Nut Mountains (Arteaga and Durbin, 1978).

The area near the prison is predominantly grassland, while the vegetation of Prison Hill is mostly sages and grasses. Juniper and pinyon pine stands are common in the Pine Nut Mountains; the Sierra Nevada has many thick stands of pines and cedars, as well as desert sage and grass groundcover.

Previous Work

Geologic studies have been carried out in Eagle Valley by Zones (1958), Eisinger (1960), Moore (1969), and Bingler (1977). Bingler mapped the New Empire (7.5') quadrangle at a scale of 1:24,000. This map was used in this study area.

The hydrology, hydrogeology, and geothermal evaluations of Eagle Valley have been carried out by Worts and Malmberg (1966), Arteaga and Durbin (1978), Trexler and others (1979 and 1980), and Szecsody and others (1983).

Geology

Geologic studies have been carried out in the area by Zones (1958), Eisinger (1960), Moore (1969), and Bingler (1977); therefore, the geology was field checked and the geologic map by Bingler was used in this study area (scale 1:24,000). See appendix A for descriptive geology.

Lithologic Interpretations

The oldest rocks in the study area are Jurassic, dacite porphyry and metavolcanic breccia (figure 15). These units have been moderately to highly metamorphosed, and in some areas the dacite porphyry grades to spotted hornfels. Outcrops are highly fractured and jointed, but are quite competent and resistant to weathering (Moore, 1969 and Bingler, 1977).

A skarn zone or contact metamorphic zone occurs between the metamorphic rocks and the Cretaceous granitic rocks to the south. The granitic rocks are predominantly hornblende-biotite granodiorite and are intruded into the older metavolcanics of Prison Hill and Hot Spring Mountain (Eisinger, 1960).

Tertiary sedimentary rocks crop out in the immediate vicinity of the State Prison. Sandstones and siltstones are competent due to calcite cementation. Much of this area could not be thoroughly investigated due to the security of the prison.

Structure

Prison Hot Spring is located along a prominent N10-20E normal fault. This fault is quite obvious on aerial photographs and extends about 1.3 km south and 2.5 km north of the State Prison. This structure may be a continuation of the fault controlling Saratoga Hot Spring to the south. According to Bingler (1977), the prison spring fault dips to the west, but field checking could not verify this.

A series of sub-parallel, northeast-trending, normal faults in the northern portion of the study area are mappable for about 1.5 km. All of the faults cut Tertiary and older units.

Hydrology

The hydrology and hydrogeochemistry of the area have been studied by Worts and Malmberg (1966), Arteaga and Durbin (1978), Katzer (1980), and Szecsody (1983).

According to Worts and Malmberg (1966), the groundwater of Eagle Valley is contained within one large unconfined aquifer. Groundwater recharge is predominantly accounted for by: 1) mountain front recharge, 2) streamflow infiltration, and 3) deep percolation (Szecsody, 1983). Approximately 95 percent of the natural

recharge comes from the Carson Range to the west, while the remainder comes from the Virginia Range to the north and the Pine Nut Mountains to the east (Worts et al., 1966).

The aquifer apparently has two discharge locations to the Carson River: 1) to the northeast, near New Empire, and 2) to the south, between Prison Hill and Hot Spring Mountain (Worts et al., (1966), and Arteaga and Durbin, 1978). Pumping fields in these discharge areas could intercept valuable groundwater that is presently not utilized (Arteaga, et al., 1978).

Two other geothermal areas occur within Eagle Valley and appear to have similar characteristics to those observed at Prison Hot Spring: 1) Carson Hot Spring, about 3 km north of Prison Hot Spring, and 2) Pinyon Hills thermal area, about 2 km to the east of Prison Hot Spring (Trexler, et al., 1979). Northerly-trending normal faults also control these thermal areas, according to Trexler, et al. (1980).

Geochemistry

Major Dissolved Constituents

An extensive hydrogeochemical study was conducted by Szecsody and others (1983). A water sample was collected at Prison Hot Spring and was analyzed by the Water

Analysis Laboratory (DRI) for major cations and anions. The results from this analysis were run through the program "WATEQ" to calculate mineral saturations, cation to anion balance, pCO_2 , etc. (table 20).

The water at Frison Hot Spring is a Na-SO₄ type water. Calculated sodium mineral saturations are well below saturation limits. Sodium can generally be accounted for two ways: 1) by dissolution of sodium salts, and 2) by dissolution of plagioclase feldspar (Drever, 1982). Sulfate concentrations can commonly be accounted for two ways: 1) by dissolution of gypsum/anhydrite, and 2) by oxidation of pyrite (Drever, 1982).

The only minerals near saturation are the silicate minerals chalcedony, cristobalite, quartz, talc, and tremolite. The high concentrations of silica are primarily derived from the dissolution of silicate minerals (Back and Freeze, 1983).

Geothermometry

The water analysis, from Szecsody (1983), was used in several chemical geothermometers (table 21). The calculated reservoir temperatures range from 38.2°C to 151.2°C. Because the hot spring discharges into a large pond, it is probable that significant cold-water mixing may have occurred at the spring discharge.

The SiO₂ geothermometers are less susceptible to

Table 20 (Prison Hot Spring WATEQ output)

*** total concentrations of input species ***				
species	total molality	total mg/liter	epm	epm fraction
Ca	0.424301e-03	17.0	0.85	0.185
Mg	0.987515e-05	0.24	0.02	0.004
Na	0.365508e-02	84.0	3.65	0.798
K	0.588413e-04	2.3	0.06	0.013
Cl	0.592543e-03	21.0	0.59	0.135
SO4	0.158288e-02	152.0	3.16	0.719
HCO3	0.644307e-03	39.3	0.64	0.146
SiO2 tot	0.616014e-03	37.0		

tds = 352.840				
*** description of solution ***				
epmcat	analytical 4.582	ph 8.490	pco2 = 0.127383e-03	
epman	4.403		log pco2 = -3.8949	
cation/anion	1.041	temperature 35.00 deg c	EC = 650.0	
			ionic strength 0.612371e-02	
**** mineral saturations ****				
	iap/kt	log iap/kt	phase	
	0.1473e-01	-1.83173	ANHYDRITE	
	0.6084e+00	-0.21578	ARAGONITE	
	0.3915e-07	-7.40732	ARTINITE	
	0.3917e-04	-4.40703	BRUCITE	
	0.8155e+00	-0.08856	CALCITE	
	0.1502e+01	0.17655	CHALCEDONY	
		-37.99195	CHRYSOTILE	
	0.4697e-02	-2.32821	CLINOENSTITE	
	0.1658e+01	0.21950	CRISTOBALITE	
	0.3719e+00	-0.42957	DIOPSIDE	
	0.2243e-01	-1.64919	DOLOMITE	
	0.1445e-06	-6.84003	FORSTERITE	
	0.1147e-01	-1.94034	GYPSUM	
	0.4298e-07	-7.36675	HALITE	
	0.8252e-02	-2.08342	MAGNESITE	
	0.7791e-09	-9.10843	NATRON	
	0.4182e+01	0.62138	QUARTZ	
	0.7486e+00	-0.12574	SEPIOLITE (C)	
	0.4739e+00	-0.32428	SiO2 (A,L)	
		0.14206	TALC	
		5.49374	TREMOLITE	
	0.2479e-14	-14.60577	TRONA	
		-3.67973	SEPIOLITE (A)	

reactions and reequilibrations due to dilution than the Na-K or Na-K-Ca geothermometers (Fournier, et al., OFR; Benjamin, 1983); therefore, the reservoir temperature is probably about $70 \pm 20^\circ\text{C}$.

Time Series Analysis Results

Data were collected for approximately one year at Prison Hot Spring, from September 22, 1983 to August 23, 1984. The mean sample interval for the study period was 13.7 days (standard deviation = 2.2 days) (table 22).

Crosscorrelation Coefficient results, at zero lag, are presented in table 23. Only two values, out of 21, are greater than 50 percent. Likewise, there are only three lagged correlations that are greater than 50 percent.

There is a direct relationship between temperature and electrical conductivity (EC), and an inverse relationship between temperature and chloride ion. The coefficients of variation for temperature and EC (1.62% and 8.81% respectively) suggest that the variability in temperature is real and cannot be accounted for by human or analytical errors; however, the EC variability may be partially due to analytical errors. The coefficient of variation for chloride ion (1.81%) suggests that all of the variation could be caused by induced errors; therefore, the relationship between temperature and EC is

Table 22 (State Prison Hot Spring temporal data)

Date	Time	T(C)	Stage (cm)	EC µmhos	pH field	pH lab	HCO ₃ mg/l	Cl mg/l	Ca mg/l	log pCO ₂	σ ¹⁰⁰ %	σD %
9/22/83	13:20	41.0	40.6	550	-	8.84	37.	19.8	18.17	-4.18	-	-
10/11/83	12:15	41.0	39.4	550	-	8.83	38.	20.1	18.17	-4.15	-	-
10/25/83	13:11	40.5	39.4	479	-	8.79	40.	20.2	17.87	-4.08	-	-
11/ 8/83	13:52	40.0	43.2	491	-	8.58	39.	20.5	18.78	-3.89	-	-
11/22/83	13:45	39.5	48.3	491	8.44	8.82	44.	21.2	18.48	-4.08	-	-
12/ 6/83	12:24	39.5	44.5	529	-	8.61	43.	21.1	19.38	-3.88	-	-
12/20/83	11:42	39.5	41.9	502	-	8.91	41.	21.2	19.08	-4.19	-15.1	-112
1/ 3/84	15:09	39.0	43.2	500	-	8.92	43.	21.1	19.38	-4.19	-	-
1/10/84	13:27	39.0	41.9	460	8.33	8.60	43.	20.9	18.93	-3.87	-	-
1/24/84	12:02	39.5	38.1	486	-	8.53	39.	20.6	19.08	-3.84	-	-
2/ 7/84	12:38	39.5	29.2	490	8.71	8.83	38.	20.6	18.48	-4.15	-	-
2/21/84	11:14	39.5	36.8	511	8.66	8.81	38.	20.8	18.78	-4.09	-	-
† 2/28/84	11:32	40.0	34.3	498	8.63	8.98	38.	-	-	-	-	-
3/ 6/84	10:50	40.0	34.3	503	8.72	9.07	38.	20.1	18.48	-4.35	-	-
† 3/13/84	11:19	40.0	34.3	487	8.68	9.00	40.	-	-	-	-	-
3/20/84	11:15	-	33.0	489	8.71	8.86	39.	20.8	18.78	-4.17	-	-
† 3/27/84	11:07	40.0	30.5	480	8.64	8.98	40.	-	-	-	-	-
4/ 3/84	11:38	40.0	29.2	497	8.64	8.95	40.	20.8	18.63	-4.24	-	-
† 4/10/84	11:32	39.0	31.8	506	8.61	8.62	38.	-	-	-	-	-
4/18/84	12:19	40.0	30.5	525	-	8.60	40.	20.8	18.32	-3.90	-	-
† 4/24/84	10:38	41.0	30.5	531	8.68	8.73	39.	-	-	-	-	-
5/ 1/84	10:37	41.0	32.4	519	-	8.64	39.	21.1	18.32	-3.95	-	-
† 5/ 8/84	10:57	40.5	30.5	525	8.73	8.58	39.	-	-	-	-	-
5/16/84	12:03	41.0	30.5	524	8.82	8.43	41.	20.5	23.34	-3.71	-15.9	-112
† 5/23/84	13:40	41.0	30.5	524	8.80	8.65	41.	-	-	-	-	-
5/30/84	13:06	41.0	47.0	512	8.92	8.72	39.	20.6	18.02	-4.02	-	-
† 6/ 6/84	13:06	40.0	38.1	502	8.65	8.55	39.	-	-	-	-	-
6/13/84	12:53	40.0	40.6	550	8.60	8.95	44.	19.8	18.17	-4.21	-	-
6/20/84	13:49	41.0	55.9	560	8.68	8.92	40.	20.5	18.17	-4.21	-	-
† 7/ 5/84	14:01	41.0	61.0	560	8.59	8.95	40.	-	-	-	-	-
7/11/84	12:56	41.0	59.7	560	8.63	8.74	39.	20.6	18.02	-4.05	-	-
† 7/17/84	11:57	40.5	59.7	504	8.65	8.70	40.	-	-	-	-	-
7/26/84	12:03	40.5	58.4	504	8.50	8.80	41.	19.8	18.32	-4.08	-	-
† 8/ 2/84	11:48	41.5	36.8	552	8.62	8.84	38.	-	-	-	-	-
8/ 9/84	12:06	41.0	31.8	552	8.65	8.96	41.	19.5	17.72	-4.24	-	-
† 8/16/84	12:04	40.5	30.5	508	8.55	8.83	40.	-	-	-	-	-
8/23/84	13:41	40.0	20.3	507	8.50	8.83	40.	20.0	17.87	-4.13	-	-
Mean		39.9	38.9	514		8.77	40.0	20.7	19.01	-4.07		
Stand Dev		0.6	9.9	26.2		0.16	2.2	0.4	1.22	0.16		
Coef Variation		1.6	25.5	5.1		1.81	5.5	1.8	6.43	3.83		

the only potentially significant correlation observed for Frison Hot Spring (figure 16).

The only significant lagged correlations are between temperature versus chloride ion ($R = -.59$, temperature leads Cl^- by two weeks), stage versus temperature ($R = -.72$, Stage leads Temperature by 12 weeks), and precipitation versus pH ($R = -.56$, precipitation leads pH by eight weeks).

Lead-lag multiple step-wise regression was not applied to this data, due to poor correlations between variables.

Summary

Frison Hot Spring is controlled by a north-trending fault on the east side of Eagle Valley. This fault forms a contact between metamorphic and granitic rocks to the east and valley-fill alluvium to the west.

The water at Frison Hot Springs is a $Na-SD_4$ type water, and had an average EC of 525 $\mu mhos/cm$. The sodium and sulfate ions are presumably derived from dissolution of basement rock minerals and salts such as plagioclase feldspar and gypsum-anhydrite, and by oxidation of sulfide minerals. Silica chemical geothermometers produced an approximate reservoir temperature of $70 \pm 20^\circ C$.

Time-series analysis showed only fair correlations between variables, due to 1) the submerged nature of the spring discharge, 2) ponding of the discharge water, and 3) local pumping.

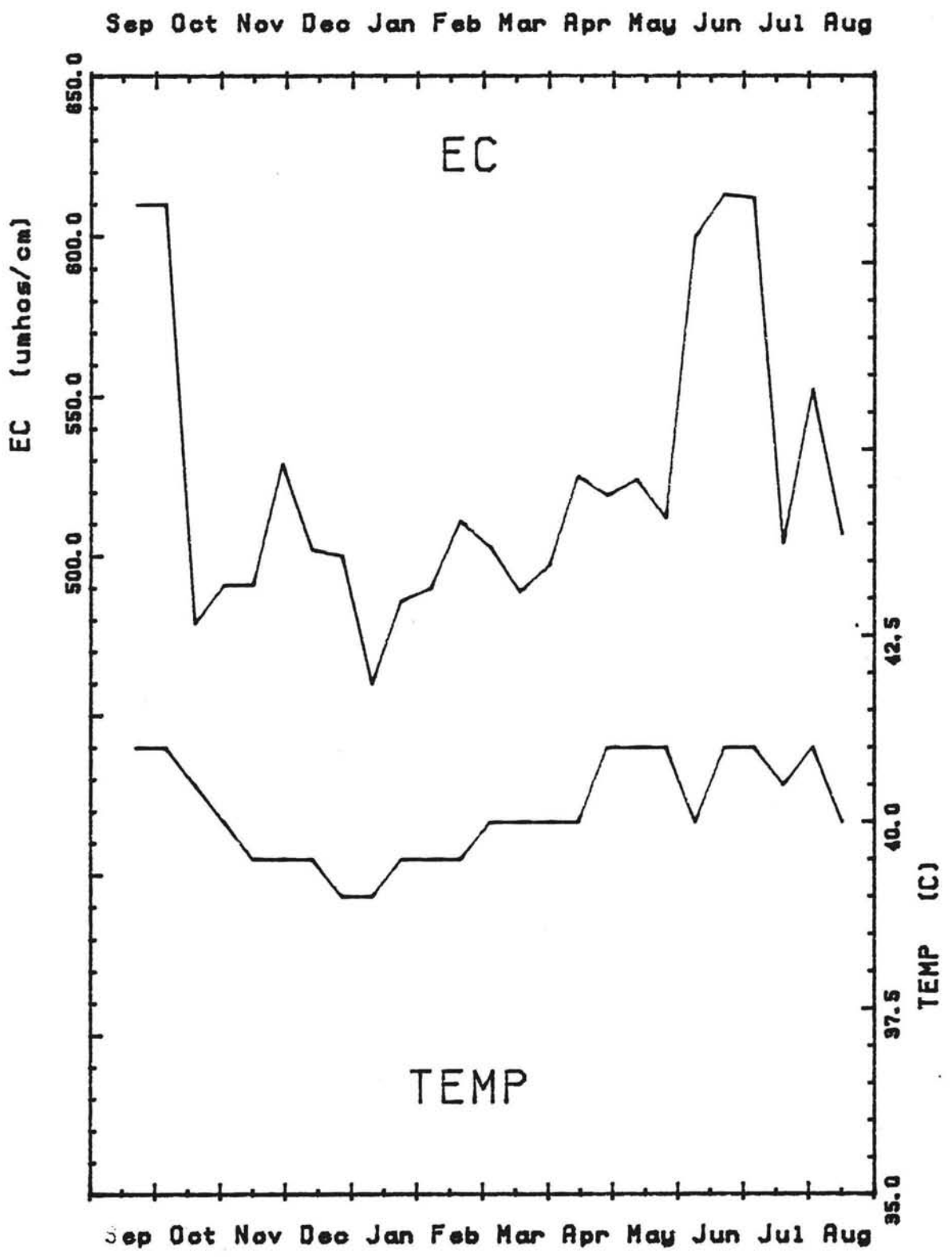


Figure 16. Prison Hot Spring
Electrical Conductivity and Temperature vs. Time

Saratoga Hot Spring

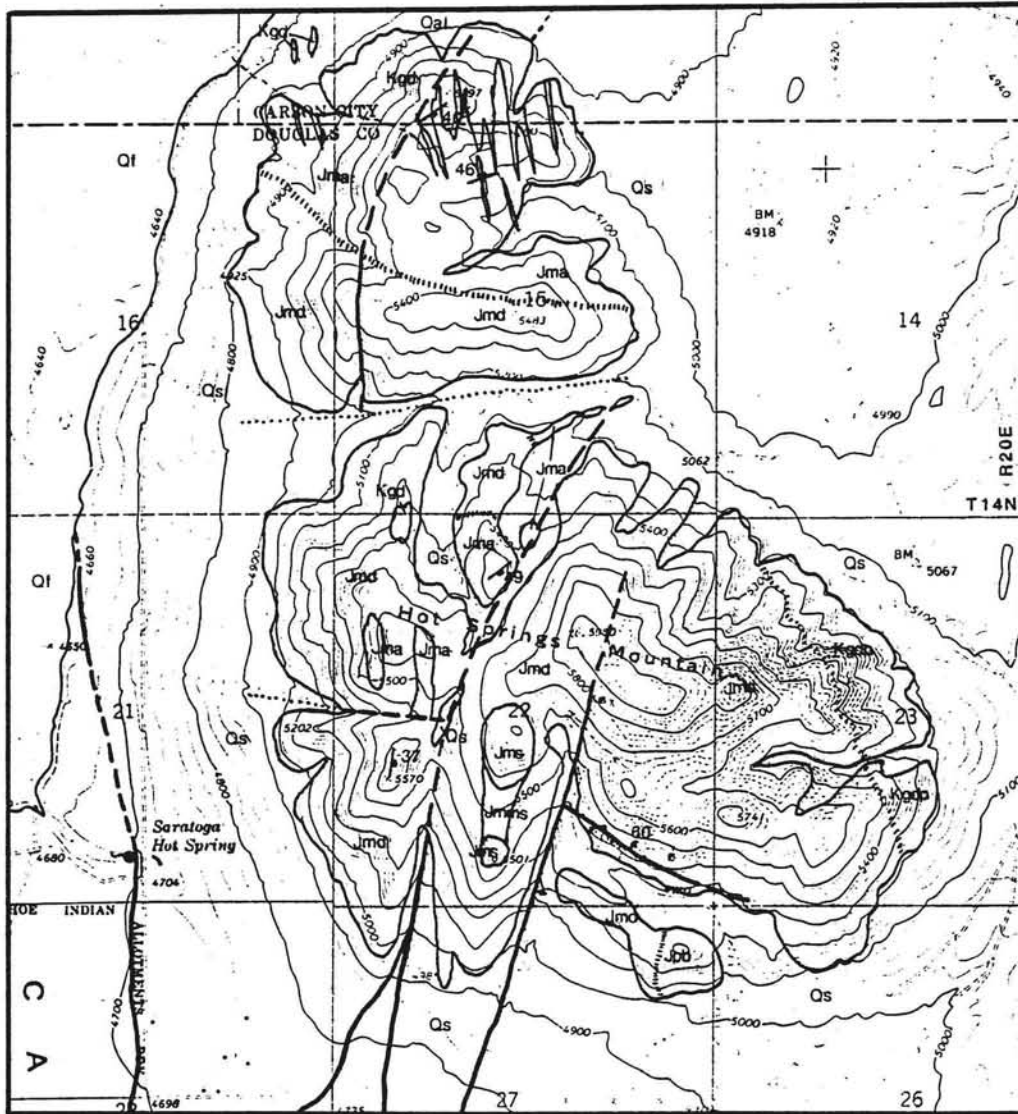
Introduction

Precise Location

Saratoga Hot Spring is in Douglas County, Nevada, about half way between Minden - Gardnerville and Carson City. Saratoga Hot Spring is on Vicky Lane, about 3.2 km east of Highway 395 and about 3.4 km north of Johnson Lane.

The hot spring is in a gully on the west side of Vicky Lane, near the U-shaped house (SW1/4, SW1/4, SE1/4 Sec 21, T14N, R20E) (figure 17). The hot spring issues from a pile of concrete rubble; apparently the rubble was dumped there to stabilize the roadside. Saratoga Hot Spring has reportedly been diverted from the yard of the house 30 m east of the current discharge, via a clay pipe (Staffen, 1984).

A concrete building and dam exist at this site. The dam was built several years ago by a previous owner to pool water for bathing; currently this facility is not used. Flow measurements were made with a 90° V-notch weir, inplaced at the downstream end of the dam underflow channel. A stilling well was constructed on the downstream side of the weir and a Stevens Type-F continuous recorder (7 day clock) was installed. From this point the hot water creek flows about 1 km west, then



Geologic Map Saratoga Hot Spring Area

(geology by B.F. Lyles, 1984)

EXPLANATION

- Qal - Alluvial-Plain Deposits
- Qf - Flood-Plain Deposits
- Qs - Windblown Sand
- Kgd - Biotite-Hornblende Granodiorite
- Kgdpr - Granodiorite Porphyry
- Jmd - Meta-Decite Porphyry
- Jpb - Meta-Welded Tuff and Breccia

- Jma - Meta-Andesite
- Jms - Metasedimentary Rocks
- Jmsm - Mottled Metasedimentary Rocks

----- Contact, dashed where approximated, hash-marked where transitional.

----- Fault, dashed where inferred or approximated, dotted where concealed, arrow shows dip.

49 Joints and Fractures, strike and dip.



Figure 17. Saratoga Hot Spring Geologic Map

north about 1 km to a marsh area at the sewage treatment facility, then north about 2 km to the Carson River.

Several more hot springs occur in the center of the Incline Village Sewage Treatment Facility, approximately 1.5 km N55W of Saratoga Hot Spring (NE1/4, NE1/4 Sec 20, T14N, R20E). These springs will from here on be called Saratoga Marsh Hot Springs, and reportedly will be preserved within the sewage ponds (Roland, personal communication, 1984). These springs contain large quantities of fish and snails, although the average temperature is about 38°C. According to Vinyard (personal communication, 1984), these fish are mosquito fish (*Gambusia affinis*) and were probably planted at the springs to cut down mosquito populations; mosquito fish thrive in warm water, as do the snails.

Climate and Vegetation

Saratoga Hot Spring is at an elevation of 1,433 m. Temperatures range from -10 to 5°C in the winter, and from 15 to 41°C in the summer. Precipitation generally falls as rain; however, small accumulations of snow were observed during this study. The average annual precipitation at Saratoga is about 254-305 mm (Spane, 1977). The Sierra Nevada accumulates approximately 2-3 m of snow annually, while the Pine Nut Mountains only accumulate about 0.5 m at the higher elevations, due to the rain-shadow effect from the Sierra Nevada.

The vegetation near Saratoga Hot Spring is predominantly desert sages and grasses. The hot water creek supports several old cottonwood trees and greasewood along its banks. Many pinyon pines occur on Hot Springs Mountain, primarily in the canyons and at the higher elevations; groundcover in this area is generally desert sages and grasses.

Geology

Geology in the Hot Spring Mountain area has been described by Eisinger (1960), Moore (1969), Spane (1977), and Bingler (1977). Geologic field mapping was conducted at a scale of 1:24,000, and was completed in four days. The descriptive geology from this area is listed in appendix A. Low sun-angle aerial photographs were used to delineate major lineations and structural trends.

Lithologic Interpretations

Ten major lithologic units occur within the study area. A geologic map was produced from the field mapping effort and is presented as figure 17.

The oldest rocks in the area have been mapped as late Triassic to early Jurassic, based on fossil occurrences in the Pine Nut Mountains (Moore, 1969). These rocks make-up five units at Hot Springs Mountain and are composed of moderately to highly metamorphosed sedimentary rocks and

volcanics. The most extensive metamorphic unit in the area has been mapped as meta-dacite porphyry. Local metamorphism has produced epidote hornfels or spotted hornfels. This unit presumably has sedimentary and volcanic interbeds throughout; these have been mapped as meta-andesite, metasedimentary rocks, meta-welded tuff and breccia, and mottled metasedimentary rocks (in decreasing abundance respectively). Metamorphism and structural complexities make depositional history interpretations difficult; however, Moore (1969) and Spane (1977) have interpreted the metamorphism to be due to intrusion of Sierran batholith granitic rocks.

Two granitic units have been mapped at Hot Spring Mountain. Granodiorite porphyry is transitional with the meta-dacite porphyry on the east side of Hot Spring Mountain. A greater abundance of spotted hornfels is apparent along this contact. Biotite-hornblende granodiorite intrudes meta-andesite in the northern portion of the study area. This granitic is a continuation of the granodiorite at Prison Hill to the north, according to Eisinger (1960), Moore (1969), and Spane (1977). Aplite and granodiorite dikes and sills cause contact metamorphism in the meta-andesite.

Three Quaternary sedimentary units have been correlated to Bingler's (1977) New Empire quadrangle geologic map, to the north. These units have been field checked, after being located by aerial photographs, and are as follows: 1) windblown sand is deposited in most

canyons, and borders about 80 percent of Hot Springs Mountain, 2) flood-plain deposits formed by the Carson River, and 3) alluvial-plain deposits occur to the north, between Hot Spring Mountain and Prison Hill.

Mineral Deposits

A mineralized area occurs in the southeast 1/4 of section 22 and has been explored by several adits, shafts, and prospect pits. These workings total approximately 300 m of tunneling, and generally follow a hydrothermal alteration zone. The zone trends approximately N60W and dips about 60NE, and is about 0.75 to 2 m wide.

The mineralization consists of quartz veining and silicification, with occurrences of crystalline calcite, chrysocolla, barite, and pyrite. Dump samples at the upper ventilation shaft (SW1/4, NE1/4 Sec 22) contained well-formed barite crystals, as vein material, and small pyrite crystals in the wallrock.

Structure

Several faults were located within the study area. Saratoga Hot Spring is controlled by a north-south trending structure which is apparent on aerial photographs for a length of approximately 2 km. Several other hot springs (Saratoga Marsh Hot Springs) occur about 1.5 km at N55W of Saratoga Hot Spring (NE1/4, NE1/4 Sec20 T14N

R20E). These springs appear to follow the same general structural trend as Saratoga Hot Spring, but the area has been disrupted by the Incline Village Sewage Treatment Facility and all surface lineations have been destroyed.

Several other lineaments are noticeable on aerial photographs and some were mapped as faults upon field verification. Most of these structures follow a N75-80E trend. The fault in the south center of section 22 (figure 17), has a near vertical dip to the east.

A shallow temperature survey was conducted at Saratoga Hot Spring by Trexler and others (1980), and showed a clear relationship between temperature-probe isotherms and fault structures. The highest temperatures occurred along the Saratoga Hot Spring controlling fault, forming the 26°C isotherm.

Gravity studies were conducted by Trexler and others (1980) to determine the basement rock configurations. A 19 km traverse was completed in the Saratoga area and showed a large structural low about 2 km west of Saratoga Hot Spring. A separate gravity study by the U.S. Geological Survey suggests the presence of a large steeply west-dipping structure in the same area; this structure appears to control the eastern boundary of Eagle and Carson Valleys (Maurer, personal communication, 1983).

Hydrology

The hydrology of Carson Valley has been studied by

Piper (1969), Glancy and Katzer (1975), and Spane (1977).

Regional

The east and west forks of the Carson River start high in the Sierra Nevada, join in Carson Valley, and flow through Carson, Eagle, Dayton, and Churchill Valleys before emptying into Lahontan Reservoir. The average Carson River discharge at the south end of Carson Valley is $11.8 \text{ m}^3/\text{sec}$ or $238,937 \text{ hm}^3/\text{year}$, for 44 years of record (Water Resources Data Nevada, 1983). Up to $3.1 \text{ m}^3/\text{sec}$ can be diverted from the East Fork of the Carson River south of Gardnerville by the Danberg Ranch; the Danberg Ranch reportedly controls most of the surfacewater rights in Carson Valley (Briant, 1984).

Recharge to alluvial aquifers is accumulated three ways: 1) by infiltration of precipitation, 2) by surface runoff from mountainous areas, and 3) by overland flow within and subsurface underflow from adjacent intra-basin mountainous areas (Spane, 1977). Spane (1977) estimated annual recharge for Carson Valley aquifers to be approximately $54,450 \text{ hm}^3$.

A large part of western Carson Valley is characterized by artesian wells and groundwater discharge to the Carson River; Carson River is a gaining river through much of Carson Valley (Spane, 1977). Inspection of Spane's (1977) potentiometric surface contour map shows the area just west of Hot Springs Mountain as a

groundwater discharge area. Much of this area is now covered by the Incline Village Sewage Treatment Facility. After dikes were constructed for leach ponds, soil that previously appeared dry produced water that accumulated on the south sides of dikes. Quick conditions were observed locally as large boulders were dumped into marsh areas to support the dikes.

Local

Saratoga Hot Spring, as previously mentioned, is controlled by a large west dipping fault. Fracture flow at Saratoga was relatively uniform during this study (less than 3 percent variation), averaging 32.35 l/s.

Recharge to Saratoga's thermal reservoir could come from three sources: 1) the Pine Nut Mountains, to the east, 2) the Carson River, and 3) the Sierra Nevada, to the west.

The Pine Nut Mountains are in the rain-shadow of the Sierra Nevada and accumulate relatively small amounts of precipitation (highest elevation precipitation = about 660 mm; Spang, 1977). Stable isotopes ($\delta D = -130$ and $\delta^{18}O = -16.2$; Trexler, et al., 1980) from Saratoga Hot Spring suggest that recharge water accumulated at elevations above 2,286 m (Szecsody, 1980); therefore, it is assumed that very little if any recharge comes from the Pine Nut Mountains.

The Carson River is at the same elevation as Saratoga

Hot Spring some 10 km south, approximately on the same line as the major north trending fault that controls Saratoga Hot Spring. Hot wells are known to exist about 1 km south of Saratoga Hot Spring along this same trend. Stable isotopes from the Carson River ($\delta D = -121$ and $\delta^{18}O = -14.0$; Trexler, et al., 1980) are considerably heavier than Saratoga thermal area; therefore, appreciable recharge is not thought to come from the Carson River.

A major range front fault on the west side of Carson Valley controls two thermal areas along the Sierra Nevada-Carson Valley boundary: Walley's and Hobo Hot Springs (see Walley's Hot Spring, structural geology). Ascending fluids along this fault could presumably communicate, at appreciable depth, with the fault on the east side of Carson Valley (figure 18). Stable isotope values from Saratoga are quite similar to those at Walley's Hot Spring (figure 19); however, stable isotopes at Hobo Hot Springs are considerably heavier, possibly due to mixing with groundwater from Jacks Valley. Therefore, it is assumed that most of Saratoga's recharge water comes from the Sierra Nevada.

Geochemistry

Major Dissolved Constituents

A water sample analysis for Saratoga Hot Spring was reported by Trexler and others (1980). This analysis was

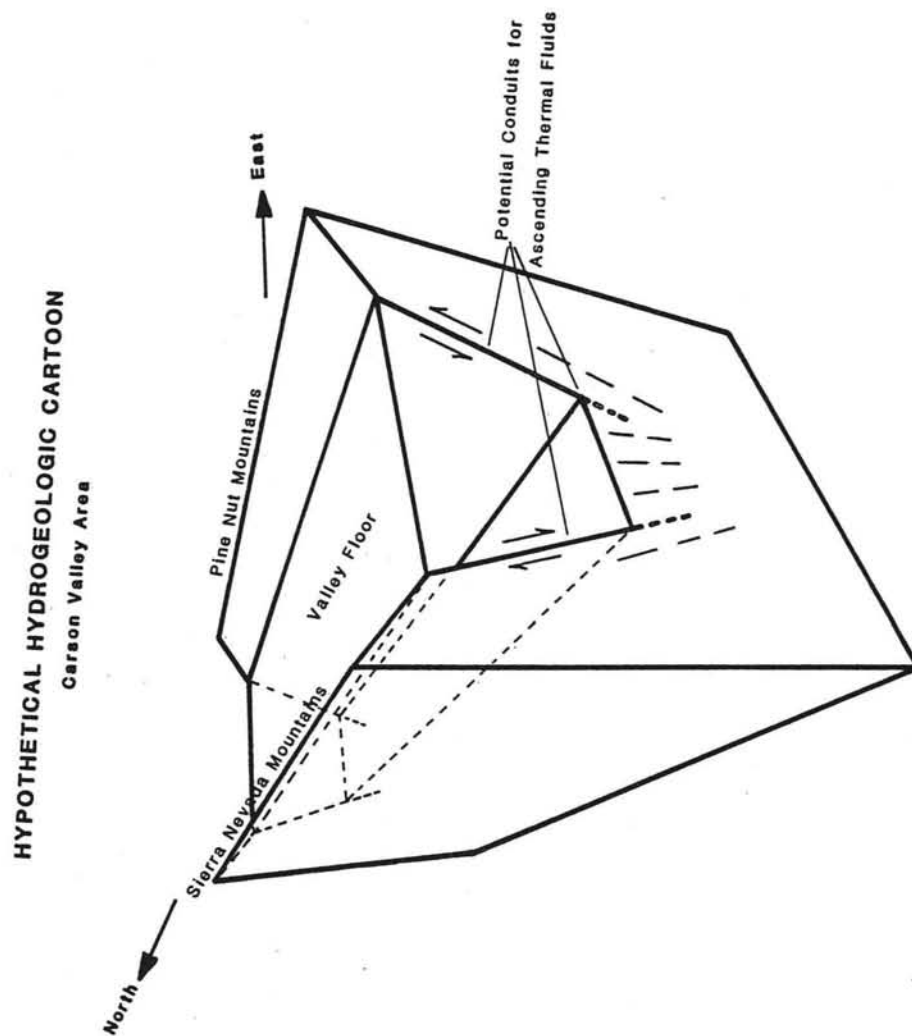


Figure 18. Carson Valley Area
Hypothetical Hydrogeologic Cartoon

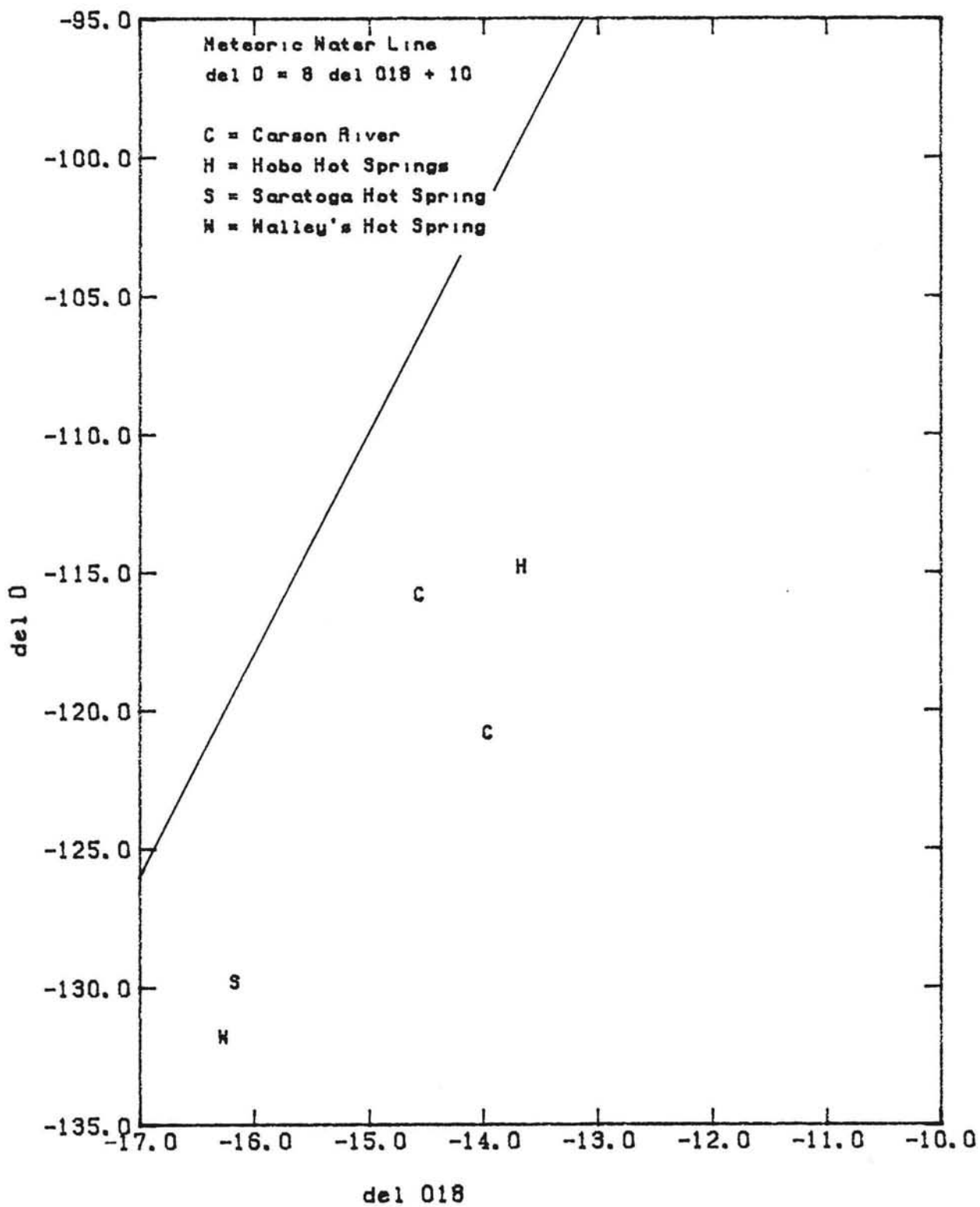


Figure 19. Carson Valley
 del D vs. del 18O

entered into the program "WATEQ" to calculate mineral saturations, cation to anion balance, $p\text{CO}_2$, etc. (figure 24).

The water at Saratoga Hot Spring is a Ca(Na)- SO_4 type water, according to White's classification scheme (1960). Calcium and sodium ions can generally be accounted for in several ways: 1) by dissolution of calcite, 2) by dissolution of gypsum or anhydrite, 3) by dissolution of plagioclase feldspar, and 4) by dissolution of sodium and calcium salts. Sulfate ion can be accounted for: 1) by dissolution of gypsum or anhydrite, 2) by oxidation of sulfide minerals such as pyrite, or 3) by minor dissolution of barite (Drever, 1982).

Based on the regional geology and hydrology, it is assumed that the calcium and sulfate ions are primarily derived from the gypsum, calcite, pyrite, and barite in the metamorphic rocks of Hot Springs Mountain; likewise, the sodium was presumably concentrated along the flow path from dissolution of plagioclase feldspar and sodium salts.

Mineral precipitation

A white precipitate occurs above water level, coating rocks, for approximately 30 m along the course of the hot water stream. A sample was X-rayed and was shown to be gypsum, according to Hefner (1983).

The water temperature along this stream section was about $50 \pm 2^\circ\text{C}$. The computer program "WATEQ" showed that

Table 24 (Saratoga Hot Spring WATEQ output)

*** total concentrations of input species ***					
species	total molality	total mg/liter	epm	epm fraction	
Ca	0.414605e-02	166.0	8.28	0.537	
Mg	0.411749e-05	0.10	0.01	0.001	
Na	0.701043e-02	161.0	7.00	0.454	
K	0.128772e-03	5.03	0.13	0.008	
Cl	0.110120e-02	39.0	1.10	0.076	
SO4	0.642968e-02	617.0	12.8	0.893	
HCO3	0.739907e-04	4.51	0.07	0.005	
SiO2 tot	0.549798e-03	33.0			
F	0.171773e-03	3.26			
B tot	0.126867e-03	1.37			
CO3	0.186833e-03	11.2	0.25		
Fe	0.716991e-06	0.04			
Li	0.144264e-06	0.001			
Sr	0.262772e-04	2.3			
Ba	0.728881e-06	0.10			
NO3	0.161446e-06	0.01			
S	0.671235e-05	0.215			
tds = 1044.14					
*** description of solution ***					
epmcat	analytical 15.495	ph 8.55	pco2 = 0.566888e-04		
epman	14.594		log pco2 = -4.2465		
cation/anion	1.062	temperature	EC = 1857.0		
co2 tot =	0.279364e-03	51.00 deg c	ionic strength 0.202410e-01		
*** mineral saturation ***					
iap/kt	log iap/kt	phase	iap/kt	log iap/kt	phase
0.3488e+00	-0.45744	ANHYDRITE	0.1192e-06	-6.92386	HALITE
0.2649e+01	0.42315	ARAGONITE	0.6305e+07	6.79970	MACKINAWIITE
0.2242e-07	-7.64929	ARTINITE	0.2072e-02	-2.68357	MAGNESITE
0.4765e+01	0.67805	BARITE	0.3488e-09	-9.45741	NATRON
0.1163e-03	-3.93424	BRUCITE	0.2094e+01	0.32104	QUARTZ
0.4168e+01	0.61991	CALCITE	0.3651e+00	-0.43765	SEPIOLITE(C)
0.1321e+00	-0.87920	CELESTITE	0.1422e+00	-0.84718	SIDERITE
0.8558e+00	-0.06760	CHALCEDONY	0.2740e+00	-0.56231	SiO2(A,L)
	-35.99951	CHRYSOTILE	0.1394e+00	-0.85584	STRONTIANITE
0.7214e-02	-2.14185	CLINDENSTITE	0.1399e-06	-6.85422	THENARDITE
0.8798e+00	-0.05563	CRISTOBALITE		7.92014	TREMOLITE
0.1085e+02	1.03533	DIOPSIDE	0.1128e-13	-13.94788	TRONA
0.3525e-01	-1.45283	DOLOMITE		-0.25809	TALC
	-53.16488	FLUORITE	0.7253e-03	-3.13948	WITHERITE
0.8168e-06	-6.08787	FORSTERITE		-2.92260	SEPIOLITE(A)
0.2334e+00	-0.63188	GYPSSUM			

the water was undersaturated with respect to gypsum; apparently gypsum is being concentrated and precipitated above water level, due to evaporation.

Geothermometry

The analytical results of the water sample reported by Trexler and others (1980) were used to calculate several chemical geothermometers (table 25). The calculated temperatures range from 40.0 to 135.1°C. The SiO₂ geothermometers are considered less susceptible to reequilibration as water ascends (Fournier, et al., OFR); Na-K-Ca may give erroneous values due to changing calcium mineral saturations. Therefore, the approximate reservoir temperature is believed to be 80±25°C.

Time Series Analysis Results

Time-variant specific electrical conductivity measurements were made from March 1973 to September 1974, by Spane (1977). A slight positive linear trend was observed during this period.

For this study, data were collected for approximately one year at Saratoga Hot Spring, from September 13, 1983 to August 23, 1984. The average sample interval was 13.5 days (standard deviation = 2.0 days) (table 26).

Crosscorrelation coefficient results, are presented in table 27. There are no significant correlations at the

Table 25 (Saratoga Hot Spring Chemical
Geothermometer Results)

Thermometer	SiO ₂	SiO ₂	Na-K	Na-K	Na-K-Ca	Na-K-Ca	Na-Li
Equation	2	4	6	7	8	9	11
Calculated Temperature (C)	54.73	83.38	134.11	100.31	39.95	50.78	50.58

Table 27 (Saratoga Hot Spring Correlation
Coefficient Matrix)

	Ca	Cl	EC	HCO ₃	Na	pCO ₂	pH	FLOW	PRCIP
PRECIP	0	0	0	0	0	0	0	0	1
FLOW	0	0	0	0	0	0	0	1	
pH	0	0	0	0	.44	-.92	1		
pCO ₂	.37	0	-.36	.32	-.35	1			
Na	-.35	0	0	0	1				
HCO ₃	0	0	0	1					
EC	-.45	0	1						
Cl	0	1							
Ca	1								

Table 28 (Saratoga Hot Spring Correlation
Coefficient Matrix at Varying Lag Positions)

Var 1	Var 2	Lag	Corr. Coef.
PRECIP	leads FLOW	by 24 weeks	.73
PRECIP	leads pH	by 22 weeks	-.53
EC	leads pH	by 2 weeks	.62

Table 26 (Saratoga Hot Spring temoral data)

Date	Time	T(C)	Flow l/s	EC µmhos	pH field	pH lab	HCO ₃ mg/l	Ca mg/l	Cl mg/l	Na mg/l	log pCO ₂	σ ¹⁸ O ‰	σD ‰
9/13/83	15:52	51.0	(31.5)	1510	-	8.84	15.36.8	171.6	166.1	-4.56	-	-	
9/27/83	14:05	51.0	(31.0)	1530	-	8.88	13.37.3	171.6	164.7	-4.63	-	-126	
10/11/83	11:45	51.0	(31.0)	1570	-	8.87	18.37.3	169.0	167.4	-4.49	-	-	
10/25/83	12:29	51.0	(31.0)	1516	-	8.91	18.37.7	170.3	165.0	-4.53	-	-	
11/ 8/83	13:12	51.0	(30.5)	1535	-	8.74	16.37.9	171.6	166.1	-4.42	-	-	
11/22/83	12:49	51.0	(30.5)	1535	8.72	8.96	17.37.3	165.1	167.8	-4.61	-16.3	-124	
12/ 6/83	11:41	51.0	(31.0)	1546	-	8.98	16.37.5	169.0	167.1	-4.66	-	-	
12/20/83	12:21	51.0	(31.5)	1605	-	9.00	16.37.3	169.0	167.4	-4.68	-	-	
1/ 3/84	12:08	51.0	(31.5)	1686	-	9.01	15.37.5	169.0	165.4	-4.73	-	-	
1/10/84	11:52	51.0	(31.5)	1535	8.86	9.16	17.37.2	167.7	168.5	-4.81	-	-	
* 1/21/84	15:38	51.0	29.03	No Sample.	-	-	-	-	-	-	-	-	
1/24/84	10:43	51.0	31.69	1663	-	8.95	13.37.7	152.3	167.4	-4.71	-	-128	
2/ 7/84	11:44	50.5	31.14	1523	8.74	9.01	15.37.5	167.7	166.4	-4.73	-	-	
2/21/84	10:24	50.5	31.14	1634	8.70	8.99	17.37.5	168.4	166.8	-4.64	-	-	
* 2/28/84	10:26	51.0	32.24	2209	8.76	9.11	16.-	-	-	-	-	-	
3/ 6/84	10:19	51.0	32.79	1626	8.89	9.04	15.37.7	169.0	167.4	-4.76	-	-	
* 3/13/84	10:32	51.0	32.24	1583	8.72	9.01	17.-	-	-	-	-	-	
3/20/84	10:20	-	32.24	1549	8.86	8.98	15.37.5	169.0	166.8	-4.70	-	-123	
* 3/27/84	10:22	50.5	32.24	1540	8.72	8.95	16.-	-	-	-	-	-	
4/ 3/84	10:49	51.0	31.69	1540	8.76	8.96	16.37.9	167.7	167.8	-4.64	-	-	
* 4/10/84	11:01	51.0	31.69	1563	8.72	8.82	16.-	-	-	-	-	-	
4/18/84	11:21	51.0	31.69	1551	-	8.86	16.37.9	167.7	164.7	-4.54	-	-	
* 4/24/84	10:02	51.0	31.14	1610	8.74	8.95	16.-	-	-	-	-	-	
5/ 1/84	10:05	51.0	33.35	1561	-	8.85	17.37.5	170.3	167.8	-4.50	-	-	
* 5/ 8/84	10:20	51.0	33.35	1561	8.74	8.96	16.-	-	-	-	-	-	
5/16/84	11:30	51.0	34.49	1561	8.74	8.98	17.37.5	169.0	165.4	-4.63	-15.6	-119	
* 5/23/84	12:47	51.0	34.49	1561	8.75	8.94	17.-	-	-	-	-	-	
5/30/84	12:08	51.0	33.35	1561	8.92	9.01	16.37.5	166.4	168.5	-4.69	-	-	
* 6/ 6/84	12:18	51.0	33.35	1561	8.83	9.02	16.-	-	-	-	-	-	
6/13/84	11:56	51.0	33.35	1583	8.83	9.01	16.37.9	169.0	165.0	-4.69	-	-	
6/20/84	12:55	51.0	33.35	1617	8.91	9.02	17.38.1	169.0	166.4	-4.67	-	-	
* 7/ 5/84	13:16	51.0	33.35	1617	8.80	9.09	17.-	-	-	-	-	-	
7/11/84	12:19	51.0	31.69	1629	8.79	8.90	16.37.5	166.4	165.4	-4.58	-	-	
* 7/17/84	11:16	51.0	31.69	1575	8.77	8.97	17.-	-	-	-	-	-	
7/26/84	11:28	51.0	31.69	1575	8.82	9.03	16.37.9	166.4	169.2	-4.71	-	-118	
* 8/ 2/84	11:19	51.0	31.69	1604	8.82	9.01	16.-	-	-	-	-	-	
8/ 9/84	11:32	51.0	31.69	1604	8.78	9.10	17.37.5	160.0	167.8	-4.75	-	-	
* 8/16/84	11:01	51.0	31.69	1638	8.75	9.01	16.-	-	-	-	-	-	
8/23/84	12:35	51.0	31.69	1638	8.75	9.01	16.37.5	167.7	167.1	-4.69	-	-	
* 8/31/84	16:56	51.0	31.69	-	8.61	-	-	-	-	-	-	-	
Mean		50.9	32.35	1569		8.96	16.37.6	167.7	166.7	-4.64			
Stand Dev		0.2	0.96	55.6		0.09	1.1	0.2	4.4	1.1	0.09		
Coef Variation		0.3	2.96	3.6		1.03	6.9	0.6	2.6	0.7	2.00		

zero lag positions; however, there is a good correlation with precipitation at a 24 week lag and two fair correlations with pH, at 22 and two week lags respectively (table 28).

There is a direct correlation between precipitation and flow, with precipitation leading flow by 24 weeks. This suggests that it takes approximately 24 weeks for the effect of a precipitation event to infiltrate down to the water table, causing a pressure pulse (figure 20).

There is an inverse relationship between precipitation and pH, with precipitation leading pH by 22 weeks. This simply suggests that 22 weeks after a precipitation event, a decrease in pH was observed. There is also a direct relationship between EC and pH, with EC leading pH by 2 weeks. It would make sense to look at the correlation between precipitation and EC at a 20 week lag; however, eventhough the correlation at this point is non-significant ($R = -.34$), an anomalous peak is obvious on the correlagram.

These relationships suggest that the pressure pulse produces a chemical and physical hydrograph that chemically starts about 20 weeks after a major precipitation event, physically peaks at 24 weeks after the event, and presumably trails out for a couple more weeks.

Lead-lag multiple step-wise regression was applied to the temporal data to get a predictive linear equation. When solving for flow, the best fit was found with two

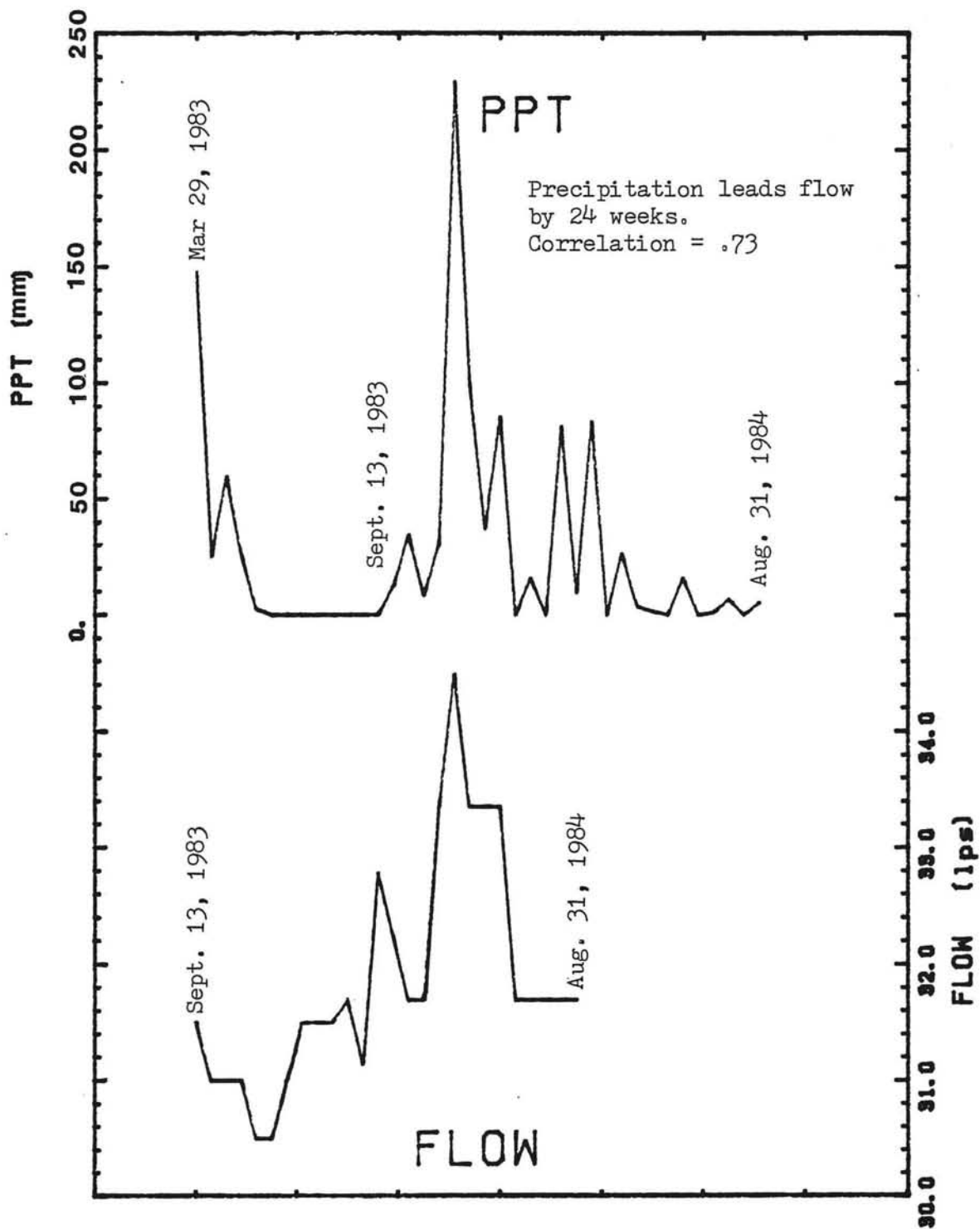


Figure 20. Saratoga Hot Spring
Precipitation and Flow vs. Time

Table 29 (Saratoga Hot Spring Lead-lag
Multiple Regression Output)

Dependent Variable = Flow			
Number of Points = 14			
Step 1			
Variable Entered Precip			
Sum of Squares Reduced in this Step ..		6.120	
Proportion Reduced in this Step528	
Multiple Corr. Coef. Adj. for D.F.727	
F-value for Analysis of Variance		13.426	
Variable	Regression Coefficient	Std. Error of Reg. Coef.	Computed t-value
Precip	.27431	.07486	3.664
Intercept	31.97781		
Step 2			
Variable Entered pH			
Sum of Squares Reduced in this Step ..		2.118	
Proportion Reduced in this Step183	
Multiple Corr. Coef. Adj. for D.F.829	
F-value for Analysis of Variance		9.908	
Variable	Regression Coefficient	Std. Error of Reg. Coef.	Computed t-value
Precip	.28339	.06131	4.623
pH	5.45941	2.07068	2.637
Intercept	-17.06827		
Step 3			
Variable Entered Ca			
Sum of Squares Reduced in this Step ..		.434	
Proportion Reduced in this Step037	
Multiple Corr. Coef. Adj. for D.F.838	
F-value for Analysis of Variance		9.908	
Variable	Regression Coefficient	Std. Error of Reg. Coef.	Computed t-value
Precip	.19590	.09350	2.095
pH	5.59113	2.02908	2.756
Ca	-.06414	.05258	-1.220
Intercept	-7.36558		

Table 29 continued

Step 4			
Variable Entered EC			
Sum of Squares Reduced in this Step ..			.200
Proportion Reduced in this Step017
Multiple Corr. Coef. Adj. for D.F.834
F-value for Analysis of Variance			7.345
Variable	Regression Coefficient	Std. Error of Reg. Coef.	Computed t-value
Precip	.16414	.10282	1.596
pH	5.69219	2.06800	2.753
Ca	-.07113	.05418	-1.313
EC	.00246	.00302	.814
Intercept	-10.91872		
Step 5			
Variable Entered HCO ₃			
Sum of Squares Reduced in this Step ..			.152
Proportion Reduced in this Step013
Multiple Corr. Coef. Adj. for D.F.825
F-value for Analysis of Variance			5.628
Variable	Regression Coefficient	Std. Error of Reg. Coef.	Computed t-value
Precip	.15628	.10657	1.466
pH	3.85765	3.41080	1.131
Ca	-.06085	.05779	-1.053
EC	.00321	.00330	.973
HCO ₃	-.16390	.23791	-.689
Intercept	5.25921		

variables entered (table 29).

The analysis of variance produced an F-value of 13.52, which surpassed the critical $F(2,11,.01)$ equal to 7.21; therefore reject the null hypothesis of "lack of fit" and conclude that there is a good fit.

The analysis of regression coefficient validity produced a t-value greater than 2.64, which surpassed the critical $t(13,.025)$ equal to ± 2.16 . Therefore, reject the null hypothesis that β equal to 0 (regression = 0) and assume each coefficient is valid.

The predictive linear equation is as follows:

$$\text{Flow} = -17.07 + 2.83 \times 10^{-1} * (\text{precip}) + 5.46 * (\text{pH}). \quad (2)$$

Summary

Saratoga Hot Spring is controlled by a north-trending fault that extends along the east side of Carson Valley and may extend into Eagle Valley. The geology east of this fault is complex (predominantly metamorphic rocks) and is a continuation of the rocks of Prison Hill, to the north. Several other small hot springs (Saratoga Marsh Hot Springs) occur about 1.5 km northwest of Saratoga Hot Spring; these springs are also controlled by north-trending faults.

The water at Saratoga Hot Spring is a Ca(Na)-SO₄ type water. The soluble ions are presumably from the dissolution of minerals such as plagioclase feldspar and gypsum-anhydrite, and by oxidation of sulfide minerals.

gypsum was observed precipitating on rocks above the water surface due to evaporative concentration. Silica chemical geothermometers yield an approximate reservoir temperature of $80 \pm 25^\circ\text{C}$. Environmental isotopes suggest that recharge occurs at relatively high elevations, and is thought to come from the Sierra Nevada.

Time-series analysis revealed interesting relationships between precipitation, spring flow, and water chemistry. Infiltration causes a pressure pulse as precipitation recharge reaches the watertable; this phenomenon produces a chemical and physical hydrograph that chemically starts about 20 weeks after a major precipitation event and physically peaks about 24 weeks after the event. Precipitation and pH variability can most suitably account for spring discharge variations.

Walley's Hot Spring

Introduction

Pioneers of the 1800's made a trail along the east side of Carson Valley (Emigrant Trail); this was also the Pony Express Route. The springs were named after David Walley, who built a 40 room hotel and mineral spa here in 1862; this facility was destroyed by fire and was completely demolished by 1929-1930 (Garside and Schilling, 1979).

Within the last five years a newly built mineral spa has been utilizing this thermal resource - "Walley's Hot Spring Resort and Country Club, Inc.". This facility obtains its hot water from two wells and the Brockliss Slough has been diverted about 300 m east by the resort owners to insure their warm water resource.

Precise Location

Walley's Hot Springs are in Douglas County, Nevada, about 3 km (1.8 miles) south of Genoa, Nevada, along Foothill Road. The hot springs occur at a topographic depression, for approximately 1 km along the Genoa Fault Zone.

All of the springs are on the east side of Foothill Road and discharge into the Brockliss Slough. The hot spring monitored in this study is about 50 m from the

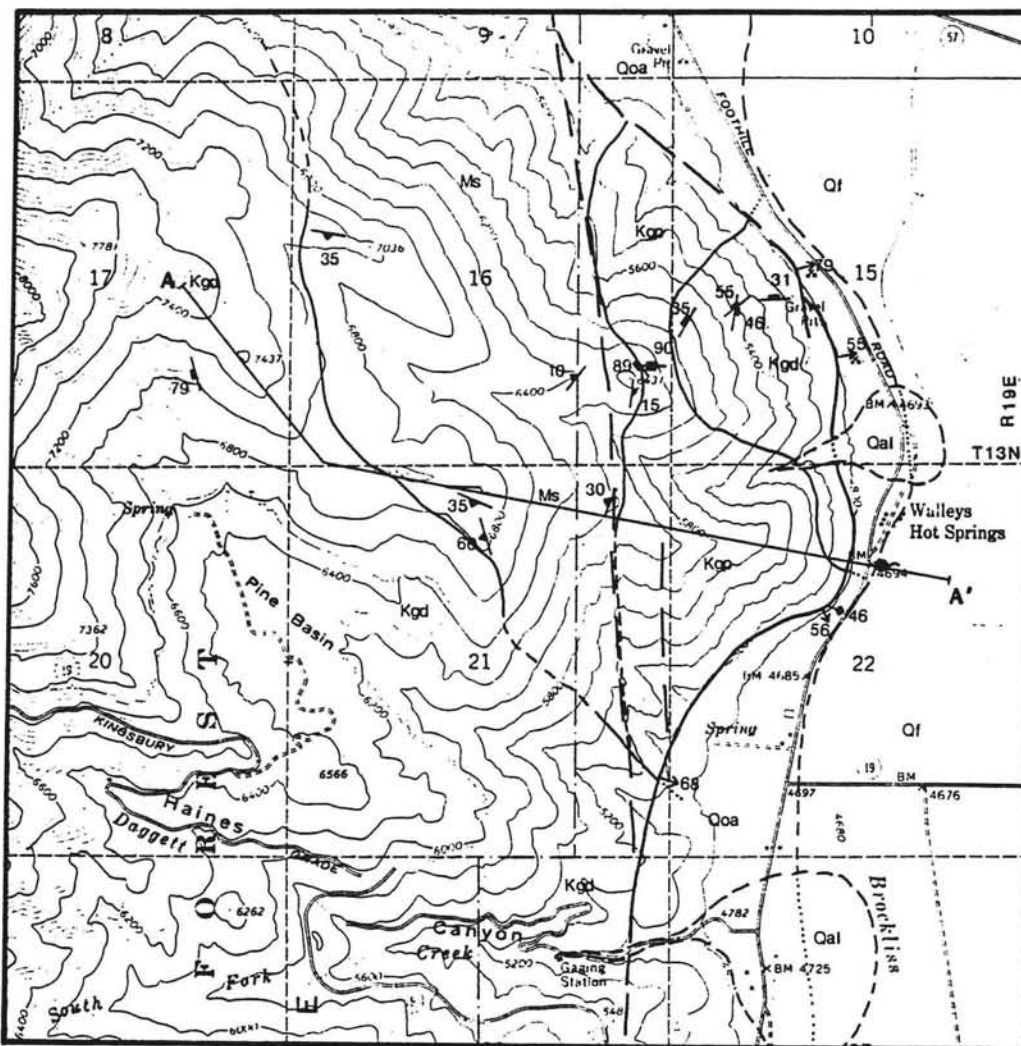
Genoa Fault scarp and 200 m south of Walley's Hot Spring Resort (NW1/4, SW1/4, NE1/4 Sec 22, T13N, R19E) (figure 21). The hot spring issues from a pool (1 m wide, 3 m long, and 6 cm deep) and flows into Brockliss Slough, about 10 m to the east. A 0.5 m long section of 4 inch ABS pipe was cemented in place, between the pool and the slough, so that a bucket and stopwatch could be used for flow measurements.

Several of the near-by pools are slightly cooler (35°C) and support many Mosquito Fish (see Saratoga Precise Location).

Climate and Vegetation

Walley's Hot Springs are at an elevation of about 1,423 m. Air temperatures range from -10 to 5°C in the winter, and from 15 to 41°C in the summer. Generally precipitation falls as rain, with occasionally accumulations of snow. Precipitation on the west side of Carson Valley is greater than an equivalent elevation on the east side; average annual precipitation at Walley's is about 381 mm. The precipitation monitoring site at Spooner Summit (13 km northwest, elevation = 2,213 m) collected 2,220 mm of snow; the total precipitation equaled 799.85 mm during the study period (Klieforth, et al., 1984).

Vegetation near the hot springs is predominated by sages and grasses. The marsh and slough areas to the east



Geologic Map Walley's Hot Spring Area

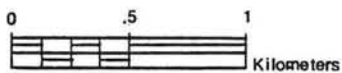
(geology by B.F. Lyles, 1984)

EXPLANATION

- Qal - Alluvial-Plain Deposits
- Qf - Flood-Plain Deposits
- Qoa - Older Alluvial-Plain Deposits
- Kgd - Homblende-Biotite Granodiorite
- Kgp - Granodiorite Porphyry
- Ms - Metamorphic Schistose Rocks

----- Contact, dashed where approximated, dotted where concealed.

----- Fault, dashed where inferred or approximated, dotted where concealed, arrow showing dip, diamond showing trend and plunge



51 Joints and Fractures, strike and dip.

10 Foliation, strike and dip.

Figure 21. Walley's Hot Spring Geologic Map

are covered with green grasses and tules year-round. The Sierra Nevada support thick forests of pines, cedars and hemlock at high elevations, and pines, junipers, sages, and grasses at lower elevations (manzonita and buckbrush occur in drainages).

Previous Work

Regional hydrology studies have been conducted by Glancy and Katzer (1975) and a water budget study for Carson Valley has been conducted by Piper (1969). The hydrogeochemistry of Carson Valley has been studied in depth by Spane (1977). The mineral and thermal resources were evaluated in 1962-1963 by U.S. Steel Inc., and an assessment of the geothermal resource was conducted by Trexler, et al. (1980). Geologic mapping of the quadrangles to the north and west was conducted by Pease (1980) and by Bonham and Burnett (1976), respectively.

Geology

No detailed geologic studies had been conducted in Walley's Hot Spring area; therefore, geologic mapping was conducted at a scale of 1:24,000 over three days (spring 1984). Major lithologic distinctions were based on the units previously mapped in the Genoa and South Lake Tahoe 7.5' quadrangles (Pease, 1980, and Bonham, et al., 1976, respectively). Refer to appendix A for detailed geologic

descriptions.

Lithologic Interpretations

Metamorphic schistose rocks make up the oldest unit in the area, and were probably volcanic rocks before metamorphism. These rocks are pre-Cretaceous and are generally located west of the Genoa Fault zone (figure 21). Foliation in these rocks is marked by light and dark stripes of plagioclase / quartz and hornblende / biotite. Although this unit is moderately to highly fractured, competent outcrops are common along ridges.

Cretaceous, hornblende-biotite granodiorite occurs west of the metamorphic rocks and in the southwest corner of section 15 (figure 21). The granitic to metamorphic contact ranges from sharp to transitional; sharp contacts have large amounts of hornblende associated with them.

Granodiorite porphyry crops out between the metamorphic rocks and the granodiorite in the southwest corner of section 15. Most outcrops are composed of a fine-grained, hornblende and biotite bearing unit with phaneritic groundmass.

The Quaternary sediments have been divided into three units: 1) older alluvial-plain deposits along the valley-mountain boundary, 2) flood-plain deposits formed by the Carson River, and 3) alluvial material primarily at the mouths of canyons.

Structure

The Genoa Fault is the most prominent structure along the west side of Carson Valley; it can be mapped for several kilometers north and south of Walley's Hot Springs. An early description of this fault was made by Lawson (1912), and a portion is as follows:

"The displacement which caused the scarp was doubtless accompanied by an earthquake of the first class. Taking forty-four feet as the measure of the displacement at Walley's Hot Spring, it may be pointed out that this figure is close to the limit of the amount of displacement which, so far as we know, may occur in a single sudden movement; and that displacements of this order cause the most violent earthquakes of which we have any knowledge."

Aerial photographs proved useful for preliminary locations of lineaments in the area. Field mapping efforts located a north trending, near linear, splay of the Genoa Fault, about 1 km west of Walley's Hot Spring (figure 22). This structure is presumably older than the current fault scarp located about 70 m west of Walley's.

The current fault scarp at Walley's Hot Spring makes a sharp bend (almost 90°) near the hot springs. This bend could possibly represent an intersection of several structures, allowing thermal fluids to ascend along highly permeable fracture channels.

A drilling program was conducted in the area by the U.S. Steel Corp., during 1962 and 1963. Down-hole

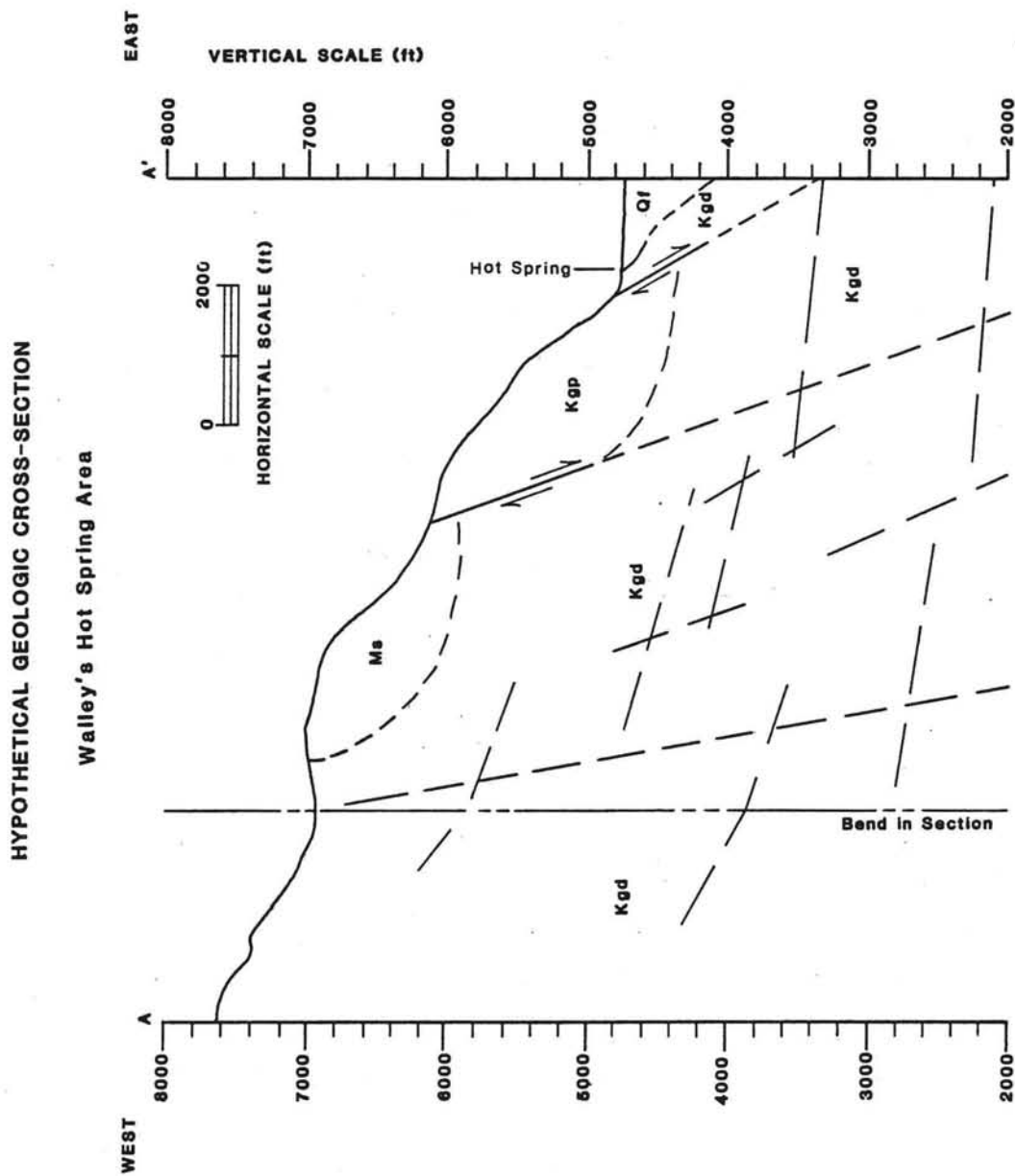


Figure 22. Walley's Hot Spring
Hypothetical Geologic Cross-section

temperature profiles were used to generate an isotherm contour map; contours represent the highest down-hole temperature (Garside and Schilling, 1979). Temperatures decreased easterly, away from the fault zone; the highest temperature was about 83°C and was within 30 m of the Genoa Fault.

Hydrology

The hydrology of Carson Valley has been studied by Piper (1969), Glancy and Katzer (1975), and Spane (1977).

Regional

The east and west forks of the Carson River start high in the Sierra Nevada, join in Carson Valley, and flow through Carson, Eagle, Dayton, and Churchill Valleys before emptying into Lahonton Reservoir. The average Carson River discharge at the south end of Carson Valley is 11.8 m³/sec or 238,939 hm³/year, for 44 years of record (Water Resources Data Nevada, 1983). Up to 3.1 m³/sec can be diverted from the East Fork of the Carson south of Gardnerville for irrigation by the Danberg Ranch; the Danberg Ranch reportedly controls most of the surfacewater rights in Carson Valley (Briant, 1984).

Recharge to alluvial aquifers is accumulated three

ways: 1) infiltration of precipitation, 2) surface runoff from mountainous areas, and 3) overland flow within and subsurface underflow from adjacent intra-basin mountainous areas (Spane, 1977). Spane (1977) estimated annual recharge for Carson Valley aquifers to be approximately 54,450 hm³).

A large part of western Carson Valley is characterized by artesian wells and groundwater discharge to the Carson River; Carson River is a gaining river for much of Carson Valley (Spane, 1977). The area near Walley's Hot Springs is characterized by several marshes and sloughs, and the east and west forks of the Carson River join about two km to the northeast.

Local

Walley's Hot Springs are controlled by the Genoa Fault zone, and appear to discharge from this point due to fault intersections and a local topographic low. Average flow from the hot springs is approximately 4.0 l/s.

voir is from the Sierra Nevada, to the west. Stable isotopes ($\delta D = -132$ and $\delta^{18}O = -16.3$; Trexler, et al., 1980) suggest that recharge occurs at relatively high elevations. These isotopic values are quite similar to those at Saratoga Hot Spring (see Saratoga Local Hydrology).

Geochemistry

Major Dissolved Constituents

A water sample analysis (Trexler, et al., 1980) was entered into the program "WATEQ" to calculate mineral saturations, cation to anion balance, pCO_2 , etc. (table 30).

The water at Walley's Hot Spring is a Na-SO₄ type water. Sodium ion is generally accounted for two ways: 1) by dissolution of plagioclase feldspar, and 2) by dissolution of sodium salts. Sulfate ion is accounted for: 1) by dissolution of gypsum - anhydrite, and 2) by oxidation of sulfide minerals such as pyrite (Drever, 1982).

The computer program "WATEQ" showed several minerals above saturation, including silicates, sulfates, and carbonates. Most of these minerals were very close to saturation. Only the silicates mackinawite and tremolite were appreciably above saturation.

Geothermometry

The results of the water analysis from Trexler and others (1980) were entered into several chemical geothermometers, results in table 31. The calculated

Table 30 (Walley's Hot Spring WATEQ output)

*** total concentrations of input species ***					
species	total molality	total mg/liter	epm	epm fraction	
Ca	0.244887e-03	9.81	0.49	0.078	
Mg	0.205766e-05	0.05	0.00	0.001	
Na	0.565761e-02	130.0	5.65	0.905	
K	0.101838e-03	3.98	0.10	0.016	
Cl	0.128405e-02	45.5	1.28	0.183	
SO4	0.213515e-02	205.0	4.25	0.610	
HCO3	0.311548e-04	1.9	0.03	0.004	
SiO2 tot	0.120392e-02	72.3			
F	0.245411e-03	4.66			
B tot	0.143460e-03	1.55			
CO3	0.710256e-03	42.6	0.97		
Fe	0.537460e-06	0.03			
Li	0.288375e-05	0.02			
Sr	0.228377e-06	0.02			
Ba	0.728497e-06	0.10			
NO3	0.968167e-06	0.06			
tds = 517.580					
*** description of solution ***					
epmcat	analytical 6.259	ph 9.08	pco2 = 0.444486e-04		
epman	7.252		log pco2 = -4.3521		
cation/anion	0.863	temperature 58.00 deg c	EC = 778.0		
			ionic strength 0.876632e-02		
*** mineral saturation ***					
iap/kt	log iap/kt	phase	iap/kt	log iap/kt	phase
0.1336e-01	-1.87404	ANHYDRITE	0.1453e+03	2.16225	KEROLITE
0.1733e+01	0.23879	ARAGONITE	0.1897e+08	7.27808	MACKINAWITE
0.2086e-05	-5.68067	ARTINITE	0.1301e-01	-1.88583	MAGNESITE
0.2157e+01	0.33388	BARITE	0.1699e-07	-7.76970	MIRABILITE
0.1919e-02	-2.71696	BRUCITE	0.4309e-05	-5.36567	NAHCOLITE
0.3043e+01	0.48337	CALCITE	0.1375e-08	-8.86178	NATRON
0.6487e-03	-3.18794	CELESTITE	0.2570e+01	0.40985	QUARTZ
0.1107e+01	0.04408	CHALCEDONY	0.1390e+03	2.14317	SEPIOLITE(C)
	-31.66337	CHRYSSOTILE	0.1253e+01	0.09800	SIDERITE
0.1479e+00	-0.83017	CLINDENSTITE	0.3563e+00	-0.44813	SiO2(A,L)
0.1105e+01	0.04344	CRISTOBALITE	0.1223e-01	-1.91275	STRONTIANITE
0.4138e+03	2.61680	DIOPSIDE		3.49762	TALC
0.1834e+00	-0.73656	DOLOMITE	0.5306e-07	-7.27523	THENARDITE
	-54.20407	FLUORITE		14.79675	TREMOLITE
0.3012e-03	-3.52112	FORSTERITE	0.2791e-12	-12.55426	TRONA
0.8773e-02	-2.05685	GYPSUM	0.7070e-02	-2.15059	WITHERITE
0.1254e-06	-6.90154	HALITE		0.06865	SEPIOLITE(A)

Table 31 (Walley's Hot Spring Chemical Geothermometer Results)

Thermometer	SiO ₂	SiO ₂	SiO ₂	Na-K	Na-K
Equation	1	2	4	6	7
Calculated Temperature (C)	69.21	91.34	119.84	132.91	99.00
Thermometer	Na-K-Ca	Na-K-Ca	Na-K-Ca	Na-Li	
Equation	8	9	10	11	
Calculated Temperature (C)	86.93	67.13	136.22	105.44	

Table 33 (Walley's Hot Spring Correlation Coefficient Matrix for 52 Weeks)

	Ca	Cl	EC	HCO ₃	pCO ₂	pH	FLOW	STAGE	TEMP	PRECIP
PRECIP	-.43	0	0	0	.36	0	.72	.53	0	1
TEMP	-.55	0	0	0	0	0	0	0	1	
STAGE	0	-.54	0	0	.38	-.40	.90	1		
FLOW	-.41	-.52	0	0	.46	-.48	1			
pH	0	.35	.33	0	-.99	1				
pCO ₂	0	-.37	-.34	0	1					
HCO ₃	0	0	0	1						
EC	0	0	1							
Cl	0	1								
Ca	1									

Table 34 (Walley's Hot Spring Correlation Coefficient Matrix at Varying Lag Positions for 52 Weeks)

Var 1		Var 2		Lag	Corr. Coef.
FLOW	leads	Ca	by	18 weeks	.92
FLOW	leads	Cl	by	2 weeks	.62
EC	leads	pH	by	5 weeks	.69

temperatures ranged from 67.1 to 136.2°C.

The calculated temperatures are in question due to the possibility of mixing thermal water with near-surface, cold water. The SiO₂ geothermometers are less susceptible to reactions and reequilibrations due to dilution than the Na-K and Na-K-Ca geothermometers (Fournier, et al., OFR, and Benjamin, 1983); therefore, the approximate reservoir temperature is estimated to be 90±20°C.

Time-Series Analysis Results

Data were collected at Walley's Hot Springs for approximately one year, from September 13, 1983 to August 23, 1984. The average sample interval was 13.5 days (standard deviation = 2.0 days) (table 32). A new hydrologic dynamic equilibrium was established in June, 1984, due to the diversion of Brockliss Slough; therefore, the data will be analyzed twice: case 1, will contain all 52 weeks of data, and case 2, will only contain the first 38 weeks of data.

Correlation coefficient results for case 1 are presented in table 33. Six of the coefficients are greater than 50 percent, of which two are greater than 70 percent. Excellent direct correlations exist between slough stage and spring flow, and between precipitation and spring flow (figures 23 and 24 respectively). The correlograms of these relationships suggest that flow is

Table 32 (Walley's Hot Spring temporal data)

Date	Time	T(C)	Flow l/s	EC µmhos fld	pH fld	pH lab	HCO ₃ mg/l	Cl mg/l	Ca mg/l	Stage (cm)	log pCO ₂	σ ² σD %	σD %
9/13/83	14:19	48.0	0.35	780	-	9.18	56.	46.6	10.47	(60.0)	-4.31	-	-
9/27/83	12:58	51.0	0.38	700	-	9.27	59.	46.0	10.18	(60.0)	-4.37	-	-122
10/11/83	10:56	49.5	0.38	870	-	9.36	57.	46.4	10.08	64.77	-4.47	-	-
10/25/83	11:18	46.5	0.34	837	-	9.23	59.	46.6	10.27	50.80	-4.35	-	-
11/ 8/83	11:13	46.0	0.37	812	9.04	9.31	54.	46.8	10.18	26.04	-4.47	-	-
11/22/83	11:59	52.0	-	812	8.52	9.19	55.	46.8	9.59	103.51	-4.31	-15.1	-115
12/ 6/83	10:57	51.0	0.74	842	-	9.04	54.	45.6	9.88	89.54	-4.18	-	-
12/20/83	12:46	48.0	0.60	836	-	9.36	57.	46.0	10.47	84.77	-4.48	-	-
1/ 3/84	11:27	50.0	0.70	903	-	9.39	59.	45.4	10.08	88.27	-4.50	-	-
1/10/84	10:56	47.0	0.57	793	9.16	9.27	60.	46.4	10.08	78.74	-4.37	-	-
1/24/84	9:55	46.0	0.48	870	-	9.26	59.	45.6	10.18	74.93	-4.38	-	-113
2/ 7/84	10:28	46.0	0.42	822	9.20	9.36	59.	45.6	10.18	68.58	-4.48	-	-
2/24/84	9:41	45.0	0.51	850	9.09	9.33	59.	45.8	10.18	72.39	-4.45	-	-
‡ 2/28/84	9:20	45.0	0.44	848	9.06	9.49	56.	-	-	67.31	-	-	-
3/ 6/84	9:34	45.5	0.41	836	9.10	9.52	56.	45.6	10.27	65.41	-4.66	-	-
‡ 3/13/84	9:39	43.0	0.42	856	9.05	9.35	57.	-	-	62.23	-	-	-
3/20/84	9:40	-	0.44	834	9.32	9.38	57.	47.4	11.15	69.22	-4.52	-	-109
‡ 3/27/84	9:30	48.0	-	819	8.94	9.35	56.	-	-	103.51	-	-	-
4/ 3/84	9:55	49.0	0.36	819	9.10	9.45	59.	46.2	10.76	66.04	-4.56	-	-
‡ 4/10/84	9:57	40.0	0.37	859	9.06	9.22	57.	-	-	78.74	-	-	-
4/18/84	10:48	45.0	0.34	835	-	9.24	59.	46.4	10.86	60.96	-4.36	-	-
‡ 4/24/84	9:11	46.0	0.28	835	9.07	9.31	56.	-	-	45.09	-	-	-
5/ 1/84	8:59	45.0	0.31	836	-	9.18	55.	46.4	10.66	45.09	-4.33	-	-
‡ 5/ 8/84	9:16	49.5	0.36	836	9.07	9.31	55.	-	-	59.69	-	-	-
5/16/84	10:32	51.5	0.49	836	9.20	9.40	50.	46.6	10.47	80.01	-4.57	-	-
‡ 5/23/84	12:11	50.5	0.42	836	9.20	9.44	55.	-	-	73.66	-	-	-
5/30/84	11:31	46.0	0.42	836	9.17	9.48	59.	47.4	10.47	73.66	-4.60	-14.1	-111
‡ 6/ 6/84	11:22	44.0	0.34	836	9.40	9.48	55.	-	-	104.14	-	-	-
6/13/84	10:57	49.0	0.26	874	9.14	9.49	59.	47.0	10.47	19.05	-4.60	-	-
6/20/84	11:43	50.5	0.25	864	9.16	9.41	60.	47.4	10.47	15.24	-4.50	-	-
‡ 7/ 5/84	12:36	53.0	0.23	836	9.12	9.55	59.	-	-	15.24	-	-	-
7/11/84	10:56	50.5	0.20	839	9.20	9.29	60.	46.4	10.27	15.24	-4.38	-	-
‡ 7/17/84	10:34	50.5	0.18	840	9.03	9.46	61.	-	-	15.24	-	-	-
7/26/84	10:53	50.0	0.18	840	9.05	9.47	59.	46.8	10.27	15.24	-4.57	-	-109
‡ 8/ 2/84	10:41	48.5	0.15	853	9.05	9.45	59.	-	-	-	-	-	-
8/ 9/84	10:57	49.5	0.14	852	9.15	9.51	56.	47.2	10.27	15.24	-4.63	-	-
‡ 8/16/84	10:26	46.5	0.13	874	9.15	9.48	56.	-	-	15.24	-	-	-
8/23/84	11:45	46.5	0.12	874	9.12	9.48	56.	47.6	10.27	15.24	-4.62	-	-
Mean		47.5	0.32	841		9.38	58.	46.1	10.36	56.84	-4.46		
Stand Dev		2.9	0.13	26.6		0.10	2.7	0.5	0.42	27.30	0.12		
Coef Variation		6.1	40.5	3.2		1.11	4.7	1.1	4.03	48.03	2.71		

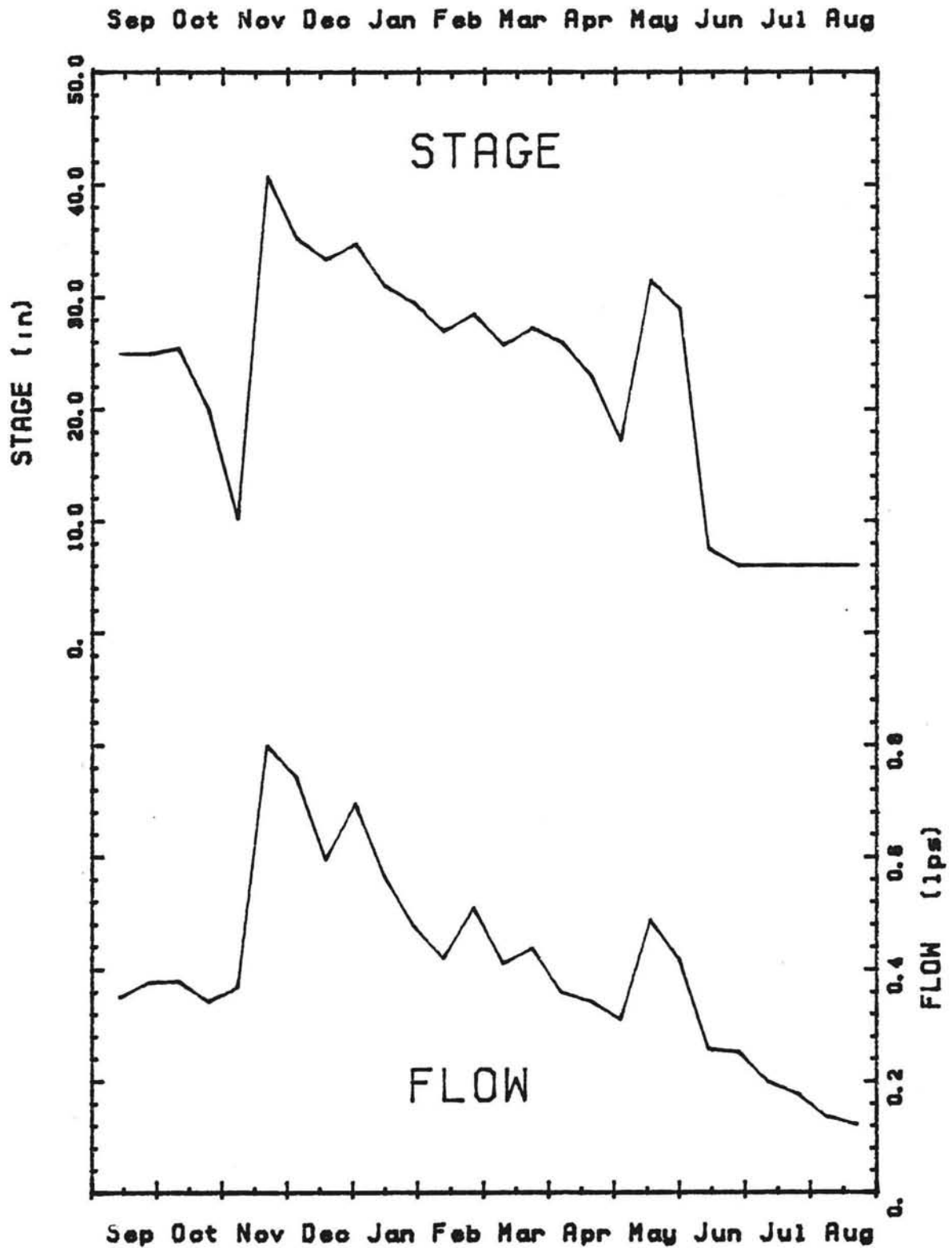


Figure 23. Walley's Hot Spring
Stage and Flow vs. Time

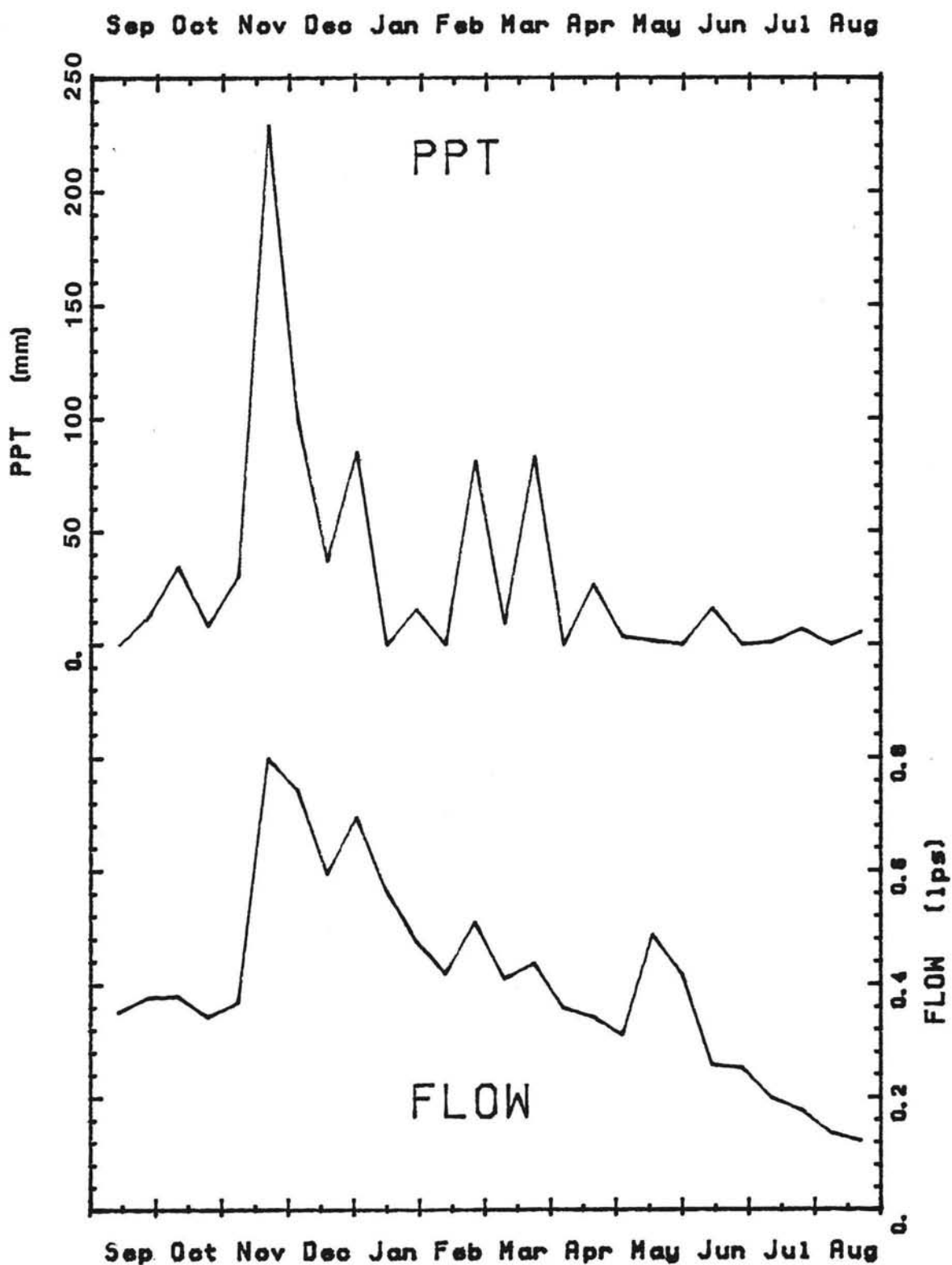


Figure 24. Walley's Hot Spring
Precipitation and Flow vs. Time

primarily controlled by slough stage fluctuations and secondarily controlled by local precipitation infiltration; each source takes somewhat less than two weeks to reach the thermal watertable, causing a pressure pulse.

A fair direct correlation exists between precipitation and slough stage (figure 25). This relationship is not as great as expected due to several factors: 1) stream diversion practices are not uniform during storms or from one storm to the next, thereby arbitrarily modifying the stream hydrographs and flood-flow frequencies, and 2) stream hydrographs are much more attenuated than the near instantaneous precipitation events that generated them due to stream hydrodynamics and stream diversion practices.

The only other relationship of interest is a fair inverse correlation between flow/stage and chloride ion. This is presumably caused by fresh (low Cl^-) surfacewater mixing with ascending thermal water; however, the coefficient of variation for chloride ion suggests that all of the variation may be accounted for by analytical and sampling errors.

Correlation coefficient results for case 2 are presented in table 35. Most of the correlation information for case 2 is very similar to case 1; however, an interesting direct relationship can now be observed between flow/stage and temperature (figure 26). This, combined with the previous information, suggests

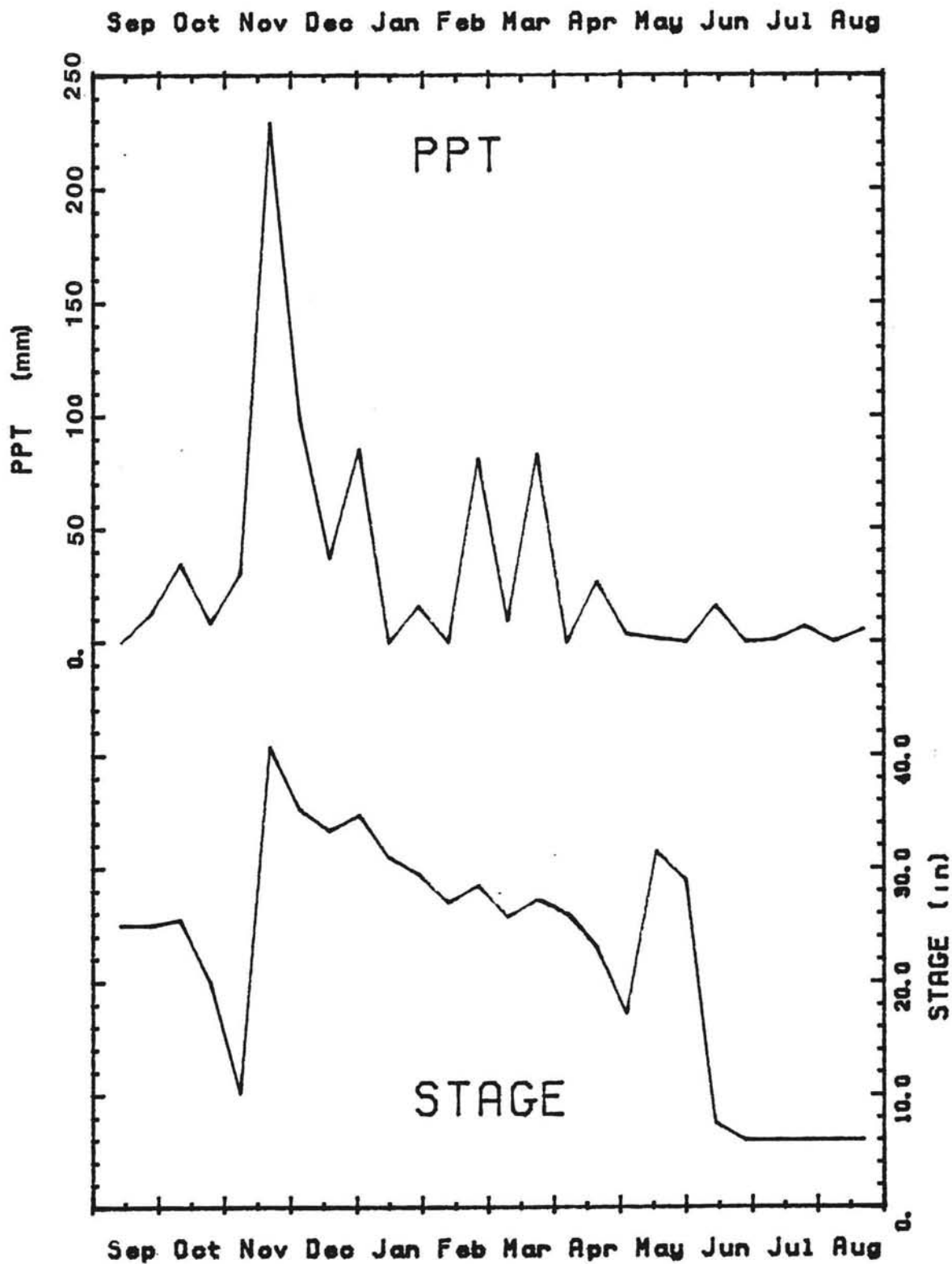


Figure 25. Walley's Hot Spring
Precipitation and Stage vs. Time

Table 35 (Walley's Hot Spring Correlation Coefficient Matrix for 38 Weeks)

	Ca	Cl	EC	HCO ₃	pCO ₂	pH	FLOW	STAGE	TEMP	PRECIP
PRECIP	-.44	0	0	0	0	0	.76	.59	0	1
TEMP	-.61	0	0	0	0	0	.49	.51	1	
STAGE	-.39	0	0	0	0	0	.84	1		
FLOW	-.60	0	0	0	0	0	1			
pH	0	0	0	0	-.99	1				
pCO ₂	0	0	0	0	1					
HCO ₃	0	0	0	1						
EC	0	0	1							
Cl	.39	1								
Ca	1									

Table 36 (Walley's Hot Spring Correlation Coefficient Matrix at varying Lag Positions for 38 Weeks)

Var1		Var2	Lag	Corr. Coef.
FLOW	leads	HCO ₃ ⁻	by 6 weeks	.60
Ca	leads	HCO ₃ ⁻	by 8 weeks	.73
FLOW	leads	Cl ⁻	by 2 weeks	-.52
pCO ₂	leads	EC	by 4 weeks	.51

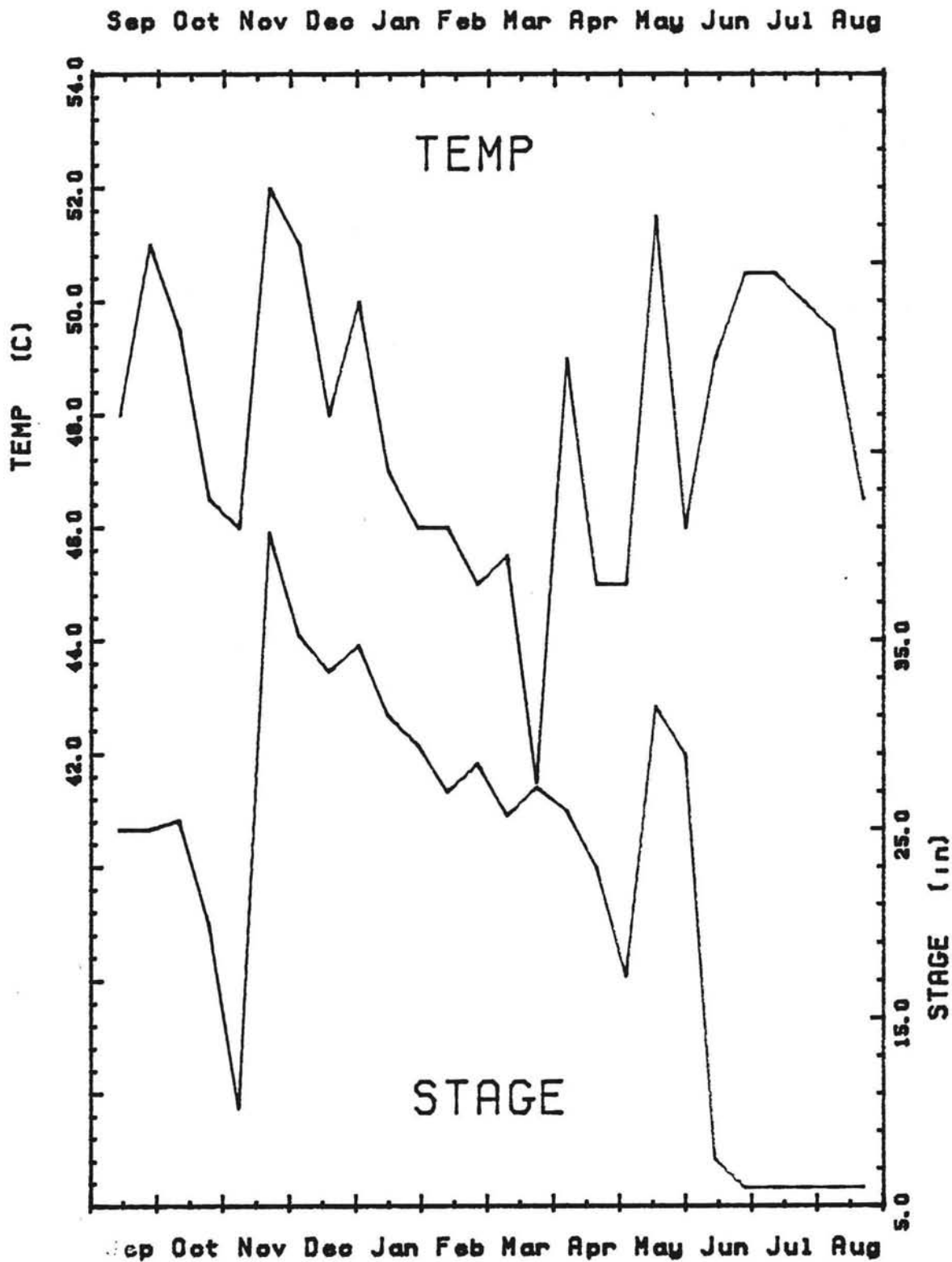


Figure 26. Walley's Hot Spring
Temperature and Stage vs. Time

that infiltrating surfacewaters produce a pressure pulse which drives the hot water in the upper part of the thermal system.

Several significant correlations exist at varying lag positions, for case 1 and case 2 (table 34 and table 36, respectively). In both cases a fair inverse correlation exists between flow and chloride ion, with flow leading chloride ion by about two weeks. This relationship suggests that it takes about two weeks for surfacewater to dilute the ascending thermal fluids; however, as previously mentioned, all of the chloride variation may be accounted for by human and analytical errors.

Lead-lag multiple step-wise linear regression was applied to the temporal data in an attempt to get a meaningful predictive equation. When solving for flow in case 1, the best fit was found when one independent variable was entered; therefore, this equation will have little or no meaning and this data will not be interpreted any further. Lead-lag regression was also applied to case 2 and when solving for flow, the best fit was obtained when three independent variables were entered (figure 37).

The analysis of variance gave an F-value equal to 44.60, which easily passes the $F(3,10,.01)$ equal to 6.55. Therefore, reject the null hypothesis of "lack of fit" and conclude the fit is good.

The analysis of regression coefficient validity

Table 37 (Walley's Hot Spring Lead-lag
Multiple Regression Output)

Dependent Variable = Flow			
Number of Points = 14			
Step 1			
Variable Entered Stage			
Sum of Squares Reduced in this Step ..		.264	
Proportion Reduced in this Step884	
Multiple Corr. Coef. Adj. for D.F.940	
F-value for Analysis of Variance		91.423	
Variable	Regression Coefficient	Std. Error of Reg. Coef.	Computed t-value
Stage	.02453	.00257	9.562
Intercept	-.20854		
Step 2			
Variable Entered EC			
Sum of Squares Reduced in this Step ..		.007	
Proportion Reduced in this Step025	
Multiple Corr. Coef. Adj. for D.F.949	
F-value for Analysis of Variance		54.630	
Variable	Regression Coefficient	Std. Error of Reg. Coef.	Computed t-value
Stage	.02238	.00269	8.326
EC	-.00055	.00032	-1.719
Intercept	.31269		
Step 3			
Variable Entered Ca			
Sum of Squares Reduced in this Step ..		.007	
Proportion Reduced in this Step022	
Multiple Corr. Coef. Adj. for D.F.958	
F-value for Analysis of Variance		44.598	
Variable	Regression Coefficient	Std. Error of Reg. Coef.	Computed t-value
Stage	.01870	.00321	5.821
EC	-.00054	.00030	-1.814
Ca	-.07490	.04218	-1.776
Intercept	1.18057		

Table 37 continued

Step 4			
Variable Entered pH			
	Sum of Squares Reduced in this Step ..		.005
	Proportion Reduced in this Step018
	Multiple Corr. Coef. Adj. for D.F.966
	F-value for Analysis of Variance		41.218
Variable	Regression Coefficient	Std. Error of Reg. Coef.	Computed t-value
Stage	.01484	.00366	4.061
EC	-.00069	.00028	-2.435
Ca	-.07770	.03839	-2.024
pH	-.23590	.13416	-1.758
Intercept	3.64371		

produced t-values less than -1.78 and greater than 5.82, which surpassed the critical $t(13, .05)$ equal to ± 1.77 . Therefore, reject the null hypothesis that $\rho = \text{zero}$ (regression coefficient = 0) and assume each coefficient is valid.

The predictive linear equation is as follows:

$$\text{FLOW} = 1.18 + 1.87 \times 10^{-2} * \text{STAGE} - 5.40 \times 10^{-4} * \text{EC} - 7.49 \times 10^{-2} * \text{Ca}^{2+}, \quad (3)$$

Summary

The Genoa Fault Zone controls the eastern boundary of the Sierra Nevada along the length of Carson Valley; Walley's Hot Spring occurs at a fault intersection on the Genoa Fault Zone. The springs discharge at a topographic low at the valley-fill alluvium contact and drain into the Carson River system. Several hot wells at Walley's Hot Spring Resort gain water from this thermal reservoir. Flow measurements were made at one spring with a bucket and stop-watch; the average flow equaled 0.32 lps.

The water at Walley's Hot Spring is a Na-SO₄ type water. The soluble ions are accounted for by dissolution of minerals such as plagioclase feldspar and gypsum-anhydrite, and by oxidation of sulfide minerals. Silica chemical geothermometers produced an approximate reservoir temperature of $90 \pm 20^\circ\text{C}$; however, this number may be in question due to the possibility of local near-surface mixing.

The Brockliss Slough flows within 10 m of Walley's Hot Springs and was a prominent controlling factor on flow at the hot spring monitored. Increased stage in Brockliss Slough caused spring flow and temperature to increase; this flushing of near-surface thermal water generally lasted about four weeks. In June, 1984, the Brockliss Slough was diverted about 100 m east of the hot springs; this caused a disruption of the dynamic equilibrium of the reservoir. Prior to this diversion, time-series analysis showed that stage, EC, and calcium ion variabilities could best explain variability in spring flow.

Discussion

Each thermal spring listed in this report is unique, and to this point has been discussed separately. Now an attempt will be made to show the similarities and differences among the springs.

Similarities

High heat flow areas are characteristic of the Basin and Range Province (Blackwell, 1983). The thermal reservoirs studied presumably derive their heat from plutonic rocks associated with the Sierra Nevada batholith, as hypothesized at the Steamboat Thermal Area by White (1968). All of the thermal springs studied issue from fractures and faults in granitic and metamorphic rocks. The metamorphics appear to be underlain by plutonic rocks, and according to Koenig and McNitt (1983), plutonic rocks in this area may extend 5 to 10 km below the surface.

Spring waters are predominantly meteoric and accumulate as snow and rain; stable isotopes suggest that most of the recharge is derived from mountainous precipitation that accumulated above about 2,100 m. All of the spring waters contain low magnesium concentrations and are considered medium conductivity waters (except Steamboat which is medium to high conductivity).

Differences

The general lithology near each spring is highly variable, primarily due to the geologic complexities within the Sierra Nevada - Basin and Range province transition zone. These local lithologic variabilities largely account for spring chemistry differences. A Durov Diagram is used to show the differing spring chemistries (see figure 27).

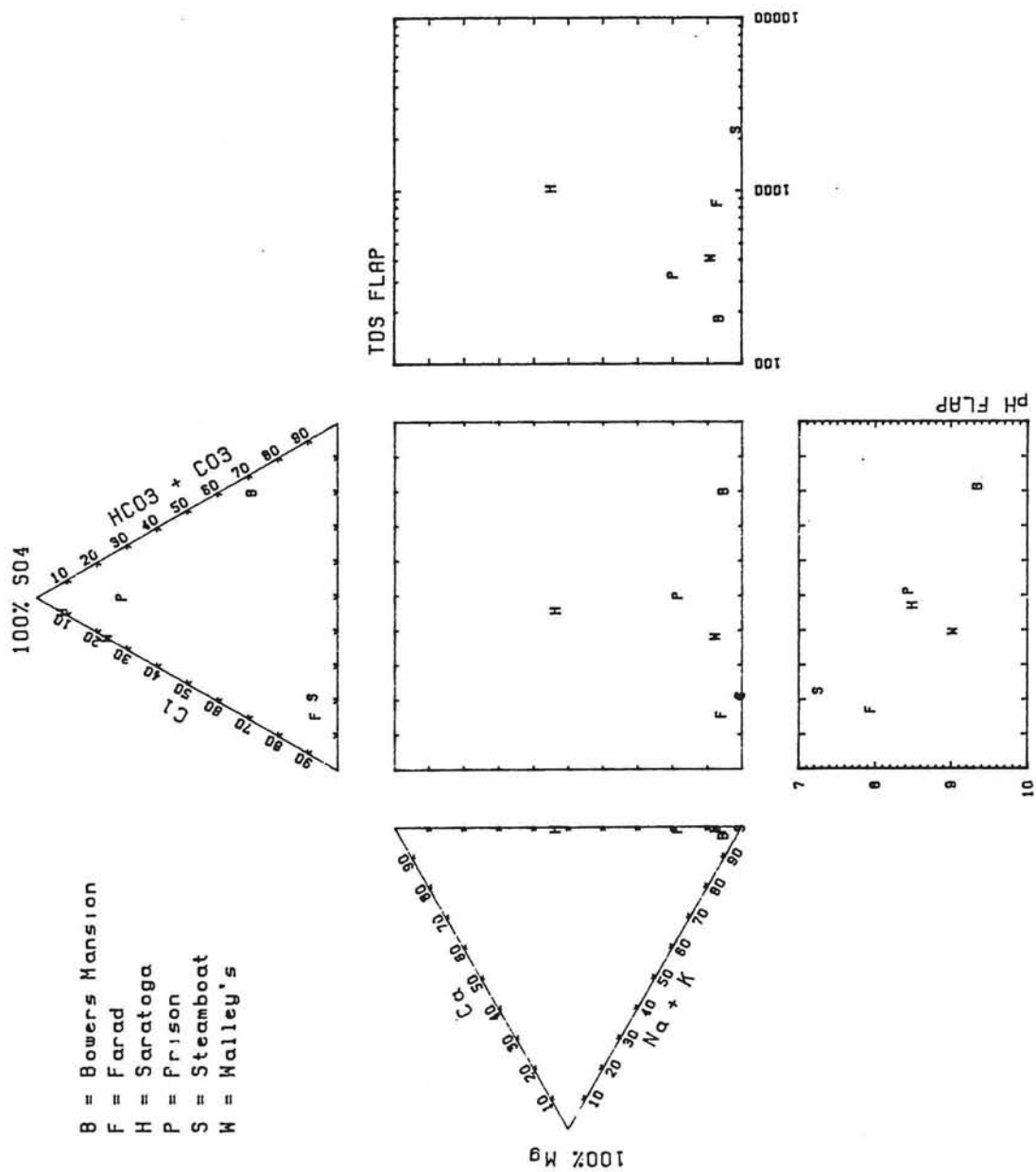
Stable isotopes are also highly variable throughout the study area. This variation can be accounted for in several ways: 1) by differing recharge elevations, 2) by varying rock-water interactions (oxygen shift), 3) by paleo-climatic variability, 4) by near-surface groundwater mixing, and 5) by isotopic fractionation during recharge and discharge. The above list of causes accounts for the variability observed in figure 28.

Based on this study the thermal springs can be categorized as follows:

	Calculated Reservoir Temp (C)	Type Water	Estimated Reservoir Size	Flow
Farad	110±25	Na-Cl	Small	Med
Steamboat	230±20	Na-Cl	Large	Med
Bowers	100±20	Na-HCO ₃	Sm-Med	Med
Prison	70±20	Na-SO ₄	Small	Low
Saratoga	80±25	Ca(Na)-SO ₄	Sm-Med	High
Walley's	90±20	Na-SO ₄	Sm-Med	Low

; where reservoir temperature is based on chemical geothermometry, type water is based on aqueous chemistry,

Figure 27
 Durov Diagram of Spring Chemistry



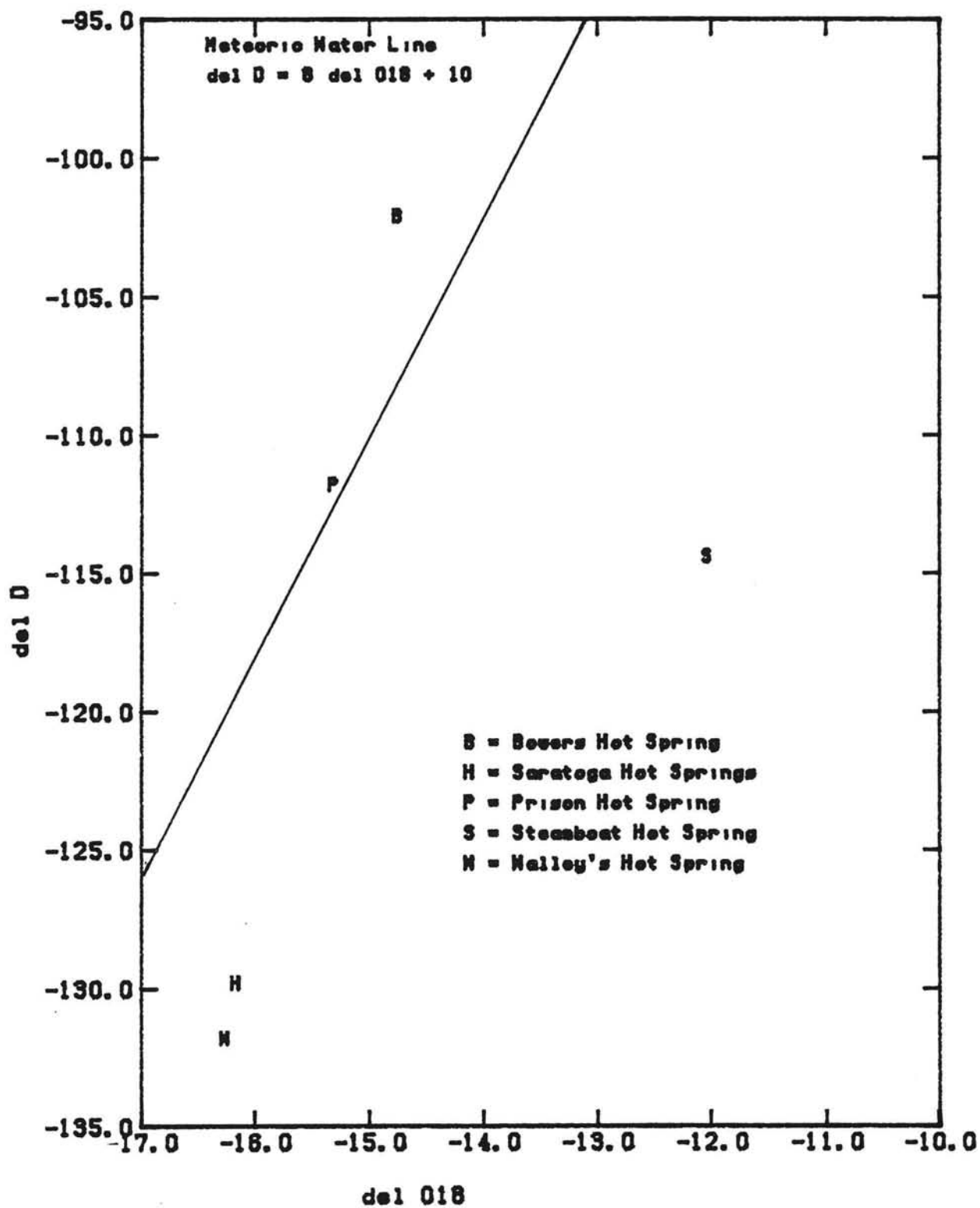


Figure 28. Stable Isotope Plot
 del D vs. del ^{18}O

relative reservoir size is based on hydrogeologic characteristics, and flow is relative (Low < 1.0 lps, 1.0 < Med < 10.0 lps, High > 10.0 lps).

Conclusion

Times-series analyses indicate interesting relationships and help to further the understanding of the springs studied; however, in some cases a more powerful statistical technique than linear cross correlation should be used to fully understand the temporal data. Cross correlation statistics produced limited results in situations where numerous unmonitored influences were present, such as local pumping, surface water stage fluctuations, snow melt, etc..

Cross correlation showed, with a defined level of confidence, how measured variables were interrelated. Lagged correlations were useful for approximating infiltration rates in the unsaturated zone; a list of the significant lagged correlations are as follows:

Significant Lagged Correlations

Farad... precipitation leads flow by six weeks, suggesting that six weeks after a precipitation event infiltrated water reaches the water table and a pressure pulse is observed at the spring discharge,

Saratoga... precipitation leads flow by 24 weeks, suggesting that 24 weeks after a precipitation event a pressure pulse is observed at the spring discharge, and

Walley's... river stage (responding to precipitation events) has a nearly instantaneous response (less than two weeks) on spring discharge.

Lead-lag multiple step-wise linear regression showed which independent variables best accounted for variations

in flow (also within defined levels of confidence) and produced linear equations, describing flow as a function of several independent variables. These linear equations are best used to show which variable accounts for the most variability in flow (the first variable entered accounts for the most variability, and so on). The linear equations are valid to within 10 per cent of the means of the independent variables and the significant equations are as follows:

Significant Linear Equations

Farad...

$$\text{Flow} = 6.79 - 5.90 \times 10^{-3} * (\text{Cl}) - 8.61 \times 10^{-2} * (\text{temp}) + 2.34 \times 10^{-2} * (\text{ppt}), \quad (1)$$

Saratoga...

$$\text{Flow} = 17.07 + 2.38 \times 10^{-1} * (\text{ppt}) + 5.46 * (\text{pH}), \quad \text{and } (2)$$

Walley's...

$$\text{Flow} = 1.18 + 1.87 \times 10^{-2} * (\text{stage}) - 5.40 \times 10^{-4} * (\text{EC}) - 7.49 \times 10^{-2} * (\text{Ca}). \quad (3)$$

Chemical and isotopic variability appear to have a greater range than was originally anticipated. This is quite significant considering that hot springs are generally considered to be relatively stable and/or constant with time. Coefficients of variation for the measured constituents are listed below:

Coefficients of Variation

	Farad	Steamboat	Bowers	Prison	Saratoga	Walley's
Flow	7.34	* 21.19	21.05	30.30	2.96	40.50
EC	4.02	2.09	6.76	5.10	3.55	3.17
Temp	1.42	2.45	1.06	1.62	0.34	6.11
pH	1.72	2.84	2.29	1.81	1.03	1.11
pCO ₂	5.06	15.5	4.67	3.83	2.00	2.71
Ca	6.54	6.41	8.31	6.43	0.64	4.03
Cl	2.61	2.31	3.27	1.81	2.59	1.09
HCO ₃	1.95	3.58	2.81	5.48	6.85	4.70
Na	-	-	-	-	0.68	-

* Steamboat flow is based on relative measurements over 24 weeks.

Prior to the cation analysis it was proposed that the major dissolved cations would be mimicked by the EC variability, but as can be seen at Saratoga Hot Spring the EC has much more variation than calcium or sodium; however, this hypothesis did hold true at Walley's and Steamboat Hot Springs.

Time-series analysis of thermal reservoirs can produce helpful information to further understand the following:

- 1) infiltration residence time,
- 2) aqueous geochemistry interrelationships,
- 3) environmental isotope variability,
- 4) relative hydrodynamic relationships, and
- 5) reservoir responses to pumping.

Temporal variability studies of physical and chemical parameters have proven useful for site specific approximations of reservoir characteristics (see discussion). The springs observed in this study are characterized by a wide variety of spring types (primarily

due to geologic heterogeneity); although these spring types are not all encompassing, the temporal approach used in this study may be applied to most springs. To use temporal variability as a tool, the following steps should be followed:

- 1) review historical spring data,
- 2) decide which variables to measure,
- 3) set up sampling and measuring devices
- 4) collect data on a regular sample interval for at least one spring cycle (biweekly for one year in this study),
- 5) interpret field geology for lithologic variability and structural controls,
- 6) interpret regional and local hydrologic characteristics, and
- 7) analyze temporal data with statistical techniques.

Before springs with limited data bases are correlated with the springs in this study, precautions should be taken:

- 1) insure that water evolutionary paths are similar,
- 2) insure that flows and temperatures are similar, and
- 3) insure that geologic controls are similar.

Further Studies

Several of the springs observed have shown complexities, primarily caused by unmonitored parameters. An attempt will now be made to outline some springs that show promise for further time-series studies.

The Steamboat thermal area has several tens of springs. It would be nearly impossible to monitor all of these springs individually, but an integrated technique could be used (previously applied by White, 1968). Flow monitoring and sample collecting devices could be installed on Steamboat Creek and on other small tributaries above and below the thermal area. The chemical and physical variabilities from the downstream station could be subtracted from the upstream station to get the integrated variability of the spring discharges. Several individual springs should also be monitored for control.

Bowers Hot Spring is influenced by local pumping from a hot well. The spring discharge variation can be easily monitored with a 30° V-notch weir and Stevens recorder, but since the hot well pumps into a pressure tank it is difficult to monitor when the well turns on and off. A current recorder would have to be installed at the pump to monitor this phenomena. At this point stochastic and numerical techniques could be used to model thermal and hydrologic reservoir characteristics.

Walley's Thermal Area is very similar to Bowers Hot

Spring except there are several hot wells which influence the flow at Walley's, where there is only one well at Bowers. Electric current recorders would have to be installed on the local wells and flow recorders would have to be installed on several thermal springs before the modeling of thermal and hydrologic characteristics could be done.

References Cited

Arteaga, F.E., and Dubin, T.J., 1978, "Development of a Relation for Steady-State Pumping Rate for Eagle Valley Ground-Water Basin, Nevada"; U.S. Geological Survey, Open-File Report 79-261, pp. 44.

Arteaga, F.E., and Nichols, W.D., 1984, "Hydrology of Washoe Valley, Washoe County, Nevada"; U.S.G.S., Open-File Report 84-465, pp. 29.

Armstrong, T.A., and Fordham, J.W., 1977, "Investigation of Groundwater Quality and its Effect on Suburban Development in Washoe Valley, Nevada"; Desert Research Institute, WRC, Project Report 48, pp. 60.

Arnorsson, S., Gunnlaugsson, E., and Svavarsson, H., 1983, "The Chemistry of Geothermal Waters. III. Chemical geothermometry in Geothermal Investigations"; *Geochemica et Cosmochemica Acta*, Volume 47, pg. 567-577.

Babuskin, V.D., Bocker, T., Borevsky, B.V., and Kovalevsky, V.S., 1975, "Regime of Subterranean Water in Karst Regions": Hydrogeology of Karst Terrains, Pub. by International Association of Hydrogeology, Paris, France, pg. 72-76.

Bateman, R.L., 1970, "Environmental Controls on Occurrence and Chemistry of Ground Water in a Basic Volcanic Terrane, Eastern Sierra Nevada"; unpublished thesis, University of Nevada Reno, pp. 115.

Bateman, R.L., and Scheibach, R.B., 1975, "Evaluation of Geothermal Activity in the Truckee Meadows, Washoe County, Nevada"; Nevada Bureau of Mines and Geology, Report 25, pp. 38.

Bear, J., 1979, Hydrolics of Groundwater, pub., McGraw - Hill Inc., pg. 55-56.

Benjamin, T., Charles, R., and Vidale, R., 1983, "Thermodynamic Parameters and Experimental Data for the Na-K-Ca Geothermometer"; *Journal of Volcanology and Geothermal Research*, Volume 15, pg. 167-186.

Berry, Roland, 1984, Personnel Communication; Civil Engineer, Harker Inc., February 28, 1984.

Bingler, E.C., 1977, New Empire Quad. Geologic Map, 1:24,000 scale, Nevada Bureau of Mines and Geology, Map No. 59.

Birkland, P.W., 1962, "Pleistocene History of the Truckee Area, North of Lake Tahoe, California"; undulished disertation, Stanford, University, Ph.D., pp 126.

Birkland, P.W., 1968, "Mean Velocities and Boulder Transport During Tahoe-age Floods of the Truckee River, California - Nevada"; Geological Society of America Bulletin, vol. 79, pg. 137-142.

Blackwell, D.D., 1983, "Heat flow in the Northern Great Basin Provence"; Geothermal Resources Council, Special Report No. 13, pg. 93.

Blattner, P., 1980, "Oxygen Isotope Shifting Capacity of Rocks - Model and Application to the Ngawha Geothermal System"; Isotope Studies in Hydrologic Processes, Northern Illinois Press, DeKalb, Illinois, pg. 9-14.

Bohm, B., 1984, "Sources of Bicarbonate in Groundwaters in the Western Basin and Range", in press, Desert Research Institute, University of Nevada System, Reno, Nevada.

Bonham, H.F., and Burnett, J.L., 1976, "Geologic Map, South Lake Tahoe Folio"; Nevada Bureau of Mines and Geology, Environmental Series, Lake Tahoe Area.

Briant, T., 1984, Personal Communication; Irrigation Forman, Danberg Ranch, Carson Valley, Nevada.

Bricker, O.P. and Garrels, R.M., 1967, "Mineralogic Factors in Natural Water Equilibria"; Chemical Hydrogeology, 1983, pub.: Hutchinson Ross Publishing Co., Strudsburg, Penn., Vol. 73, pg. 268-274.

Combarrous, M.A., and Bories, S.A., 1975, "Hydrothermal Convection in Saturated Porus Media"; Advances in Hydroscience; pub.: Academic Press, New York, Volume 10, pg. 231-307.

Coyle, T., 1984, Personal Communication, Bowers Mansion Park Ranger.

Daugherty, R.L., and Franzini, J.B., 1977, Fluid Mechanics with Engineering Applications; pub.: McGraw-Hill Book Company, seventh edition, pp. 564.

Davis, J.C., 1973, Statistics and Data Analysis in Geology; pub.: John Willey and Sons, New York, pp. 550.

Drever, J.I., 1982, The Geochemistry of Natural Waters; pub.: Prentice-Hall, Inc., Englewood Cliffs, N.J., pp 361.

Eisinger, V.J., 1960, "Geology of Prison Hill-Brunswick Canyon Area, Ormsby County, Nevada"; unpublished thesis, University of Nevada Reno, M.S..

Ellis, A.J., and Mahon, W.A., 1977, Chemistry of Geothermal Systems; pub.: Academic Press, New York, pp 392.

EPA, Method 273.1, March 1979, "Methods for Chemical Analysis of Water and Wastes"; EPA -600/4-79-020, Atomic Absorption, Direct Aspiration.

EPA, Method 325.1, March 1979, "Methods for Chemical Analysis of Water and Wastes"; EPA -600/4-79-020, Colorimetric.

Feth, J.H., Roberson, C.E., and Polzer, W.L., 1964, "Sources of Mineral Constituents in Water from Granitic Rocks, Sierra Nevada, California and Nevada"; U.S.G.S., Water Supply Paper, 1535-I.

Flynn, T., and Ghush, G., Jr., 1984, "Geologic and Hydrologic on the Moana Geothermal System, Washoe County, Nevada"; EOS, Transactions, American Geophysical Union, Vol. 65, No. 45, pg. 883.

Fontes, J.C., 1980, "Environmental Isotopes in Groundwater Hydrology"; Handbook of Environmental Isotope Geochemistry, Elsevier Scientific Publishing Co., New York, pg. 75-140.

Fouillac, C., and Michard, G., 1981, "Sodium/Lithium Ratio in Water Applied to Geothermometry of Geothermal Reservoirs"; Geothermics, Volume 10, Number 1, pg. 55-70.

Fournier, R.O., and Truesdell, A.H., 1973, "An Empirical Na-K-Ca Geothermometer for Natural Waters"; *Geochemica et Cosmochemica Acta*, Volume 37, pg. 1255-1275.

Fournier, R.O., 1977, "Chemical Geothermometers and Mixing Models for Geothermal Systems"; Geothermics, Volume 5, pg. 41-50.

Fournier, R.O., White, D.E., and Truesdell, A.H., OFR, "Geochemical indicators of Subsurface Temperatures Part 1: Basic Assumptions", Preliminary, U.S. Geological Survey, Open-file Report.

Fournier, R.O., 1979, "A Revised Equation for the Na/K Geothermometer"; Geothermal Resources Council, Transactions, Volume 3, pg. 221-224.

- Fournier, R.O., and Potter, R.W., III, 1979, "Magnesium Correction to the Na-K-Ca Chemical Geothermometer"; *Geochemica et Cosmochemica Acta*, Volume 43, pg. 1543-1550.
- Garside, L.J., and Schilling, J.H., 1979, "Thermal Waters of Nevada"; Nevada Bureau of Mines and Geology, Bull. 91, pp. 163.
- Glancey, P.A., and Katzer, T.L., 1975, "Water Resources Appraisal of the Carson River Basin, Western Nevada"; Nevada Division of Water Resources, Water Resources Reconnaissance Series, No. 59, pp. 126.
- Glancey, P.A., and Katzer, T.L., 1977, "Flood and Related Debris Flow Hazards Map, Washoe City Folio"; Nevada Bureau of Mines and Geology, Environmental Series, Washoe Lake Area.
- Glancey, P.A., 1983, Personal Communication, Hydrologist, U.S.G.S., Carson City, Nevada.
- Gross, G.W., Hoy, R.N., Duffy, C.J., and Rehfeld, K.R., 1980, "Isotope Studies in the Roswell Basin"; Isotope Studies of Hydrologic Processes, Northern Illinois University Press, DeKalb, Illinois, pg. 25-33.
- Hefner, M.L., 1983, Personal Communication, Graduate Student, Geology Dept., University of Nevada Reno.
- Hyndman, D.W., 1972, Petrology of Igneous and Metamorphic Rocks; pub.: McGraw-Hill Book Co., New York, pp. 533.
- Jacobson, R.L., and Dangmuir, D., 1974, "Controls on the Quality Variations of some Carbonate Springs"; *Journal of Hydrology*, Vol. 23, pg. 247-265.
- Johnson, C.A., 1980, "Environmental Controls on Occurrence and Chemistry of Groundwater in a Carbonate Terrane of Eastern Nevada"; Desert Research Institute, Pub. No. 41066, pp. 101.
- Katzer, T., 1980, "Carson City Quadrangle General Groundwater Map"; Nevada Bureau of Mines and Geology, No. 1Af.
- Klieforth, H., Albright, W., and Ashby, J., 1984, "Measurement, Tabulation and Analysis of Rain and Snowfall in the Truckee River Basin"; ASC, Desert Research Institute, University of Nevada System, Stead, Nevada.

Koenig, J.B., and McNitt, J.R., 1983, "Controls on the Location and Intensity of Magmatic and Non-magmatic Geothermal Systems in the Basin and Range Province"; Geothermal Resources Council, Special Report No. 13, pg. 93.

Lawson, A.C., 1912, "The Recent Fault Scarps at Genoa, Nevada"; Bulletin of the Seismological Society of America, Vol. II, No. 3, pg. 20.

Lovejoy, E.M., 1972, "Nonantecedent Development of Truckee River Canyon, Northern Carson River, Nevada and California"; Geological Society of America Bull., Vol. 83, pg. 885-894.

Maurer, D., 1984, Personal Communication, USGS, Water Resources Center, Carson City, Nevada.

Mero, F., 1963, "Application of Groundwater Depletion Curves in Analysing and Forcasting Spring Discharge Influences bt Well Fields"; Symp. Intern. Assoc. for Scientific Hydrology, IUGG, Berkley, California, Pub. No. 63, pg. 107-117.

Moore, J.G., 1969, "Geology and Mineral Deposits of Lyon, Douglas, and Ormsby Counties, Nevada"; Nevada Bureau of Mines and Geology, Bull. 75, pp. 45.

Nehring, N.L., 1980, "Geochemistry of Steamboat Springs, Nevada"; U.S. Geological Survey, Open-File Report, 80-887, pp. 61.

Norris, R.M., and Webb, R.W., 1976, Geology of California, John Wiley and Sons, Inc., New York, pp. 365.

Pease, R.C., 1980, "Geologic Map, Genoa 7.5 Minute Quadrangle"; Nevada Bureau of Mines and Geology, Map 1Cg.

Piper, A.M., 1969, "A Water Budget of the Carson Valley, Nevada"; U.S.G.S. Profesional Paper 417-F, pp. 8.

Rush, F.E., 1964, "Groundwater Appraisal of Meadow Valley Area, Clark County"; Nevada Department of Conservation and Natural Resources, Groundwater Resources Reconnaissance Series Report 27, pp. 43.

Shuster, E.T., and White, W.B., 1971, "Seasonal Fluctuations in the Chemistry of Limestone Springs: a Possible Means for Characterizing Carbonate Aquifers", Journal of Hydrology, Vol. 14, pg. 93-128.

- Silberman, D.E., White, D.E., Keith, T.E.C., and Dockter, R.D., 1979, "Duration of Hydrothermal Activity at Steamboat Springs, Nevada, from Ages of Spacially Associated Volcanic Rocks"; U.S. Geological Survey, Professional Paper, 458-D.
- Spane, F.A., Jr., 1977, "Evaluation of Factors Influencing the Inorganic Water-Quality Regimen of Carson River, Carson Valley, Nevada-California"; unpublished dissertation, University of Nevada Reno, Ph.D..
- Staffin, Darrel, 1984, Personal Communication, Homeowner at Saratoga Hot Spring.
- Stewart, J.H., 1980, Geology of Nevada, Nevada Bureau of Mines and Geology, Reno, Nevada, Special Pub. No. 4, pp. 136.
- Stewart, M.K., and Downes, C.J., 1980, "Isotope Hydrology of Waikoropupu Springs, New Zealand"; Isotope Studies of Hydrologic Processes, Northern Illinois Press, DeKalb, Illinois, pg. 15-24.
- Szecsody, J.E., Jacobson, R.L., and Campana, M.E., 1983, "Environmental Isotopes and Hydrogeological Investigation of Recharge and Subsurface Flow in Eagle Valley, Nevada"; Desert Research Institute, University of Nevada Reno, Water Resources Center, Publication No. 42037, pp. 120.
- Tabor, R.W., and Ellen, S.E., 1975, "Geologic Map, Washoe City Folio"; Nevada Bureau of Mines and Geology, Environmental Series, Washoe Lake Area.
- Tabor, R.W., Ellen, S.E., Clark, M.M., Glancey, P.A., and Katzer, T.L., 1983, "Geology, Geophysics, Geologic Hazards, and Engineering and Geologic Hazards of Earth Material in Washoe Lake Area"; Nevada Bureau of Mines and Geology, open-file report 83-7, pp. 87.
- Thompson, G.A., and White, D.E., 1964, "Regional Geology of the Steamboat Springs Area Washoe County, Nevada"; U.S. Geological Survey, Professional Paper, 458-A, pp. 52.
- Trexler, D.T., Flynn, T., and Koenig, B.A., 1979, "Assessment of Low- to Moderate- Temperature Geothermal Resources of Nevada"; U.S. Department of Energy, NVO/01556-1, pp. 30.
- Trexler, D.T., Koenig, B.A., Flynn, T., and Bruce, J.L., 1980, "Assesment of the Geothermal Resouces of Carson-Eagle Valleys and Big Smoky Valley, Nevada"; U.S. Department of Energy, DOE/NV/10039-2, pp. 161.

USGS, 1971, Reno Topographic Map, U.S. Geological Survey, Scale 1:250,000.

Vinyard, G.L., 1984, Biology Professor; University of Nevada Reno, Personal Communication, February 28, 1984.

WATEQ, 1974, A Computer Program for Calculating Chemical Equilibria of Natural Waters; USGS Journal Research, Vol. 2, pg. 233-248.

Water Resources Data Nevada, 1983, USGS Water Data Report, NV-83-1, Carson City, Nevada.

Watters, R.J., 1983, "A Landslide induced Water-Debris Flow"; Bulletin, International Association of Engineering Geology, No. 28, Paris, France, pg. 177-182.

White, D.E., and Brannock, W.W., 1950, "The Source of Heat and Water Supply of Thermal Springs, with Particular Reference to Steamboat Springs, Nevada"; Transactions: American Geophysical Union, Volume 31, number 4, pg. 566-574.

White, D.E., 1960, "Summary of Chemical Characteristics of some Waters of Deep Origin"; U.S. Geological Survey, Professional Paper, 400-B, pg. 452-454.

White, D.E., Thompson, G.A., and Sandberg, C.H., 1964, "Rocks, Structure, and Geologic History of Steamboat Springs Thermal Area, Washoe County, Nevada"; U.S. Geological Survey, Professional Paper 458-B, pp. 63.

White, D.E., 1968, "Hydrology, Activity, and Heat Flow of the Steamboat Springs Thermal System, Washoe County, Nevada"; U.S. Geological Survey, Professional Paper 458-C, pp. 109.

White, D.E., 1983, "Summary of Steamboat Springs Thermal Area, Nevada with Attached Road-log Commentary"; Geothermal Resources Council Meeting, Field Trip Road-log.

Worts, G.F., and Malmberg, G.T., 1966, "Hydrologic Appraisal of Eagle Valley, Ormsby County, Nevada"; Water Resources-Reconnaissance Series, State of Nevada Department of Conservation and Natural Resources, Report 39, pp. 55.

Yeaman, F., 1983, "Basin and Range Geothermal Hydrology: an Empirical Approach"; Geothermal Resources Council, Special Report No. 13, May 1983, pg. 159-175.

Zones, C.P., 1958, "Petrographic and Petrofabric Study of the Metamorphic Rocks North of Carson City, Nevada"; Masters Thesis, University Nevada Reno, pp. 80.

APPENDIX A

Geologic Unit Descriptions

Lithologic descriptions were made during geologic field mapping, which was carried out in the Spring and Summer of 1984. Descriptions were primarily made from hand samples with a 10X hand lens; however, selected samples from Hot Spring Mountain were cut into thin sections by Larry Garside, of the Nevada Bureau of Mines and Geology, and were analyzed with a cross-polarizing microscope to identify the bulk mineral compositions.

The symbols defined in this appendix correspond to units on the geologic maps within the text. For example, Qrg represents Quaternary River Gravel, where Quaternary is a term describing the age of the unit. The units are listed oldest to youngest and age terms follow the general geological time table compiled by F.W.B. van Eysinga (1978). A synopsis of the symbols used and their relative ages are as follows:

Q = Quaternary (0 - 1.8 million years old)

T = Tertiary (1.8 - 65 million years old)

K = Cretaceous (65 - 140 million years old)

J = Jurassic (140 - 195 million years old)

M = rock older than Cretaceous (> 140 million years old).

Farad Hot Spring

Qrg = River Gravel. This unit is primarily composed of granitic and andesitic material ranging from sand to boulder sized and is thought to be deposited during high flow along the Truckee River. The rocks are unconsolidated and cobbles range from angular to rounded.

Qls = Land Slide. The slide material consists of andesitic rocks, cobble- to boulder-sized, in a granitic to andesitic sandy groundmass. The andesitic rock fragments are angular to slightly rounded and are generally unconsolidated.

Ql = Latite. This unit ranges from brown to green. Pyroxene and hornblende phenocrysts are abundant, and olivine may also be present. The outcrops are moderately to highly fractured. Cooling joints are uniformly spaced at 3 cm intervals.

Qmf = Mudflow; Lahar. This unit is composed of fragments of andesitic and dacitic rocks, medium grey to red-brown. The fragments range from a few mm in diameter to 10 cm, with a few fragments up to 50 cm in diameter. Approximately 5% of the cobbles are biotite granodiorite (locally varying 0 to 20%). The granitic cobbles are moderately rounded and exhibit good sphericity, while the volcanic fragments are generally angular. The groundmass consists of fine-grained volcanic rock fragments. The unit is somewhat resistant to weathering.

Ta = Andesite. This unit varies from light brown to

dark grey-green. Small crystals of pyroxene, plagioclase quartz and hornblende can be identified with a hand lens. Most of the outcrops are moderately to highly fractured. Fractures are accented by iron oxide stains and salt crusts. Cooling joints are quite apparent locally, with very small joints (2 cm spacing) near the top of outcrop exposures and large joints (10 cm spacing) at the ground surface. These joint patterns are bent, conforming to the topography.

Kgd = Hornblende Biotite Granodiorite. These rocks are composed of 15-20% quartz, 40-50% plagioclase, 15-20% orthoclase, 5% biotite and 15% hornblende. Most outcrops are highly fractured, with red-brown iron staining along fractures. Coarse granitic derived soil occurs around most outcrops.

Bowers Mansion

Qaf = Alluvial Fan. This unit forms the valley fill material from the mountain flanks to Washoe Lake. The material is fine to coarse, poorly to moderately sorted, granodioritic sand. Some areas contain significant amounts of clay minerals, particularly in the pasture areas.

Qba = Basin Alluvium. Many of the high basins and canyons are partially filled with poor to well sorted, boulder- to silt-size granitic fragments. Most of this material was water-lain, due to ponding during high

moisture periods. In general this material was distinguished from decomposed granitic material by the abundance of silty material and presence of minor sedimentary structures.

Qsd = Slide Mountain Debris Flows; undifferentiated. The flows are composed of angular granitic rock fragments, ranging from boulder to sand size. Size sorting occurs locally, with boulders deposited exclusively in one area and cobbles in another area. Subtle compositional variations are noticeable, similar to those seen in granitic rock outcrops. No attempt was made to delineate different debris flows.

Kgd = Hornblende-Biotite Granodiorite. The granitic rocks in the study area range in composition from hornblende-biotite granodiorite (90%) to hornblende granodiorite (10%), but these distinction were not mapped. The rock is highly fractured and jointed near faults, and is in varying stages of decomposition. The ridge between Little Valley and Bowers Mansion has the appearance of gently rolling hills composed of extremely weathered granitic outcrops surrounded by a layer of coarse granitic sand (1 m to 10 m thick). Minor iron staining is caused by oxidizing pyrite crystals. Pegmatite and aplite is noticeable in contact with the granitic rocks locally.

Ts = Sedimentary Rocks. This unit is made up of sandstone; composed of medium to well rounded, moderately spherical, quartz grains with calcite cement. Interbedded siltstone is laterally discontinuous, and exhibits crossbedding and minor load structures. Most outcrops are highly fractured.

Kgd = Hornblende-Biotite Granodiorite. Most outcrops are moderately to highly and jointed. Long prismatic hornblende crystals are evident on fresh surfaces, as well as small epidote crystals and possible minor pyroxene (stained iron red-brown by iron oxides).

Jb = Metavolcanic Breccia. Composed of light grey-brown to dark grey-brown andesitic to dacitic rock fragments. The breccia also contains minor coarse granitic material (about 5 percent). Outcrops are moderately to highly fractured; some areas are punky, composed of weathered coarse rock fragments.

Jd = Dacite Porphyry. Quartz crystals are easily recognizable by well formed crystal faces. The groundmass is composed of altered hornblende and minor altered pyroxene. Weathered outcrops exhibit a spotted appearance.

Saratoga

Qal = Alluvial-Plain Deposits; restricted to the northern (granitic) area. 30-50% of the material is cobble to bolder size, primarily composed of granitic rocks, while

the remainder is decomposed granitic rock and wind blown sand.

Qf = Flood-Plain Deposits; deposited by the Carson River. This unit is silty, medium to coarse sand, unconsolidated and moderately well sorted.

Qs = Windblown Sand. 20% of this unit is composed of material >2mm (metavolcanic), 60% is medium rounded and medium spherical quartz sand grains, and the remaining 20% is medium rounded and medium spherical metavolcanic and granitic fragments.

Kgd = Biotite-Hornblende Granodiorite; primarily located at the northern boundary of Hot Springs Mountain. The unit is phaneritic and contains 20% quartz, approximately 2% biotite mica (commonly as books), 50% plagioclase, 20% orthoclase and minor occurrences of sphene/pyroxene (starting to show weathering effects). The granodiorite grades into a pegmatite, and forms a sharp contact with the fine-grained metavolcanic unit (Jma). Most of the contacts are mapped as dikes of pegmatite or granitic rocks into metamorphosed andesitic volcanics.

Kgdp = Granodiorite Porphyry; along the eastern boundary of Hot Springs Mountain. The unit is phaneritic and contains approximately 15% quartz, 50% feldspar (predominantly plagioclase), approximately 1% biotite mica and small iron stains (possibly from minor sphene/pyroxene). The contact with the metavolcanic is transitional and is only approximately located by the percent composition of float and by minor outcrops in

drainages.

Jmd = Meta-Dacite Porphyry. The unit is cream to grey-green; some areas can be easily distinguished by a light to dark spotted appearance. Other areas show the same spotted appearance with inclusions of epidote (epidote hornfels or spotted hornfels). The main mineralized areas are within this unit and follow a trend of approximately N60W dipping about 60NE. Several adits and shafts explore this hydrothermally altered zone (approximately .75-2m wide). Mineralization consists of quartz veining and silicification, with occurrences of crystalline calcite, chrysocolla, barite and pyrite. Ore production was probably small (no production figures are available and claim notices have expired since 1973).

Jpb = Meta-Welded Tuff and Breccia. This unit is grey to brown and has a distinctive weathered appearance with pumice fragments flattened and preferentially weathered out. A thin section showed the approximate composition to be 60% plagioclase (An=10-30, oligoclase), 30% chloritized mica, 5% actinolite (14 degree extinction) and 5% opaque minerals (magnetite?). The breccia is similar to that found near the State Prison (dacite to andesite).

Jma = Meta-Andesite. The unit is grey to black, aphanitic and in particular orientations lineations of altered mica crystals are quite distinct. Very small quartz crystals are noticeable and plagioclase appears to be the predominant feldspar. There also appears to be minor pyroxene dispersed throughout. The contact is

generally sharp at the granitic boundaries, but is generally transitional at the meta-dacite porphyry contacts (the two dikes in the western part of section 22 are mapped based primarily on percent change in float composition).

Jms = Metasedimentary Rocks. This unit is a coarse to medium coarse grained sandstone (ranging from angular to rounded), composed of quartz, chert and epidote. Lineations are noticeable along certain orientations of the samples.

Jmms = Mottled Metasedimentary Rocks. This unit is medium to fine grained and has a cream/brown plagic matrix with green Epidote splotches. Two outcrops of Jmms are separated by coarse-grained metasedimentary rocks (Jms).

Walley's Hot Springs

Qal = Alluvial-Plain Deposits. This unit is composed of sand to boulder size material (although, most is cobble size) fragments are angular to sub-rounded granitic and metamorphic rocks. Very few plants grow on this unit, primarily due to the scarcity of soil.

Qf = Flood-Plain Deposits; from the Carson River. This unit is composed of sand- to mud-sized material. Many sedimentary structures can be distinguished in some areas.

Qoa = Older Alluvial-Plain Deposits. This unit is composed of poorly sorted sands and gravels along the Genoa Fault. The gravels consist of granitic and metamorphic

pebbles (primarily granitic in the gravel pits).

Kgd = Hornblende-Biotite Granodiorite. This unit is moderately to highly fractured and moderately jointed. The hornblende/biotite ranges from <2% to 25%. The biotite occurs in books and as individual flecks, locally chloritized. Plagioclase feldspar and quartz are easily identifiable, while orthoclase is a minor constituent. Sphene is a possible accessory mineral. The granitic to metamorphic contact ranges from sharp to transitional; the sharp contacts usually have large amounts of hornblende associated with them (up to 25% in the granitic rocks and 80% in the metamorphic rocks). In some areas the granitic rocks are decomposed to a depth of 2-3 m.

Kgp = Granodiorite Porphyry. This unit has been slightly to intensely metamorphosed. The rocks only lightly metamorphosed are porphyritic with a fine-grained phaneritic groundmass; white specks on a green-grey groundmass are caused by quartz and plagioclase on altered hornblende and biotite. Some hornblende crystal structures can still be identified. The more heavily metamorphosed rocks can be described as spotted hornfels, with the quartz and plagioclase minerals slightly deformed.

Ms = Metamorphic Schistose Rocks. This unit is composed of quartz, plagioclase, biotite, hornblende and minor pyrite. Foliation is accentuated by irregular masses of biotite. In areas of higher metamorphism grains cannot be distinguished (phyllitic), but foliation is marked by white streaks of plagioclase-quartz on dark hornblende -biotite.

The unit is moderately to highly fractured.

Fault Gouge; along the Genoa Fault Zone. The fault gouge is composed of granitic and metamorphic rocks. The rocks are generally crushed to a chalky powder. The crushed zone is up to 6 m wide and the scarp is up to 5 m high (10 m in areas exposed in gravel pits). Small amounts of Natrolite occurs as seams in the crush zone.

APPENDIX B

Temporal Data

Appendix B contains temporal data from the flowing wells and miscellaneous temporal data in this study. Several symbols used in this appendix are defined as follows:

- * = Value is not used in statistical analysis,
- = no data is available, and
- () = approximate value.

Appendix B.1 (Bowers Mansion Hot well)

Date	Time	On	Off	Volume Fumed Since Previous Time (gals)
6 /12	5:45PM		X	-
6 /13	2:02PM	X		42272230
6 /14	11:00AM		X	-
6 /14	4:00PM	X		-
6 /15	8:30AM			423695--
6 /16	9:39AM			424265--
6 /17	9:59AM		X	424531--
6 /18	12:00PM		X	425403--
6 /19	9:45AM			42606250
6 /20	10:15AM		X	42673600
6 /20	5:00PM	X		42688800
6 /21	10:00AM		X	42715500
6 /21	5:30PM	X		42729100
6 /22	9:45AM	X		42744450
6 /22	2:00PM		X	42760000
6 /22	5:15PM	X		42764100
6 /23	10:00AM	X		42801700
6 /25	9:30AM		X	42863470
6 /25	5:10PM	X		42689700
6 /26	9:45AM		X	42904060
6 /26	5:00PM	X		42910500
6 /27	9:45AM		X	42968842
6 /27	5:00PM	X		42977700
6 /28	9:30AM	X		42983900
6 /29	10:30AM	X		43055540
6 /29	5:30PM		X	
6 /30	10:00AM	X		43141420
(6/30	4: PM		Turned down?)
7 /2	9:30AM		X	43204560
7 /2	5:30PM	X		43211230
7 /3	9:30AM		X	43236620
7 /3	5:00PM	X		
7 /4	9:30AM		X	43298870
7 /5	11:45AM			43315600
7 /5	5:15PM	X		43321890
7 /6	9:30AM		(X)	43357630
(7/6	5: PM	X?)
7 /7	9:30AM		(X)	43423180
(7/7	5: PM	X?)
7 /8	9:30AM		X	43478600
7 /8	5:00PM	X		43486680
7 /10	9:30AM		X	43565480
(7/10	5:00PM	X?)
7 /11	9:30AM		X	43629750
7 /11	5:30PM	X		43637200
7 /12	9:30AM		X	43664100
7 /12	5:30PM	X		43670800
7 /13	9:30AM		(X)	43691460
7 /14	5:30PM	(X)		43708760
7 /15	9:30AM		X	43754760

Appendix B.1 Continued

Date	Time	On	Off	Volume Pumped (gals)
7 /15	5:30PM	X		43760830
7 /16	9:30AM		X	43785350
7 /16	5:20PM	X		43789930
7 /17	9:37AM		X	43817132
7 /17	5:17PM	X		43820320
7 /18	11:42AM		X	43882200
7 /18	5:31PM	X		43887360
7 /19	9:32AM		X	43921070
7 /19	5:31PM	X		43928330
7 /20	10:00AM		X	43959200
7 /21	11:45AM	X		43989920
7 /21	7:12PM	X		44007500
7 /22	9:31AM		X	44031920
7 /22	5:17PM	X		44043700
7 /23	9:32AM		X	44099260
7 /23	2:15PM	X		44103940
7 /24	9:35AM		X	44143880
7 /25	5:28PM	X		44162415
7 /26	9:39AM		X	44200920
7 /26	5:29PM	X		44206200
7 /28	7:30PM	X		44339720
7 /29	9:55AM		X	44375810
7 /29	5:33PM	X		44380430
7 /30	9:30AM		X	44411500
7 /30	4:33PM	X		44416410
7 /31	9:40AM		X	44449255
7 /31	5:17PM	X		44455000
8 /1	12:05PM	X		44487600
8 /2	9:29AM		X	44539400
8 /2	5:10PM	X		44547560
8 /3	9:35AM	X		44577470
8 /4	9:45AM	X		44623830
8 /5	9:44AM	X		44641710
8 /6	9:45AM		X	44714380
8 /6	5:24PM	X		44722380
8 /7	9:37AM		X	44772480
8 /7	5:30PM	X		44778690
8 /8	9:52AM		X	44816520
8 /8	5:35PM	X		44821710
8 /9	9:35AM		X	44855660
8 /9	5:16PM	X		44861190
8 /10	10:32AM		X	44898560
8 /11	12:00PM	X		44921140
8 /12	3:00PM		X	44929000
8 /12	5:00PM	X		44961590
8 /13	9:45AM		X	45019485
8 /13	5:18PM	X		45026025
8 /14	9:40AM		X	45074130
8 /14	5:18PM	X		45080000
8 /15	9:45AM		X	45094685

Appendix B.1 Continued

Date	Time	On	Off	Volume Pumped (gals)
8 /15	4:30PM	X		45100310
8 /16	9:40AM		X	45123728
8 /16	4:32PM	X		45133065
8 /17	5:22PM	X		45198500
8 /18	10:45AM	X		45256230
8 /19	9:41AM		X	45333500
8 /19	5:05PM	X		45337565
8 /20	9:40AM	(X)	?	45385900
(8/20	5: PM	X?)
8 /21	9:25AM		X?	45452800
8 /21	4:37PM	X?		45456555
8 /22	9:52AM		X	45504950
8 /22	5:20PM	X		45509570
8 /23	9:48AM		X	45561460
8 /23	5:02PM	X		45567980
8 /24	12:00PM		X	-
8 /24	5:00PM	X		45637100
8 /25	10:00AM		X	45693600
8 /25	5:00PM	X		45698700
8 /26	10:00AM		X	45759300
8 /26	5:00PM	X		45761300
8 /27	9:37AM		X	45818330
27	5: PM	?		
8 /28	9:33AM		X	45875910
8 /28	5:22PM	X		45883170
8 /29	9:36AM		X	45927380
8 /29	5:05PM	X		45933358
8 /30	9:46AM		X	45986880
8 /30	4:24PM	X		45999975
8 /31	3:08PM	(XX)		46052300
9 / 3	9:35AM		X	46224780
9 /13	1:31PM	(XX)		46463450

Appendix B.2 (Bowers Mansion Hot Well)

Date	Time	On	Off	Volume (gal)	avg used (gal)	del T (hr)	avg Rate (lps)
7 /2	9:30AM		X	43204560	-	-	-
7 /2	5:30PM	X		43211230	6670	8.0	0.88
7 /3	9:30AM		X	43236620	25390	16.0	1.67
(7/3	5:00PM	X)	-	-	-
7 /4	9:30AM		X	43298870	62250	24.0	2.73
7 /5	11:45AM			43315600	(16730	26.25	0.67)
7 /5	5:15PM	X		43321890	23020	31.75	0.76
7 /6	9:30AM		(X)	43357630	35740	16.25	2.32
(7/6	5: PM	X?)	-	-	-
7 /7	9:30AM		(X)	43423180	65550	24.0	2.88
(7/7	5: PM	X?)	-	-	-
7 /8	9:30AM		X	43478600	55420	24.0	2.43
7 /8	5:00PM	X		43486680	8080	7.5	1.13
7 /10	9:30AM		X	43565480	78800	40.5	2.05
(7/10	5:00PM	X?)	-	-	-
7 /11	9:30AM		X	43629750	64270	24.0	2.82
7 /11	5:30PM	X		43637200	8450	8.0	1.11
7 /12	9:30AM		X	43664100	26900	16.0	1.77
7 /12	5:30PM	X		43670800	6700	8.0	0.88
7 /13	9:30AM		(X)	43691460	20660	16.0	1.36
7 /14	5:30PM (X)			43708760	17300	32.0	0.57
7 /15	9:30AM		X	43754760	46000	16.0	3.03
7 /15	5:30PM	X		43760830	6070	8.0	0.80
7 /16	9:30AM		X	43785350	24520	16.0	1.61
7 /16	5:20PM	X		43789930	4580	7.9	0.61
7 /17	9:37AM		X	43817132	27202	16.25	1.76
7 /17	5:17PM	X		43820320	3188	8.0	0.42
7 /18	11:42AM		X	43882200	61880	18.5	3.52
7 /18	5:31PM	X		43887360	5160	6.25	0.87
7 /19	9:32AM		X	43921070	33710	16.0	2.22
7 /19	5:31PM	X		43928330	7260	8.0	0.96
7 /20	10:00AM		X	43959200	30870	16.5	1.97
7 /21	11:45AM	X		43989920	30720	25.75	1.26
7 /21	7:12PM	X		44007500	10580	7.5	1.49
7 /22	9:31AM		X	44031920	31420	14.25	2.32
7 /22	5:17PM	X		44043700	17380	7.75	2.36
7 /23	9:32AM		X	44099260	49960	16.25	3.24
7 /23	2:15PM	X		44103940	4680	4.75	1.04
7 /24	9:35AM		X	44143880	39940	19.25	2.18
7 /25	5:28PM	X		44162415	18535	32.0	0.61
7 /26	9:39AM		X	44200920	38505	16.1	2.52
7 /26	5:29PM	X		44206200	5280	7.9	0.70
7 /28	7:30PM	X		44339720	132820	50.0	2.80
7 /29	9:55AM		X	44375810	36790	14.5	2.67
7 /29	5:33PM	X		44380430	4620	7.5	0.65
7 /30	9:30AM		X	44411500	31070	16.0	2.04
7 /30	4:33PM	X		44416410	4910	7.0	0.74
7 /31	9:40AM		X	44449255	32845	17.0	2.03
7 /31	5:17PM	X		44455000	5745	7.5	0.81

Appendix B.3 (Temporal Data from Bowers Mansion Hot Spring)

Date	Time (hr)	Barometric (in Hg)	Flow (lps)	Date	Time (hr)	Barometric (in Hg)	Flow (lps)
8/01/84	12:00	30.13	0.48		12:00	30.17	0.50
	18:00	30.13	0.48		18:00	30.09	0.49
8/02/84	24:00	30.16	0.47	8/10/84	24:00	30.13	0.47
	6:00	30.17	0.47		6:00	30.12	0.48
	12:00	30.15	0.47		12:00	30.10	0.48
8/03/84	18:00	30.05	0.50	8/11/84	18:00	29.98	0.48
	24:00	30.09	0.50		24:00	29.98	0.48
	6:00	30.11	0.50		6:00	29.93	0.48
	12:00	30.13	0.50		12:00	29.86	0.48
	18:00	30.11	0.49		18:00	29.72	0.48
8/04/84	24:00	30.16	0.52	8/12/84	24:00	29.74	0.48
	6:00	30.16	0.55		6:00	29.72	0.48
	12:00	30.18	0.57		12:00	29.74	0.48
	18:00	30.11	0.57		18:00	29.73	0.48
8/05/84	24:00	30.14	0.57	8/13/84	24:00	29.89	0.48
	6:00	30.14	0.57		6:00	29.97	0.48
	12:00	30.15	0.58		12:00	30.02	0.48
	18:00	30.09	0.59		18:00	30.00	0.48
	24:00	30.09	0.58		8/14/84	24:00	30.09
6:00	30.11	0.58	6:00	30.10		0.48	
12:00	30.10	0.57	12:00	30.02		0.48	
8/06/84	18:00	30.02	0.57	8/15/84	18:00	30.05	0.48
	24:00	30.03	0.56		24:00	30.09	0.48
	6:00	30.00	0.56		6:00	30.09	0.47
	12:00	30.01	0.55		12:00	30.04	0.48
8/07/84	18:00	29.94	0.53	8/16/84	18:00	29.97	0.49
	24:00	29.99	0.51		24:00	29.99	0.49
	6:00	30.01	0.50		6:00	30.00	0.47
	12:00	30.08	0.50		12:00	30.01	0.49
	18:00	30.03	0.50		18:00	29.96	0.49
8/08/84	24:00	30.10	0.48	8/17/84	24:00	30.05	0.51
	6:00	30.12	0.48		6:00	30.10	0.51

Appendix B.3 Continued

Date	Time (hr)	Barometric (in Hg)	Flow (lps)	Date	Time (hr)	Barometric (in Hg)	Flow (lps)
8/17/84	12:00	30.11	0.49		12:00	30.08	0.48
	18:00	30.04	0.49		18:00	30.10	0.48
8/18/84	24:00	30.14	0.50	8/26/84	24:00	30.19	0.48
	6:00	30.18	0.49		6:00	30.16	0.47
	12:00	30.20	0.47		12:00	30.11	0.47
	18:00	30.16	0.48		18:00	30.02	0.48
8/19/84	24:00	30.22	0.50	8/27/84	24:00	30.07	0.49
	6:00	30.23	0.49		6:00	30.07	0.48
	12:00	30.22	0.		12:00	30.06	0.48
	18:00	30.20	0.48		18:00	30.06	0.49
8/20/84	24:00	30.22	0.49	8/28/84	24:00	30.15	0.49
	6:00	30.21	0.49		6:00	30.19	0.48
	12:00	30.17	0.48		12:00	30.17	0.48
	18:00	30.10	0.48		18:00	30.12	0.48
8/21/84	24:00	30.04	0.49	8/29/84	24:00	30.18	0.50
	6:00	29.97	0.50		6:00	30.19	0.49
	12:00	29.94	0.48		12:00	30.19	0.49
	18:00	29.84	0.51		18:00	30.12	0.51
8/22/84	24:00	29.85	0.49	8/30/84	24:00	30.16	0.51
	6:00	29.81	0.50		6:00	30.14	0.51
	12:00	29.85	0.48		12:00	30.09	0.50
	18:00	29.79	0.48		18:00	29.99	0.52
8/23/84	24:00	29.81	0.49	8/31/84	24:00	29.93	0.51
	6:00	29.75	0.48		6:00	29.85	0.51
	12:00	29.72	0.48		12:00	29.76	0.52
	18:00	29.68	0.48		18:00	29.80	0.53
8/24/84	24:00	29.71	0.49	9/01/84	24:00	29.84	0.52
	6:00	29.72	0.49		6:00	29.89	0.52
	12:00	29.79	0.49		12:00	29.99	0.52
	18:00	29.81	0.48		18:00	30.01	0.52
8/25/84	24:00	29.87	0.50	9/02/84	24:00	30.01	0.52
	6:00	30.01	0.48		6:00	30.03	0.52

Appendix B.4 (West Washoe flowing well temporal data)

Date	Time	T(C)	Flow l/s	EC µMHOS	pH field	pH lab	HCO ₃ ⁻ mg/l
9/13/83	11:21AM	13.0	1.737	159	-	6.40	89.
9/27/83	11:44AM	12.5	1.782	159	-	6.59	93.
10/11/84	9:26AM	12.5	1.788	170	-	6.63	94.
10/25/83	9:43AM	13.0	1.798	175	6.61	6.64	94.
11/ 8/83	9:32AM	12.5	1.804	170	6.59	6.63	96.
11/22/83	10:22AM	12.5	1.887	170	6.87	6.11	93.
12/ 6/83	9:42AM	13.0	1.944	166	6.65	6.50	96.
12/20/83	10:46AM	12.5	2.025	177	-	6.68	99.
1/ 3/84	9:57AM	13.0	2.043	170	-	6.85	96.
1/10/84	9:07AM	12.5	2.005	162	6.54	6.21	98.
1/24/84	8:37AM	12.5	1.993	176	-	6.44	98.
2/ 7/84	8:57AM	12.5	1.935	161	6.66	6.55	98.
2/21/84	8:20AM	12.5	1.956	173	6.62	6.56	96.
* 2/28/84	8:06AM	12.5	2.025	174	6.85	6.66	99.
3/ 6/84	8:10AM	12.5	2.008	172	6.74	6.70	98.
* 3/13/84	7:59AM	12.5	1.998	174	6.76	6.72	100.
3/20/84	7:59AM	-	2.049	164	6.70	6.58	95.
* 3/27/84	8:05AM	13.0	1.961	162	6.87	6.76	94.
4/ 3/84	8:11AM	13.0	1.942	167	6.80	6.71	98.
* 4/10/84	8:07AM	13.0	1.945	170	6.87	6.19	94.
4/18/84	9:34AM	13.0	1.839	176	-	6.21	93.
* 5/ 8/84	7:47AM	13.0	1.870	170	6.93	6.53	96.
5/23/84	10:47AM	13.0	1.770	194	7.17	6.72	107.
5/30/84	9:08AM	13.0	1.754	177	7.17	6.55	98.
* 6/ 6/84	9:45AM	13.0	-	-	-	-	-
6/13/84	9:30AM	13.0	1.732	173	6.93	6.92	95.
6/20/84	9:10AM	13.0	1.652	172	6.89	6.86	96.
* 7/ 5/84	11:02AM	13.0	1.601	172	6.91	6.86?	98.
7/11/84	9:27AM	13.0	1.607	183	6.93	6.64	95.
* 7/17/84	8:33AM	13.0	1.544	172	6.71	6.87	98.
7/26/84	9:32AM	13.0	1.325	172	7.02	6.78	96.
* 8/ 2/84	9:19AM	13.0	1.266	164	6.85	6.86	98.
8/ 9/84	9:23AM	13.0	1.280	175	6.73	6.88	98.
* 8/16/84	8:51AM	13.0	1.159	173	6.83	6.87	102.
8/23/84	9:54AM	13.0	1.066	-	6.92	-	-
Mean		12.8	1.792	171		6.60	96.2
Stand Dev		0.25	0.245	7.8		0.21	3.26
Coef Variation		1.98	13.7	4.6		3.19	3.39

Appendix B.5 (Boat Ramp flowing well temporal data)

Date	Time	T(C)	Flow l/s	EC µMHOS	pH field	pH lab	HCO ₃ ⁻ mg/l
9/13/83	5:15PM	18.0	1.480	150	-	6.76	89.
9/ 2/83	2:53PM	18.0	1.443	170	-	7.10	93.
10/11/83	1:05PM	18.0	1.497	180	-	6.88	93.
10/25/83	1:47PM	18.0	1.498	182	-	6.77	93.
11/ 8/84	2:27PM	18.0	1.524	183	-	6.30	94.
11/22/83	2:34PM	18.0	1.667	183	6.68	6.89	93.
12/ 6/83	1:13PM	18.0	1.700	183	-	6.34	93.
12/20/83	10:19AM	18.0	1.681	187	-	7.00	92.
1/ 3/84	4:02PM	18.0	1.726	182	-	6.79	92.
1/10/84	2:16PM	18.0	1.752	189	6.78	6.41	95.
1/24/84	12:45PM	18.0	1.720	189	-	6.50	92.
2/ 7/84	1:11PM	18.0	1.677	180	6.73	6.89	98.
2/21/84	11:57AM	17.5	1.690	180	6.88	6.92	109.
* 2/28/84	12:11PM	18.0	1.747	187	6.83	7.10	110.
3/ 6/84	11:32AM	18.0	1.711	184	6.84	7.21	113.
* 3/13/84	12:07PM	18.0	1.691	180	6.87	7.31	110.
3/20/84	11:59AM	18.0	1.722	176	6.76	6.98	88.
* 3/27/84	11:53AM	18.0	1.690	167	6.80	7.13	112.
4/ 3/84	12:19PM	18.0	1.688	179	6.68	7.17	113.
* 4/10/84	12:16PM	18.0	1.670	183	6.80	6.54	110.
4/18/84	12:58PM	18.0	1.702	189	-	6.54	109.
5/ 8/84	11:37AM	18.0	1.650	183	7.02	6.60	110.
5/23/84	2:16PM	18.0	1.615	189	7.25	6.81	107.
5/30/84	1:39PM	18.0	1.598	195	6.80	7.20	110.
6/13/84	1:29PM	18.0	1.521	185	6.80	7.34	106.
6/20/84	2:29PM	18.0	1.496	189	6.75	7.25	115.
* 7/ 5/84	2:36PM	18.0	1.413	189	7.12	7.55	112.
7/11/84	1:33PM	18.0	1.417	193	6.95	7.20	117.
* 7/17/84	12:37PM	18.0	1.366	189	6.89	7.12	110.
7/26/84	12:42PM	18.0	1.254	191	6.97	7.12	110.
* 8/ 2/84	12:26PM	18.0	1.149	191	7.05	7.20	111.
8/ 9/84	12:42PM	18.0	1.096	186	6.90	7.34	109.
* 8/16/84	12:46PM	18.0	0.994	-	7.19	-	-
8/23/84	2:32PM	18.0	0.930	-	7.20	-	-
Mean		18.0	1.556	183		6.89	101.3
Stand Dev		0.09	0.202	8.8		0.31	9.58
Coef Variation		0.48	12.90	4.82		4.51	9.46

Appendix B.6 (Accumulated Precipitation at
Spooner Summit (mm))

Date	Precip	Date	Precip
3/15/83	-	12/20/83	37.8
3/29/83	150.4	1/ 3/84	86.9
4/12/83	25.9	1/10/84	0.0
4/26/83	60.5	1/24/84	16.0
5/10/83	25.7	2/ 7/84	0.0
5/24/83	2.3	2/21/84	82.6
6/ 7/83	0.0	3/ 6/84	9.7
6/21/83	0.0	3/20/84	84.6
7/ 5/83	0.0	4/ 3/84	0.0
7/19/83	0.0	4/18/84	26.9
8/ 2/83	0.0	5/ 1/84	3.6
8/16/83	0.0	5/16/84	1.5
8/30/83	0.0	5/30/84	0.0
9/13/83	0.0	6/13/84	16.3
9/27/83	12.7	6/20/84	0.0
10/11/83	35.1	7/11/84	1.0
10/25/83	8.6	7/26/84	6.9
11/ 8/83	30.5	8/ 9/84	0.0
11/22/84	232.9	8/23/84	5.3
12/ 6/83	101.1		
Mean			27.9
Stand Deviation			49.0
Maximum			232.9
Total			1064.3

* Precipitation amount is total from
previous date to current date.

APPENDIX C

Chemical Geothermometry Equations

The following equations have been developed through experimentation, using thermodynamic and kinematic relationships. Listed with each equation will be information such as: 1) the input concentration units, 2) the equilibrium mineral for the equation, 3) the temperature validity range, and 4) the reference. Following this listing will be a discussion of the equations and their application suitabilities.

The equations are incorporated in the FORTRAN program D.1 (appendix D). This program calculates all 12 equations, and outputs temperatures and base assumption violations.

The equations are as follows:

1) $Temp^{\circ}C = (1000/4.78 - \log(SiO_2)) - 273.15$, SiO_2 as Cristobalite in ppm, valid 0-250°C; Fournier, 1977,

2) $Temp^{\circ}C = (1112/4.91 - \log(SiO_2)) - 273.15$, SiO_2 as Chalcedony in ppm, valid 25-180°C; Arnorsson, et al., 1983,

3) $Temp^{\circ}C = (1264/5.31 - \log(SiO_2)) - 273.15$, SiO_2 as Chalcedony in ppm, after adiabatic steam loss, valid 100-180°C; Arnorsson, et al., 1983,

4) $Temp^{\circ}C = (1309/5.19 - \log(SiO_2)) - 273.15$, SiO_2 as Quartz in ppm, valid 150-225°C; Fournier, 1977,

5) $Temp^{\circ}C = (1522/5.75 - \log(SiO_2)) - 273.15$, SiO_2 as Quartz in ppm, after steam loss, valid 150-225°C; Fournier, 1977,

6) $Temp^{\circ}C = (1217/1.483 + \log(Na/K)) - 273.15$, Na and K in ppm, valid 150-200°C; Fournier, 1979,

7) $Temp^{\circ}C = (933/0.993 + \log(Na/K)) - 273.15$, Na and K as

low Albite / K-Feldspar in ppm, valid 25-250°C; Arnorsson, et al., 1983,

8) $Temp^{\circ}C = (1647/2.24 + \log(Na/K) + \beta * \log(\sqrt{Ca}/Na)) - 273.15$, Na, K and Ca in Molar, $\beta = 4/3$ when $\sqrt{Ca}/Na > 0$, $\beta = 1/3$ when $\sqrt{Ca}/Na < 0$, valid 4-340°C; Fournier, et al., 1973,

9) $Temp^{\circ}C = (-22200/\log(Na/K) - 6.3 * \log(\sqrt{Ca}/K) - 64.2) - 273.15$, Na, K and Ca in Molar, valid 0-100°C; Benjamin, et al., 1983,

10) $Temp^{\circ}C = (1416/\log(Na/K) + 0.055 * \log(\sqrt{Ca}/Na) + 1.69) - 273.15$, Na, K and Ca in Molar, valid +100°C; Benjamin, et al., 1983,

11) $Temp^{\circ}C = (1000/\log(Na/Li) + .38) - 273.15$, Na and Li in Molar; Fouillac, et al., 1981, and

12) $R = (Mg/K + Ca + Mg)$, Mg, K and Ca in EPM, $T = (K)$ from equation 8,

$dt = -1.03 + 59.971 * \log R + 145.05 * (\log R)^2 - 36711 * (\log R)^2 / T - 1.67e7 * \log R / T^2$, for $.5 < R < 5$
 $dt = 10.66 - 4.741R + 325.87(\log R)^2 - 1.032e5 * (\log R)^2 T - 1.968e7(\log R)^2 / T^2 + 1.605e7(\log R)^3 / T^2$; for $5 < R < 50$,
 $Temp8^{\circ}C = (temp8(K) - dt) - 273.15$
 If $Temp8 < 70^{\circ}C$, Mg correction cannot be made,
 if $R > 50$, water is too cool and Mg correction cannot be made,
 if $R < .5$, Mg correction cannot be made,
 if $dt < 0$, Mg correction cannot be made; Fournier, et al., 1979.

Silica geothermometers are generally based on mineral solubility. Equations 1 and 2 should be used for systems that may have precipitated cristobalite or chalcedony, respectively, upon ascent. Equation 3 should be applied if chalcedony is thought to have precipitated adiabatically (by boiling). Equation 4 and 5 should be used for reservoirs above 150°C that are thought to have quartz precipitated upon ascent; Equation 4 is for conductive cooling systems and equation 5 is for adiabatically cooled systems.

Na-K and Na-K-Ca geothermometers are based on

exchange reactions. Equation 6 is good for reservoirs around 200°C and will give arbitrarily high readings for reservoirs below 100°C. Equation 7 should be used in low-albite / microcline solution equilibrium. Equation 8 should be used for measuring the last temperature of water-rock interaction; do not continue to apply Na-K geothermometers when square root $(M_{Ca})/M_{Na}$ ratio is greater than 1. Equations 9 and 10 are based on relationships established in equation 8. Equation 11 is an experimental geothermometer, for which little information is available. Equation 12 is a Magnesium correction for equation 8.

APPENDIX D

Program Descriptions

Program D.1 calculates potential reservoir temperatures by applying chemical geothermometers (see table 38 for FORTRAN code). A complete description of these equations is covered in Appendix C. Input data are real values and should be entered in columnar format. An example is as follows:

Example: Geothermometry test input/output
Input data should be entered SiO₂, Na, K,
Ca, Li, and Mg, in mg/l. Enter 0.01 for
values are not available.

287.
675.
82.
4.2
.017
7.8

See table 39 for program output

Program D.2 does lead-lag multiple step-wise linear regression. The data is first run through a crosscorrelation routine to determine the maximum correlation positions. The data is then shifted to its maximum correlation position and data points are removed from the front of each data set, redefining each set at maximum lag positions. A linear equation is developed by entering the independent variable of highest correlation (at any lagged position) solving for the dependent variable. The analysis of variance and correlation coefficient validity are computed as each variable set is entered; therefore, step-wise equation

validity can be measured statistically. A program listing is not included, due the lengthy nature of the code; however, SPSS routines can be coupled to yield the same results and a conceptual flow chart is presented in figure 29.

Program D.3 was used to calculate $p\text{CO}_2$ values. The $p\text{CO}_2$ values are calculated as a function of pH, HCO_3^- (mg/l), temperature (C), EC $\mu\text{mhos/cm}$. This program approximates the ionic strength as a function of the EC and uses the Debye-Huckel equation to calculate the HCO_3^- activity coefficient. From this the partial pressure of CO_2 is calculated. A FORTRAN code listing of this program is listed in Table 40.

Table 38 (FORTRAN Code Listing for Program D.1)

```

program therm
c*****
c      Program by Brad F. Lyles   March 28, 1985      *
c  This program will execute 12 goethermometry equations from *
c  various authors.  Data should be entered as ppm (mg/l), the *
c  program is capable of doing any needed conversions.  The data *
c  can be input for any file name and should be arranged in a *
c  single column format.  Six ions will be entered so enter 0.01 *
c  when ions are not available.                          *
c  Needed subroutines: readm.                              *
c*****
c
      dimension a(14), title(2), ratio(3), dt(2), temp(12)
      character*80 output,input,title
      print*, 'Do you want references printed out?'
      print*, '0=no and 1=yes'
      read(5,*) inst
      if (inst .eq. 1) then
3         go to 1
         inst=0
         write(2,1099)
         write(2,1100)
         go to 2
      else
         go to 1
      end if
1         print*, 'Enter the input and output file names.'
         read(5,10) input,output
10        format (a)
         open(1,file=input,status='old')
         rewind 1
         open(2,file=output,status='new')
         if(inst .eq. 1)goto 3
         write(2,1099)
c
c.. Enter data
c      a(1)=SiO2
c      a(2)=Na
c      a(3)=K
c      a(4)=Ca
c      a(5)=Mg
c      a(6)=Li
c
2         call readm(a,n,6,err)
         if (err .eq. 1.)go to 2000
         print*, 'Enter the title (up to two 80 character lines).'
         read(5,10) title
         write(2,*) '*****'
         write(2,*) title
         write(2,*) '*****'
         write(2,*) ' '
c

```

```

c.. Convert data to the proper units.
c   Eq.: 1-7 in ppm           a(7)=Molar Na
c       8-11 in Molar        a(8)=Molar K
c       12 in EPM           a(9)=Molar Ca
c                               a(10)=Molar Li
c                               a(11)=EPM Na
c                               a(12)=EPM K
c                               a(13)=EPM Ca
c                               a(14)=EPM Mg
c
c       a(7)=a(2)/22.98977/1000.
c       a(8)=a(3)/39.098/1000.
c       a(9)=a(4)/40.08/1000.
c       a(10)=a(6)/6.941/1000.
c
c       a(11)=a(2)*1./22.98977
c       a(12)=a(3)*1./39.098
c       a(13)=a(4)*2./40.08
c       a(14)=a(5)*2./24.305
c
c.. Now calculate temperatures.
c
c       temp(1)=1000./(4.78-log10(a(1)))-273.15
c       temp(2)=1112./(4.91-log10(a(1)))-273.15
c       temp(3)=1264./(5.31-log10(a(1)))-273.15
c       temp(4)=1309./(5.19-log10(a(1)))-273.15
c       temp(5)=1522./(5.75-log10(a(1)))-273.15
c       temp(6)=1217./(1.483+log10(a(2)/a(3)))-273.15
c       temp(7)=933./(.993+log10(a(2)/a(3)))-273.15
c
c.. Ratios are all in Molar.
c
c       ratio(1)=log10(a(7)/a(8))
c       ratio(2)=(a(9)**.5)/a(7)
c       ratio(3)=log10(ratio(2))
c
c.. Check assumptions for the Na-K-Ca thermometer, and do calculations.
c
c       if(ratio(2) .ge. 0) then
c         b=4./3.
c       else
c         b=1./3.
c       end if
c
c       temp(8)=1647./(2.24+ratio(1)+b*ratio(3))-273.15
c       if(ratio(2) .ge. 0 .and. temp(8) .gt. 100) then
c         b=1./3.
c         go to 4
c       end if
4     temp(8)=1647./(2.24+ratio(1)+b*ratio(3))-273.15
c
c       temp(9)=-22200./(ratio(1)-6.3*ratio(3)-64.2)-273.15
c       if(temp(9) .gt. 100) then
c         write(2,102)
c         write(6,102)

```

```

102  format(5x,'ERROR: Temp for eq. (9) should be < 100.')
```

$$\text{temp}(10) = 1416. / (\text{ratio}(1) + .055 * \text{ratio}(3) + 1.69) - 273.15$$

```

    end if
    if(temp(10) .lt. 100) then
      write(2,103)
      write(6,103)
103  format(5x,'ERROR: Temp for eq. (10) should be > 100.')
```

$$\text{temp}(11) = 1000. / (\log_{10}(a(7)/a(10)) + .38) - 273.15$$

```

    end if
    if(a(10) .gt. 0) then
      if(temp(11) .le. 0) then
        write(2,13)
13   format(5x,'ERROR: Li value is too small.')
```

$$\text{temp}(11) = 0.$$

```

      else
        write(2,14)
14   format(5x,'ERROR: Li value = 0')
```

$$\text{temp}(11) = 0.$$

```

      end if
    c
c.. Now calculate the Mg correction for the Na-K-Ca thermometer.
c
    r=(a(14)/(a(12)+a(13)+a(14)))*100.
    if(temp(8) .lt. 70) then
      write(2,104)
      write(6,104)
104  format(5x,'Temp in eq. (8) is < 70; therefore Mg correction cannot
&  'be made.')
```

$$\text{temp}(12) = \text{temp}(8)$$

```

    else if(r .gt. 50) then
      write(2,105)
      write(6,105)
105  format(5x,'Assume: Aquifer water is relatively cold and Mg correction'
&  ' cannot be made.')
```

$$\text{temp}(12) = \text{temp}(8)$$

```

    else if(r .lt. .5) then
      write(2,106)
      write(6,106)
106  format(5x,'ERROR: Mg correction cannot be made.')
```

$$\text{temp}(12) = \text{temp}(8)$$

```

    else if(r .gt. 5 .and. r .le. 50) then
      dt(1)=10.66-4.741*r+325.87*(log10(r))**2-1.032*10.**5*(log10(r))**2/
&  temp(8)-1.968*10.**7*(log10(r))**2/(temp(8))**2+1.605*10.**7*(log10(r)
&  )**2
      if(dt(1) .ge. 0) then
        temp(12)=temp(8)-dt(1)
      else
        write(2,107)
        write(6,107)
107  format(5x,'ERROR: Mg del(T) < 0; no Mg correction is made.')
```

$$\text{temp}(12) = \text{temp}(8) - dt(1)$$

```

    else if(r .gt. .5 .and. r .le. 5) then
      dt(2)=-1.03+59.97*log10(r)+145.05*(log10(r))**2-36711.*(log10(r)
&  )**2/temp(8)-1.67*10.**7*log10(r)/temp(8)**2
```

```

        if(dt(2) .ge. 0) then
            temp(12)=temp(8)-dt(2)
        else
            write(2,107)
            write(6,107)
        end if
    end if

c
c.. Printout of calculated temps
c
    write(2,*) ' '
    write(2,1000)
    write(2,999)
    write(2,1001)
    write(2,999)
    write(2,1002) (temp(i),i=1,12)
    write(2,1003)
    write(2,1004) (a(i),i=1,6)
    write(2,1005)

c
c.. Format statements
c
999    format('-----I-----')
&'-----')
1000   format('Thermometer',2x,'I',3x,'SiO2',6x,'SiO2',6x,'SiO2',6x,'SiO2',
&        6x,'SiO2',6x,'Na-K',6x,'Na-K',3x,'Na-K-Ca',3x,'Na-K-Ca',3x,'Na-K-Ca'
&        ,4x,'Na-Li',3x,'Na-K-Ca (-Mg)')
1001   format('Eq. No.',6x,'I',5x,'1',9x,'2',9x,'3',9x,'4',9x,'5',9x,
&        '6',9x,'7',9x,'8',9x,'9',9x,'10',8x,'11',8x,'12')
1002   format('Calculated',3x,'I',/'Temperatures',1x,'I',f8.2,11f10.2)
1003   format('    (C)      I',/'      I')
1004   format(' Input Ion  I  SiO2    Na      K      Ca      Mg  '
&        'Li'
&        /'ConcentrationI',f7.2,5f9.2)
1005   format('=====')
&'=====','/,/)
1099   format(/,20x,'*** GEOTHERMOMETRY PROGRAM ***',/)
1100   format('Eq.1,4-5 = Fournier, 1977, "Chemical
& Geothermometers and Mixing',/
& Models for Geothermal systems",Geothermics,vol. 5,pp.41-50.',/,/
& Eq.2-3,7 = Arnorsson,etal, 1983, "The Chemistry of
& geothermal Waters in Iceland',/
& Chemical Geothermometry in Geothermal Investigations",
& Geochemica et Cosmocimica Acta',/
& ,Vol 47,pp 567-577.',/,/
& Eq.6 = Fournier, 1979, "A Revised Edition for the Na/K
& Geothermometer",Geothermal',/
& Resources Council, Transactions,Vol 3,pp 221-224.',/,/
& Eq.8 = Fournier,etal, 1973, "An Empirical Na-K-Ca
& Geothermometer for Natural',/
& Waters", Geochemica et Cosmochemica Acta,Vol 37,pp
& 1255-1275.',/,/
& Eq.9-10 = Bejamin,etal, 1983, "Thermodynamic perameters
& and Experimental data for the Na-K-Ca ',/
& Geothermometer",Jour. of Volcanology and Geothermal

```

```

&Research,Vol 15,pp 167-186.',/,/
&'Eq.11 = Fouillac,etal, 1981, "Sodium/Lithium Ratio in
& Water Applied to Geothermometry of',/
&'Geothermal Reservoirs", Geothermics,Vol 10,pp 55-70.'
&,/,/
&'Eq.12 = Fournier,etal, 1979, "Magnesium Correction of
& the Na-K-Ca Chemical Geothermometer"',/
&',Geochemica et Cosmochemica Acta,Vol 43,pp
&1543-1550.')
```

```

      print*, 'Do you want to make another run?'
      print*, '0=no and 1=yes'
      read(5,*) ins
      if (ins .eq. 1) go to 1
2000  continue
      end
```

```

c***** Subroutine Readm *****
      subroutine readm(a,n,n1,err)
      dimension a(n1)
      print*, 'Enter the number of ions to be evaluated.'
      print*, 'Enter all six values; use 0.01 when ions are not available.'
      read(5,*) n
      if (n .ne. 6) then
      print*, 'ERROR: 6 values must be entered from input file.'
      print*, 'Run is terminated.'
      err=1.
      go to 2000
      end if
      do 100 i=1,n
      read(1,*) a(i)
100  continue
2000  return
      end
```


Table 39(Example output from program D.1)

*** GEOTHERMOMETRY PROGRAM ***

 Test data for program geotherm.

ERROR: Mg correction cannot be made.

Thermometer	I	SiO2	SiO2	SiO2	SiO2	SiO2	Na-K	Na-K	Na-K-Ca	Na-K-Ca	Na-K-Ca	Na-Li	Na-K-Ca (-Mg)
Eq. No.	I	1	2	3	4	5	6	7	8	9	10	11	12
Calculated	I												
Temperatures (C)	I	157.49	180.34	170.03	205.97	189.17	234.25	215.72	236.19	95.80	230.60	283.30	236.19
Input Ion Concentration	I	SiO2	Na	K	Ca	Mg	Li						
	I	287.00	675.00	82.00	4.20	0.02	7.80						

Figure 29 (Conceptual Flowchart of Lead-lag Multiple Step-wise Linear Regression)

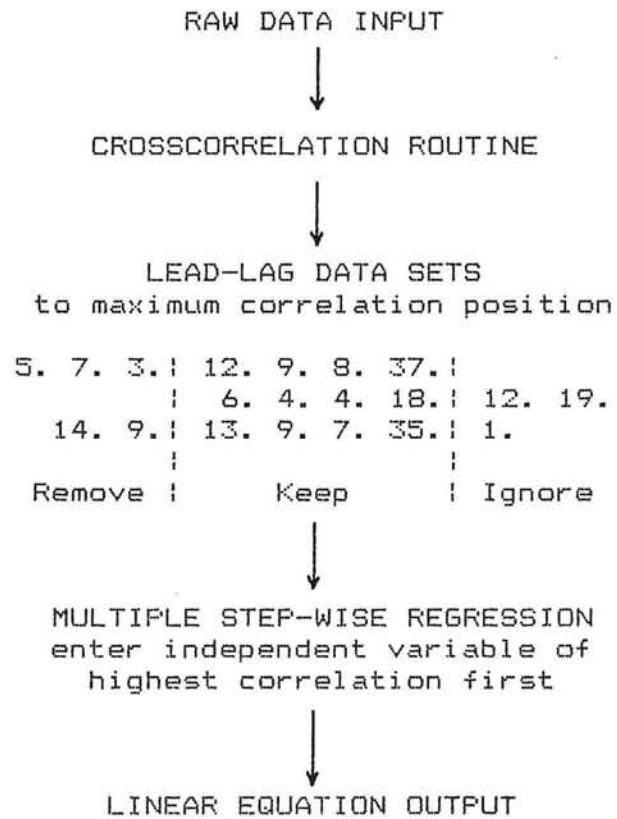


Table 40 (FORTRAN code listing Program D.3)
 program pco2

```

c*****
c      Program by Brad F. Lyles May 5, 1985      *
c      This program does the following:         *
c      1) converts HCO3 from ppm to Molality with density *
c      as a function of temperature,           *
c      2) calculate the Debye-Huckel constants f(temp), *
c      3) approximates ionic strength f(temp),  *
c      4) calculates activity coefficient of HCO3, *
c      5) pK1 and pKCO2 are calculated based on temp, and *
c      6) pCO2 is calculated as a function of hydrogen *
c      and bicarbonate ion activities, and as a function *
c      of temp and EC.                          *
c*****
      dimension t(30),ec(30),ph(30),rho(21)
      real hco3(30),is,lpco2
      character*20 arg(10)
      data rho(1),rho(2),rho(3),rho(4)/.99987,.99999,.99973,.99913/
      data rho(5),rho(6),rho(7),rho(8)/.99823,.99707,.99567,.99406/
      data rho(9),rho(10),rho(11),rho(12)/.99224,.99025,.98807,.98573/
      data rho(13),rho(14),rho(15),rho(16)/.98324,.98059,.97781,.97489/
      data rho(17),rho(18),rho(19),rho(20)/.97183,.96865,.96534,.96192/
      data rho(21)/.95838/
      n=0

c
      numarg=iargc()
      call getarg(1,arg(1))
      call getarg(2,arg(2))
      call getarg(3,arg(3))
      call getarg(4,arg(4))
      open(1,file=arg(1),status='old')
      open(2,file=arg(2),status='old')
      open(3,file=arg(3),status='old')
      open(4,file=arg(4),status='old')
      open(7,file='OUT',status='new',err=5)
      goto 6
5      open(7,file='OUT',status='old')
6      rewind 7
c
c.... Enter data files
c
      do 100 i=1,30
        read(1,*,end=100) ph(i)
        read(2,*,end=100) ec(i)
        read(3,*,end=100) t(i)
        read(4,*,end=100) hco3(i)
        n=n+1
100    continue
c
c.... Calculate Molality with density=f(temp)
c
      do 200 i=1,n
        hco3(i)=hco3(i)*61./1000.
        itemp=nint(t(i)/5.)

```

```

        rhho=rho(itemp+1)
        hco3(i)=1000.*hco3(i)/(61.*(1000.*rhho-hco3(i)))
200  continue
c
c..... Calculate Debye-Huckel constants
c
        write(7,20)
        do 300 i=1,n
            s1=374.11-t(i)
            s2=s1**.333
            s3=(1.+1.1342489*s2-3.94623e-03*s1/3.1975-.3151548*s2-1.203374e-03
& *s1+(7.48908e-13*s1)**4.)**.5
            temp=273.16+t(i)
            if(temp .lt. 373.16)then
                c1=87.741-t(i)*(t(i)*(1.41e-06*t(i)-9.398e-04)+.4008)
            else
                c1=5321./temp+233.76-temp*(temp*(8.29e-07*temp-1.417e-03)+.9279)
            end if
            c2=(c1*temp)**.5
            a=.49+8.9989e-04*t(i)
            b=.32406+1.6158e-04*t(i)
c            a=1824600.*s3/c2**3
c            b=50.29*s3/c2
c
c..... Calculate ionic strength
c
            is=1.4271e-05*ec(i)**.95184
c
c..... Calculate GAMMA with Debye-Huckel equation
c
            gamma=10.**((-1)*a*is**.5/(1+b**4.*is**.5))
            ahco3=hco3(i)*gamma
            pk1=6.71*t(i)**-.0168
            pkco2=.8800*t(i)**.1638
            ten=10.
            ah=ten**(-1)*ph(i)
            pco2=ah*ahco3/(ten**((-1)*pk1)*ten**((-1)*pkco2))
            lpco2=log10(pco2)
            write(7,10) rhho,is,gamma,ahco3,pco2,lpco2
300  continue
10  format (6f10.5)
20  format (' H2O',7x,' Ionic      Gamma      activity  pCO2',
& ' log',/, ' Density      Strength',15x,' HCO3',15x,' pCO2')
        end

```

APPENDIX E

Thesis Addendum

The following isotopic information became available just prior to the presentation of this thesis; therefore, the data will be mentioned here as an addendum to the previously addressed information. Stable isotope samples were collected on each sample date of this study. All isotopic analyses were conducted at the Desert Research Institute Stable Isotope Laboratory, Las Vegas, Nevada.

Hydrogen isotopes are generally considered stable along lengthy tortuous flow paths, but oxygen isotopes are susceptible to ^{18}O enrichment by exchange with silicate mineral oxygen. The oxygen ^{18}O enrichment is referred to as an "Oxygen Shift", and has been discussed by White and others (1968), Ellis and Mahon (1977), and Blattner (1980). In an attempt to alleviate the oxygen shift interpretation problems, more emphasis was focused on the hydrogen isotopes. From the six geothermal springs studied 38 hydrogen and 14 oxygen isotopes were analyzed; six cold water sources from potential recharge areas were also analyzed for oxygen and hydrogen (table 41). These analysis results are plotted on figure 30 along with the previously referenced values. The world average meteoric water line has been added to figure 30 for reference.

In most cases the previously referenced values are similar to those measured in this study; the only values that are significantly different are from Saratoga and

Table 41 (Stable Isotope Data)

Name	Date	$\delta^{18}O$	δD	Location
Farad	9/13/83	-	-108	se, se, s12, 18n, 17e
"	11/08/83	-	-115	"
"	1/03/84	-13.8	-106	"
"	3/06/84	-	-107	"
"	5/16/84	-	-102	"
"	7/11/84	-13.7	-106	"
$\delta D=13\%$.	MEAN δD =	-107.3	SDEV δD = 4.27	Coef. Var. = 4.0
Steamboat	10/25/83	-11.8	-112	sw, se, s28, 18n, 20e
"	12/20/83	-	-109	"
"	2/21/84	-	-106	"
"	4/18/84	-10.8	-105	"
"	6/20/84	-	-109	"
"	8/23/84	-	-120	"
$\delta D=15\%$.	MEAN δD =	-110.2	SDEV δD = 5.42	Coef. Var. = 4.9
Bowers	9/13/83	-	-109	nw, nw, s03, 16n, 19e
"	10/11/83	-	-105	"
"	11/08/83	-14.8	-104	"
"	12/06/83	-	-105	"
"	1/10/84	-	-108	"
"	2/07/84	-14.9	-106	"
"	3/06/84	-	-103	"
"	4/18/84	-	-102	"
"	5/16/84	-14.5	-105	"
"	6/13/84	-	-101	"
"	7/11/84	-	-104	"
"	8/23/84	-14.7	-105	"
$\delta D=8\%$.	MEAN δD =	-104.8	SDEV δD = 2.26	Coef. Var. = 2.2
Prison	12/20/83	-15.1	-112	sw, se, s16, 15n, 20e
"	5/16/84	-15.9	-112	"
$\delta D=0\%$.				
Saratoga	9/27/83	-	-126	sw, se, s21, 14n, 20e
"	11/22/83	-16.3	-124	"
"	1/24/84	-	-128	"
"	3/20/84	-	-123	"
"	5/16/84	-15.6	-119	"
"	7/26/84	-	-109	"
$\delta D=10\%$.	MEAN δD =	-123.0	SDEV δD = 3.90	Coef. Var. = 3.2
Walley's	9/27/83	-	-122	sw, ne, s22, 13n, 19e
"	11/22/83	-15.1	-115	"
"	1/24/84	-	-113	"
"	3/20/84	-	-109	"
"	5/30/84	-14.1	-111	"
"	7/26/84	-	-109	"
$\delta D=13\%$.	MEAN δD =	-113.2	SDEV δD = 4.92	Coef. Var. = 4.3

Table 41 continued

Name	Date	$\sigma^{18}O$	σD	Location
Brockliss Slough	7/11/84	-13.1	-96	se,nw,s22,13n,19e
Kingbury Grade spg.	6/07/84	-14.6	-106	ne,ne,s20,13n,19e
Ritter Spring	6/22/84	-14.9	-106	se,sw,s33,17n,19e
Ritter Spring Overflow	12/15/84	-15.2	-108	nw,nw,s03,16n,19e
Thomas Creek Spring	12/15/84	-16.3	-118	nw,se,s29,18n,19e
Stock Spring	12/15/84	-15.6	-113	nw,ne,s22,18n,19e
Name	Date	$\sigma^{18}O$	σD	Reference
Bowers	-	-14.8	-102.3	Garside (1979)
Steamboat	7/12/77	-12.0	-115	Nehring (1980)
Prison	10/15/81	-15.2	-112	Szecody (1983)
Saratoga	-	-16.2	-130	Trexler (1980)
Walley's	-	-16.3	-132	"
Carson River	-	-14.6	-116	"
Thomas Creek Spring	6/08/77	-15.9	-122	Nehring (1980)
Stock Spring	6/08/77	-15.6	-118	"

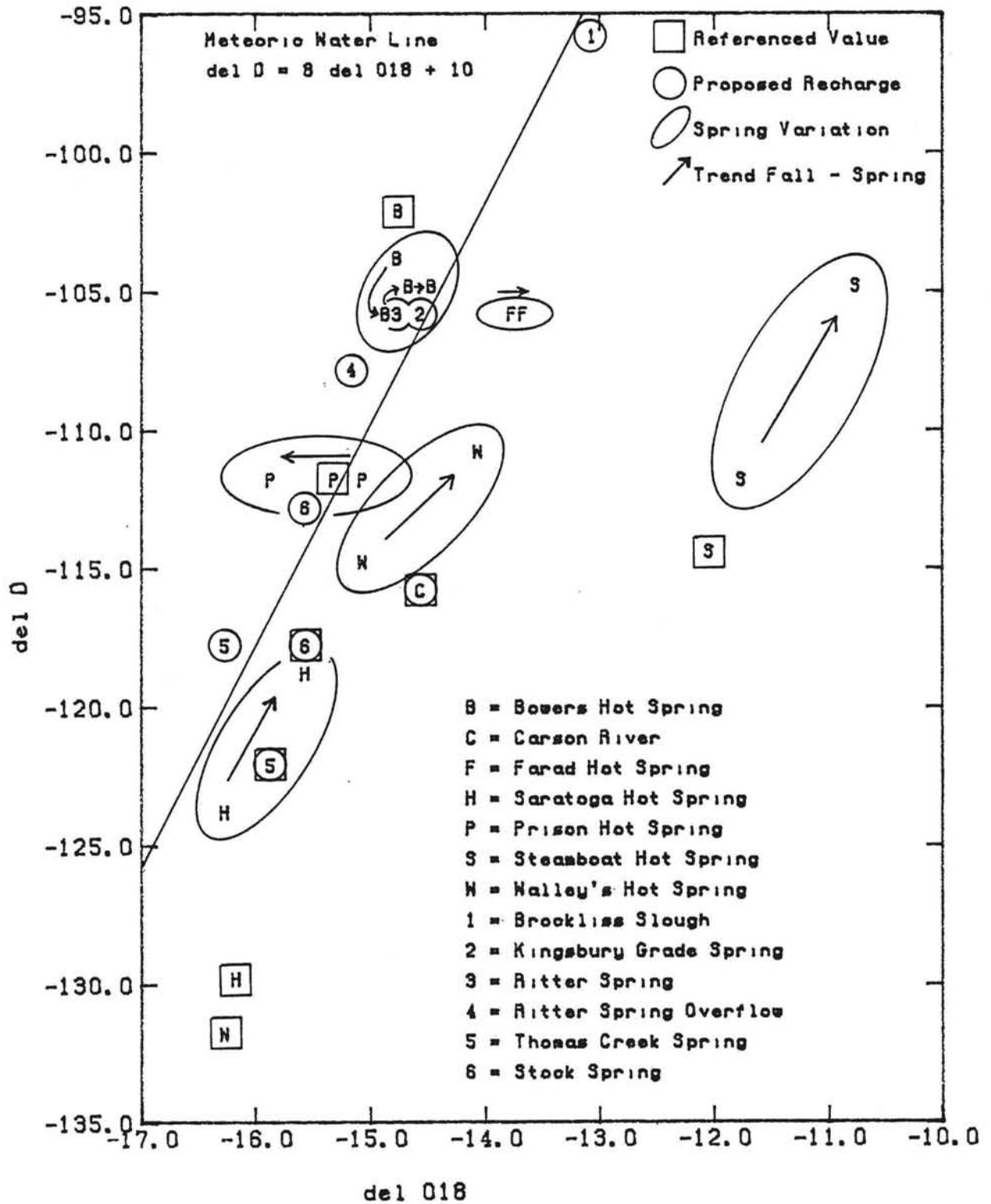


Figure 30. Study Area Isotope Plot
 δD vs. $\delta^{18}O$

Walley's hot springs. Saratoga and Walley's hot springs were isotopically light according to Trexler and others (1980) ($\delta^{18}O = -16.2$, $\delta D = -130$ and $\delta^{18}O = -16.3$, $\delta D = -132$, respectively); however, recent measurements from Saratoga and Walley's hot springs plot isotopically heavier in $\delta^{18}O$ and δD . This enrichment is probably due to surface water and ground water mixing (dilution), such as Walley's Hot Spring reservoir water mixing with Sierran recharge water (similar to Kingsbury Grade Spring) and Carson Valley surface water (similar to Brockliss Slough water), resulting in an intermediate composition water. A similar comparison is observed at Saratoga Hot Spring.

Bowers Hot Spring water is similar isotopically to the water at Ritter cold Spring, suggesting that both springs gain their recharge from similar areas. In this case recharge is probably derived from infiltration around Price Lake and Mount Rose Meadows. A similar relationship exists between Steamboat Springs and two cold springs (Thomas Creek Spring and Stock Spring). The general vicinity of this two cold springs has been proposed by Nehring (1980) as a major recharge area for the Steamboat Geothermal System; however, further work is necessary to justify this proposed theory.

All of the geothermal springs were observed to be highly variable with respect to δD , with the exception of Prison Hot Spring. The change in δD ranged from 0% to 15%, with most springs showing a change of 10%; coefficients of variation paralleled this trend, with values ranging

from 2.2 to 4.9 percent. Stewart and Downes (1980) presented data from New Zealand springs that produced a δD coefficient of variation of 2.1 percent.

Assuming that hydrogen isotopes are stable along the flow path, which is not unreasonable considering the low abundance of hydrous minerals in the study area, isotopic variability can be accounted for in at least two ways:

1) quick infiltration of surface water near spring discharge points that is markedly different (isotopically) from the reservoir water, and

2) recharge waters that keep their isotopic integrity along the entire reservoir flow path, due to poor mixing.

Each theory has certain drawbacks, intuitively and theoretically. Without further study no final hypothesis can be posed; however, the data does show that the isotopic variability is higher than was previously expected.